A DISTRIBUTED KINEMATIC MODEL OF UPLAND WATERSHEDS

by
Edward W. Rovey, David A. Woolhiser
and Roger E. Smith

July 1977

HYDROLOGY PAPERS
COLORADO STATE UNIVERSITY
Fort Collins, Colorado

93

A DISTRIBUTED KINEMATIC MODEL OF UPLAND WATERSHEDS

by
Edward W. Rovey, David A. Woolhiser and Roger E. Smith

HYDROLOGY PAPERS
COLORADO STATE UNIVERSITY
FORT COLLINS, COLORADO 80523

July 1977

No. 93

TABLE OF CONTENTS

ACKNOWLEDGEMENTS

This paper is based upon the M.S. Thesis "A Kinematic Model of Upland Watersheds" by Edward W. Rovey. The work was supported by the Agricultural Research Service of the U. S. Department of Agriculture and the Colorado Experiment Station under project number LS114 "Investigation of Small Watershed Floods."

Mr. G. L. Ducret, Jr. furnished the U. S. Geological Survey's data for the Denver urban area. Data for the Hillcrest Drain watershed was made available by the Public Works Department of the City of Northglenn.

David C. Clutter did much of the programming for the KINGEN 75 model presented in the Appendix. The help and advice of Professor E. F. Schulz and Dr. Freeman Smith is also sincerely appreciated.

ABSTRACT

A parametric infiltration model is incorporated with a surface routing model, based upon a kinematic cascade of planes and channels to constitute a watershed model. Relationships are developed to compute flows by the kinematic approximation in channels of circular cross-section for routing through storm drains. The infiltration model is tested on some infiltrometer experiments; model parameters are estimated from measured data and by comparison to characteristics of soils used in a previous study. Two types of flow resistance relationships are considered: the Chezy formula and a friction relationship that is initially laminar and then becomes turbulent (Chezy) above a transition Reynolds number. The watershed model is used to compute discharge from: a) a 0.6 acre impervious experimental rainfall-runoff facility, b) a 27 acre experimental agricultural watershed, and c) a 165 acre urban watershed.

A computer program of a general kinematic watershed model is described and documented. This program, called KINGEN 75 may be used to predict hydrographs of individual storms for small rural and urban watersheds, based on basin topography and field measurements of infiltration parameters.

FOREWORD

The basic KINGEN program for computing the runoff hydrograph from a complex configuration of impervious planes and channels was written by D. A. Woolhiser in 1969. The philosophy adopted at that time was to test the model on successively more complicated systems, beginning with the CSU Experimental Rainfall-Runoff Facility and progressing to more complicated rural and urban watersheds. As his M.S. Thesis topic E. W. Rovey added an infiltration subroutine (developed by R. E. Smith) to the model, added a routine to handle unsteady flow in circular conduits and performed extensive tests using apriori information.

Because the KINGEN program used by E. W. Rovey had evolved over a period of 5 years, it had become quite unwieldy. Consequently, we decided to completely reprogram the model, making extensive use of subroutines, and simplifying the input as much as possible. The KINGEN 75 model, presented in the Appendix, is the result of this effort.

David A. Woolhiser
Research Hydraulic Engineer
USDA-ARS

July 1977
Fort Collins, Colorado

DISCLAIMER

The programs listed herein are furnished with the express understanding that the United States Department of Agriculture or Colorado State University give no warranties, expressed or implied, concerning the accuracy, completeness, reliability, usability, or suitability for any particular purpose of the information and data contained in these programs or furnished in connection therewith, and the USDA or Colorado State University shall be under no liability whatsoever to any person by reason of any use made thereof.

The programs herein belong to the USDA. Therefore, the recipient further agrees not to assert any proprietary rights therein or to represent these programs to anyone as other than USDA programs.

LIST OF SYMBOLS

Symbol	Chapter	Definitions (dimensions)
a	2	Regression coefficient**
A	3	Cross-sectional area (L^2)
A	3	Coefficient of R. Smith's parametric, decay-type infiltration function (T^{α})
b	2	Regression exponent
B	3	Geometric parameter of a trapezoidal channel as shown in Fig. 3-1 (L)
B_p	3	Dimensionless ponding coefficient in Equation (3-60)
c	2	Parameter related to soil cover complex in regards to infiltration (T^{-1})
c	3	Constant of integration
c	3	Wave celerity, when used in the context of flow in a channel (L/T)
C	3,5	Chezy friction factor ($L^{1/2}T^{-1}$)
C_1	3,5	Constant relating T_o and relative saturation (T)
CF	5	Coefficient greater than unity used to calculate a Δt for infiltration computation
D	3	Diameter of a circular conduit (L)
e	2	Base of natural logarithm system
f	2,3	Darcy-Weisbach friction factor
f	2,3,5	Infiltration rate (LT^{-1})
f_*	3	Dimensionless infiltration
f_o	2	Initial infiltration rate (LT^{-1})
f_∞	2,3,5	Steady-state infiltration rate (LT^{-1})
F	3,5	Accumulated infiltration (L)
F_o	2	Froude number for normal flow
F_p	3	Accumulated infiltration at time of ponding (L)
F'	5	Factor that is used to limit the infiltration on recession
g	3	Acceleration due to gravity (LT^{-2})
h	3	Depth of flow (L)
h_{max}	3	Maximum depth (L)
h_o	3	Initial depth (L)
$\tilde{h}$	3	Depth error term (L)
HD	3	Hydraulic depth (L)
H_o	2	Normal depth (L)
i	3	Rainfall rate (L/T)
i_*	3	Dimensionless rainfall rate
IC	5	Intensity coefficient used in variable flow resistance relationship
k	2,3,5	Laminar flow roughness constant
k'	5	Empirical constant used to limit infiltration on recession
K	2	Kinematic flow number, measures applicability of kinematic wave theory
K_s	2	Saturated conductivity (LT^{-1})
K_r	2	Relative conductivity
ℓ	3	Length of a plane (L)
L	2,5	Length of flow (L)
n	2,3,5	Manning's flow resistance factor ($L^{1/6}$)
N	3	Exponent for overland flow that is related to surface roughness and geometry
O.F.	5	Objective function used in studying infiltration sensitivity
P	3	Wetted perimeter (L)
q	3	Lateral inflow (LT^{-1})
Q	3	Discharge per unit width for overland flow (L^2T^{-1})
Q	3	Discharge in a channel (L^3T^{-1})
R	3	Hydraulic radius (L)
R_e	2	Reynolds number
s	2	"Sorptivity" or influence of capillarity of a soil ($LT^{-1/2}$)
S	2,3	Surface slope of channel or plane
S_a	2	Relative saturation

LIST OF SYMBOLS - CONTINUED

Symbol	Chapter	Definitions (dimensions)
S_f	3	Friction slope
S_i	3,5	Initial relative volumetric water content of a soil
S_o	3,5	Maximum relative volumetric water content of a soil
t	2,3	Elapsed time (T)
t_*	3	Dimensionless time
t_o	3	The vertical asymptote of the infiltration function (T)
t_o	3	Initial time when referring to surface flow (T)
t_{o*}	3	Dimensionless form of t_o related to infiltration
t_p	3,5	Time to ponding (T)
t_{p*}	3	Dimensionless time to ponding
Δt	3,5	Time increment (T)
TI	5	Time at the beginning of a rainfall pulse (T)
T_o	3,5	Normalizing time (T)
x	3	Distance in the direction of flow (L)
x_o	3	Initial position on the x axis (L)
Δx	3,5	Length increment (L)
z	2	Vertical distance below surface (L)
α	3,5	Coefficient for overland flow that is related to surface roughness and geometry ($L^{1/2}T^{-1}$--turbulent and LT^{-1}--laminar)
α	3,5	Exponent of R. Smith's parametric, decay-type infiltration function
β	3,5	Exponent of relationship between t_{p*} and i_*
γ	3,5	Coefficient of relationship between t_{p*} and i_*
θ	3	Central angle to the water surface of a partially full circular conduit
ν	3	Kinematic viscosity (L^2T^{-1})
ϕ	2	Porosity
ψ	2	Soil capillary potential (L)
ω	3,5	Weighting factor used in an implicit finite difference scheme

**no dimensions listed indicate dimensionless quantity

Chapter 1
INTRODUCTION

The increase in world population has resulted in increased development in natural floodways in both rural and metropolitan areas. As a consequence of this development, property values have risen and more people are exposed to flood danger. The increased potential for flood losses warrants the development of more accurate techniques for estimating flood peaks.

Watershed models of various types have been used to estimate flood peaks. A watershed model may be defined as a physical or mathematical representation of the real watershed. Any useful model involves simplification of the real system and therefore inevitably results in distortion. However, the model developer attempts to minimize distortion of the most crucial watershed characteristics, and it is assumed that the most important aspects are accurately portrayed.

Mathematical models are usually more useful than physical models in hydrologic studies. The models consist of differential or partial differential equations which may have analytic solutions for only a few, highly simplified problems. Consequently numerical methods must be used to obtain solutions for most mathematical models.

There are four important phases in using mathematical models as aids in understanding and predicting hydrologic phenomena. The first phase is to determine the equations, and appropriate boundary conditions that describe the physical processes being investigated and to consider possible simplifications. The second phase is to develop an efficient and accurate computer algorithm to solve the equations and to handle the logical steps. Methods of parameter estimation must then be developed using rainfall, runoff, topographic, and soil data from a variety of watersheds. The final and most important phase of modeling comes when the calibrated model is used to predict the response of a system using only knowledge of the system and its inputs.

The major objectives of this study are:

1. To develop a flow routing procedure for circular conduits, based on the kinematic approximations of unsteady free surface flow equations, and compare the solutions to those obtained by other methods of routing,
2. To incorporate an infiltration model with a surface runoff model, based on the kinematic approximation,
3. To compare observed hydrographs with computed hydrographs from the model for:
    a) a small impervious experimental watershed at Colorado State University,
    b) an experimental agricultural watershed at Edwardsville, Illinois,
    c) an experimental urban watershed at Denver, Colorado,
4. To test the sensitivity of the model parameters,
5. To document a computer program for estimating surface runoff hydrographs from complex watersheds described as a cascade (logical flow sequence) of overland flow planes and channels.

Chapter 2
PREVIOUS STUDIES OF KINEMATIC WATERSHED MODELS

2.1 Kinematic Wave Theory

The continuity and momentum equations for gradually varied unsteady flow were developed by De Saint Venant in 1871 (Yevjevich, 1960). Direct solution of these equations, even by numerical means, was not possible before electronic computers were available, except for extremely simplified initial and boundary conditions. Graphical methods were used for approximate solutions but even these were tedious. Usually, simplified methods, considering only continuity or approximations to the momentum equation, were used to route flows (Yevjevich and Barnes, 1970).

Many investigators have studied gradually varied unsteady flow and found conditions for which a simplification of the complete momentum equation and the continuity equation are sufficiently accurate.

Lighthill and Whitham (1955) considered propagation of flood waves in rivers as mainly kinematic, a balance of bed slope and friction slope; they also investigated kinematic shock waves. Wooding (1965) applied kinematic wave theory to a catchment formed by two planes in a V-shape, each discharging into a stream at the center. He concluded that kinematic theory was applicable to gradually varied unsteady flow if the Froude number was less than 2. Woolhiser and Liggett (1967) showed how the use of dimensionless continuity and momentum equations could reduce the number of parameters for overland flow on a plane from five to two. A parameter of the dimensionless momentum equation was used to measure the applicability of kinematic wave theory. The parameter was

$$K = \frac{SL}{H_o F_o^2} \qquad (2\text{-}1)$$

where S is surface slope; L is length of flow; H_o is normal depth; and F_o is the Froude number for normal flow. Figure 2-1 shows that for $K > 10$, the kinematic wave solution, labeled $K = \infty$, is a good approximation. The kinematic wave parameter is often several thousand or more for many cases of overland flow. Foster, et. al. (1968) simulated rainfall on an erodible fallow plot and found that a kinematic wave model satisfactorily predicted overland flow. Observed hydrograph data were analyzed to estimate retention storage and surface roughness. These results were used to predict hydrographs. A comparison was made between a constant Darcy-Weisbach f or Manning's n and a variable friction factor of the form

$$f = aR_e^b \qquad (2\text{-}2)$$

where a and b are constants and R_e is the Reynolds number. The constant friction factor gave results as good as a variable factor, which would indicate the flow was turbulent. Henderson (1963) and Eagleson (1970) have utilized the kinematic wave theory, but they limit the kinematic waves to a non-subsiding state. They do not account for the subsidence property of kinematic shock waves that may exist. Kinematic shocks result when waves travel faster and overtake slower waves that originated downstream. This phenomenon is represented mathematically by an upstream characteristic intersecting a characteristic that originated below it; there is a discontinuity at the intersection (see section on *Kinematic Equations for a Plane* for mathematical definition of a characteristic). Kibler (1968) and Kibler and Woolhiser (1970) developed dimensionless kinematic equations for a cascade of planes and developed a parameter based upon the widths, slope, and roughness of adjoining planes to predict occurrence of kinematic shocks. A method for tracing the shock waves was also presented.

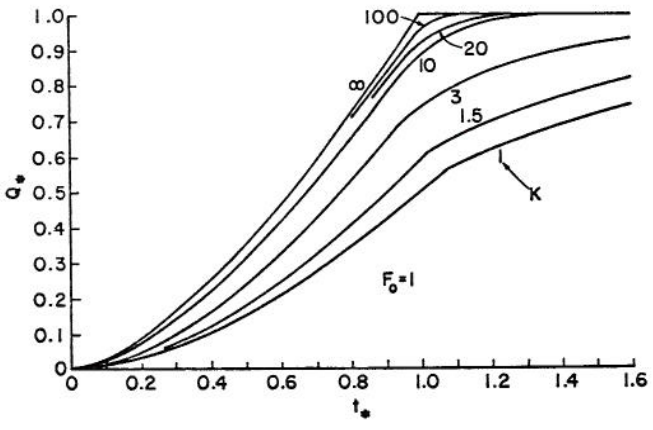

Fig. 2-1 Variation of Dimensionless Hydrograph with Kinematic Flow Number (after Woolhiser and Liggett, 1967)

The kinematic wave models that have been formulated have been solved by a variety of finite difference methods, some implicit and some explicit. Brakensiek (1967a) tested three types of finite difference methods on a kinematic model of flood routing and found that a four point implicit scheme, which centered on the two upper points, gave the most satisfactory results. Kibler and Woolhiser (1970) found that an explicit finite difference scheme with second order accuracy was the most satisfactory numerical method for their studies of overland flow.

Kinematic models have usually been used to simulate hydrographs of individual runoff events. Such simulations require that the surface geometry or macroscale features of the watershed, like length, width and slope of overland flow areas and channel lengths, slopes, and cross-sections, be measured from topographical maps and incorporated into the model geometry.

Although this procedure is subjective, it can be done with reasonable accuracy. The mesoscale features of rills and obstructions to flow and the microscale features of surface roughness cannot be measured as

easily and are generally lumped in a hydraulic roughness parameter or parameters that are often estimated by optimization techniques.

Several researchers have worked on the problem of resistance to overland flow. Some of the results of this work are plotted in Fig. 2-2 for Darcy-Weisbach f vs. Reynolds number. In this analyses, they assumed that the friction law was of this form. Woo and Brater (1962) simulated rainfall for conditions of laminar flow but found that raindrop impact affected flow resistance. Iwagaki (1955) solved the characteristic equations for kinematic waves in steep channels and found good agreement between calculated and observed results. He observed an increase in discharge momentarily after lateral inflow abruptly went to zero. Yu and McNown (1964) experimented with data obtained from Crops of Engineers rainfall experiments on a concrete surface. They could model the sudden increases of discharge after rainfall ceased by lowering the friction coefficient when rainfall stopped. Henderson and Wooding (1964) applied a kinematic wave model to experiments on tarred gravel, clipped sod, and tarred sand surfaces. They obtained good agreement between computed and observed hydrographs.

The variation in hydraulic resistance is quite large as shown in Fig. 2-2. Of course, one would expect the research results to vary when the experiments were conducted on the different types of surfaces or under different conditions. Morgali and Linsley (1965) simulated some hydrographs with a kinematic model and found laminar flow conditions best fit discharge over a painted wood surface, while the best fit for the rising limb of roughened surfaces was with a turbulent friction factor, n = .017 for crushed slate, and n = 0.4 - 0.5 for turf. The friction factor had to be lowered for the recession hydrograph. Morgali (1970) found the range of the laminar roughness constant, k , which is the product of the friction factor, f , and the Reynolds number was 14-35 for asphalt, 20-65 for crushed slate, and 5,000 - 14,000 for turf. As Reynolds' number increased, transition to turbulent flow occurred, and resistance could be modeled by Manning's law. Kibler (1968) and Kibler and Woolhiser (1970) verified their work on the Colorado State University experimental rainfall-runoff facility and their results indicated that observed hydrographs rose more slowly during the initial periods of rainfall than did the predicted hydrographs. Computed peak rates varied both above and below the observed rates but the timing of the peaks agreed fairly well and the recession hydrographs were accurately simulated.

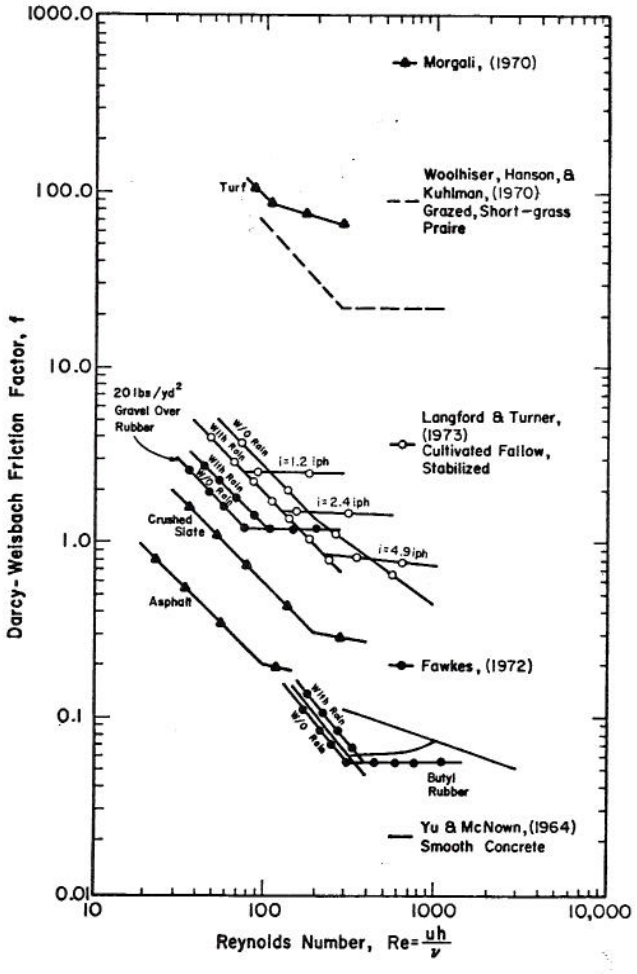

Fig. 2-2 Darcy-Weisbach f vs. Reynolds number

Woolhiser (1969) proposed a portion of a cone at the upstream end of an area to approximate the convergence of flow on many watersheds. This was combined with two planes and a channel to represent an entire watershed. He derived the dimensionless equations for a converging section, tested it on observed data, and obtained good agreement on the steeply rising early portion of the hydrograph. Fawkes (1972) tested several roughness relationships on the Colorado State University facility and found that a mixed laminar-turbulent roughness relationship gave the best results. He found good agreement using "disturbed" laminar conditions during rainfall and "undisturbed" laminar conditions without rainfall. For both cases a constant turbulent friction coefficient was used above a "transitional" Reynolds number. The laminar roughness constant was about 25 for butyl rubber and 100 for rubber roughened with 20 lbs. per square yard gravel. The transition Reynolds number was about 400 for the smooth rubber and 80 for the roughened rubber.

Kinematic wave models have been used to simulate runoff from agricultural areas and found to give satisfactory results. Woolhiser, Hanson and Kuhlman (1970) modeled runoff as beginning under laminar conditions and changing to turbulent flow at a Reynolds number of 300 for a short-grass, grazed prairie. The average value of the parameter k was about 7,000. Langford and Turner (1973) simulated rainfall on a stabilized fallow surface with a friction relationship in the form of laminar-turbulent Manning's n that varied with rainfall intensity. The surface retention showed a hysteresis effect because of changing hydraulic roughness under conditions of rain and no rain. Brakensiek (1967b) depicted a mixed-cover, agricultural watershed in Wisconsin as a distributed system by utilizing a hypsometric curve and contour length-elevation curve. He fitted hydrographs by varying Manning's n and obtained satisfactory results with values of 0.08 to 0.10 for n . These values seem low for an agricultural area. Overton and Brakensiek (1970) also applied the kinematic wave model for a V-shape configuration. They derived a lag time based on watershed dimensions, roughness, and rainfall rate. Their relation between lag time and rainfall rate agreed well with observed data for several events on a Hastings, Nebraska, experimental watershed. A sensitivity analysis showed the solution

more sensitive to errors in rainfall than to errors in averaging geometry and roughness.

2.2 Urban Hydrology

The development of rural areas into urban communities has a significant effect on the hydrologic response because the impervious area is drastically changed and conveyance systems for drainage are often installed. Schulz (1971) summarized the salient features of unit hydrographs generally changed by urbanization--increase of peak discharges, reduction of response time, and reduction of hydrograph base length. Runoff volumes also increase. These changes have been observed since the Nineteenth Century but were not quantitatively investigated until the Twentieth Century. In urban hydrology there is still a shortage of accurate rainfall-runoff field data. Considerable emphasis has been placed on this problem in the last 5 years (ASCE Urban Hydrology Research Council, 1968).

Horner and Flynt (1936) quantitatively studied the runoff from two different city blocks in St. Louis, Missouri. Izzard (1946) studied flow over paved and turf surfaces and in gutters from which he developed some empirical curves to estimate the maximum rate of runoff. Much of the early work in calculating runoff from urban areas was based upon the well-known rational formula. Introduction of the unit hydrograph permitted its use in urban hydrology. A survey of current practicing engineers indicated they use the rational method for areas less than 5 square miles, while larger areas are calculated by the unit hydrograph method (Committee on Flood Control, 1969).

Several "hydrograph" methods, which permit estimation of runoff, have been developed in particular regions of the country. Caution must be used if these methods are applied to conditions that may be different than the ones under which they were derived. The Los Angeles Hydrograph Method, developed by Hicks (1944) for use in southern California, is based upon a substantial amount of data from that region. The procedure uses two methods of computing discharges--the peak-rate method (which is a rational type method) and summing hydrographs (used when the time of concentration exceeds 60 minutes or a flow retention structure is part of the system)(Chow, 1964). Tholin and Keifer (1960) published one of the classic reports on urban hydrology, the Chicago Hydrograph Method. A step-by-step design procedure based upon a unit size of 10 acres was presented. Abstractions from design rainfalls were calculated. Overland flow was computed by Izzard's procedure. Routing through all sewers was done by a time-offset method because of its simplicity. From the storm sewer hydrographs, it was possible to develop a series of design charts for peak discharge based on percent of directly connected impervious area, type of land use, and travel time. The time-offset method of routing in storm sewers is often used. This method seems to give satisfactory results under some conditions, but its limitations have not been fully evaluated. Harris (1970) used a progressive average-lag method for routing in storm sewers. He compared this technique with the method of characteristics for the full dynamic equation of motion. He found a satisfactory comparison of the two methods and thus chose the simplified method; however, this method requires observed hydrographs (at least three) to evaluate the routing constants.

Since the mid-1950's, the Johns Hopkins University has conducted extensive research in storm sewer drainage. An inlet hydrograph method was developed, based on a rational type formula for peak flows and an assumed triangular shape. These hydrographs are summed to obtain the total hydrograph, after each inlet hydrograph is reduced by a factor based on the time characteristics of the event (Viessman and Geyer, 1962). Schaake (1970) applied a kinematic wave model by separating the catchment into segments over which the model parameters were assumed uniform. He presented a technique to compute the kinematic parameter, based upon geometrical characteristics and assumed types of flow for a segment. The model was tested on an 0.4-acre experimental catchment in Baltimore, Maryland. The University of Cincinnati developed a runoff model for urban watersheds (1972). Infiltration on pervious segments was computed by Horton's equation with surface retention estimated by an exponential relationship recommended by Linsley, Kohler, and Paulus (1949); average values for impervious and pervious segments were given if measured data were not available on the watershed. Overland flow was assumed to be turbulent and computed by a storage routing procedure, while gutter flow was computed strictly by continuity and was assumed to occur over relatively short lengths. Sewer routing was performed by undistorted lagging of the inflow hydrograph. This procedure results in higher peaks at later times than more exact methods. The model was applied to a 13-acre watershed in Chicago with satisfactory agreement between observed and computed hydrographs, except on the recession portion.

In 1969, the Denver Regional Council of Governments published an urban storm drainage criteria manual. This manual outlined design requirements for urban storm drainage projects in the Denver region. Rainfall-frequency maps were prepared up to the 100-year return period. The rational formula was used to compute runoff in areas which did not contain storm sewers and were less than 200 acres. The unit hydrograph method was used for areas larger than 200 acres or if storm sewers or channels were present. The manual outlined procedures to estimate the rainfall excess and compute runoff by the rational formula with typical coefficients or from the specified unit hydrograph method.

2.3 Infiltration

Any watershed model simulating runoff from a partially or totally pervious surface must have a means of estimating infiltration. The process of infiltration has remained as one of the most complex problems faced by the watershed engineer. Many methods have been developed for estimating infiltration quantitatively--some empirical and some based on theoretical relationships. Horton's (1940) infiltration equation accounts for the time variability of infiltration. The equation is

$$f = f_{\infty} + (f_0 - f_{\infty})e^{-ct} \qquad (2\text{-}3)$$

where f is infiltration rate at time t; f_{∞} is the steady-state infiltration rate; f_0 is the initial infiltration rate; and c is a parameter related to the soil cover complex.

Philip (1969) developed a theory of infiltration based upon the governing relationship for movement of a fluid in porous media. An algebraic form of his relationship for infiltration from a ponded surface is

$$f = 1/2\ st^{-1/2} + A \qquad (2\text{-}4)$$

where s is the "sorptivity" of the soil, a measure of the influence of capillarity, and A is an approximate value of the steady state infiltration rate. Several empirical methods are merely indices of infiltration and assume a constant loss rate throughout the entire hydrograph. The ϕ Index and W Index are the best known of this type. These indices are best suited for major storms occurring on wet soils or storms when the peak rates and durations occur after infiltration can be approximated as a constant.

The partial differential equation that governs one-dimensional flow of water in an unsaturated porous medium (ignoring air counter-flow) is often referred to as Richard's equation (Smith and Woolhiser, 1971)

$$\frac{\partial(S_a\phi)}{\partial t} = K_s \frac{\partial}{\partial z}\left[K_r \frac{\partial \psi}{\partial z}\right] - K_s \frac{\partial K_r}{\partial z} \qquad (2\text{-}5)$$

where S_a is relative saturation; ϕ is porosity; K_s is saturated conductivity; K_r is relative conductivity; ψ is soil capillary potential; and z is distance below the surface. The solution of this nonlinear differential equation requires a knowledge of the functional relationships among ψ, S, and K_r and the values of ϕ and K_s for a particular soil. Richard's equation can be solved analytically only if severely simplifying assumptions are introduced. The usual means of solution is by finite difference methods. Smith and Woolhiser (1971) used an implicit finite difference method to solve Eq. (2-5) for a wide variety of rainfall rates and initial conditions. These results were summarized by parameteric relations reported by Smith (1972)(discussed in Chapter 3).

2.4 Sensitivity

Sensitivity is a measure of the effect of change in a parameter on a response. The role of sensitivity analysis in hydrologic models is often inherent in models that utilize optimization techniques to fit observed data. A sensitive parameter may converge quickly, while the converse applies to an insensitive parameter.

McCuen (1973) presented a mathematical framework for sensitivity analysis. He gave explicit relationships which can be applied to models if the governing equations can be differentiated. The most common form of sensitivity analysis is by parameter perturbation. One parameter is varied, while the others are held constant and the response to this change is recorded. The means of estimating a response is usually by an objective function. The choice of an objective function is at least partly a subject matter. Ibbitt (1970) presents a review of some of the common objective functions and the features which they emphasize. Probably the most common objective function that is used is the sum of the squared deviations between the observed and computed response. One reason this formulation is used so extensively is that it has some statistical significance for linear systems. The sum of the squared deviations divided by the number of degrees of freedom is the variance of the deviations for linear models.

Dawdy (1969) emphasizes the importance of having model parameters that are physically significant, particularly on urban watersheds where little observed rainfall-runoff data exists and the transferability of a model is essential to usefulness. Lichty, Dawdy, and Bergmann (1968) presented an objective function that was the sum of deviations of the logarithms of observed and computed response with the peak values weighted twice that of the volume. This objective function removes some of the emphasis of the extreme values. The objective function utilized should be related to the goal of the model, i.e., peak-predicting models should emphasize the large flows, while a water quality model needs to predict the total volume as well as the peak rate.

2.5 Summary

This review has provided a limited summary of the development of kinematic wave theory as an appropriate means of computing some categories of gradually varied, unsteady flow. Much of the work discussed referred to laboratory or small scale experiments, but some work has been conducted on small watersheds, either agricultural or urban areas. The extensive research related to kinematic wave theory makes its application to field problems possible. The variety of surfaces and cover conditions to which the kinematic theory has been applied make possible the preselection of approximate roughness factors for a watershed. These factors can be varied to give a better fit to observed data.

There are mathematical watershed models, such as the Stanford Model, that utilize some aspects of kinematic theory plus other mathematical functions to simulate the hydrologic processes for a continuous period of time, generally, for several months or years. The model that is developed in this study is designed to have the capability of predicting storm runoff from agricultural or urban watersheds for discrete periods of time, generally, for several hours to no more than 1 or 2 days.

Chapter 3
MATHEMATICAL MODEL

The model developed herein is classified as nonlinear, deterministic, and distributed. Input to the model is: (1) the hyetograph of precipitation as measured on or near the watershed and is assumed constant over the watershed, (2) the geometry and topography as determined from a map of the area, (3) two parameters, which relate to the surface roughness characteristics and the regime of flow (laminar or turbulent) which would be expected to occur, and (4) infiltration characteristics for pervious areas. The watershed is segmented into a series of planes cascading onto other planes or connected with other planes by channels as shown in Fig. 3-1. The planes

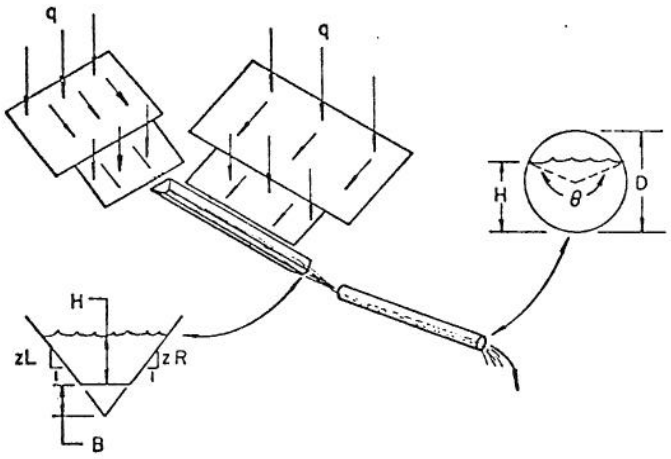

Fig. 3-1 Watershed Represented as a Kinematic Cascade

are either impervious, i.e., streets or parking lots, or are pervious, i.e., rural open areas or lawn areas. The channels are assumed to have either a trapezoidal or circular cross section.

3.1 Surface Water Routing

The governing equations of motion for spatially varied, unsteady flow over a plane surface are derived by applying the principles of conservation of mass and momentum.

Equations of Motion

The one-dimensional continuity equation with lateral inflow is written as

$$\frac{\partial h}{\partial t} + \frac{\partial (uh)}{\partial x} = q \qquad (3\text{-}1)$$

where h is the depth of flow; u is the local average velocity; q is the lateral inflow; x is the distance from the upstream end; and t is time. The momentum equation for one-dimensional gradually-varied, unsteady flow can be written as

$$\frac{1}{g}\left(\frac{\partial u}{\partial t} + u\frac{\partial u}{\partial x}\right) + \frac{\partial h}{\partial x} = S - S_f - \frac{q}{g}\cdot\frac{u}{h} \qquad (3\text{-}2)$$

where g is the acceleration due to gravity; S is the slope of the bed surface; and S_f is the friction slope. These equations for gradually varied, unsteady flow are based on the following assumptions (Yevjevich and Barnes, 1970):

i. The slope of the bed surface, S, is small and is approximately equal to the sine of the angle of inclination.
ii. The flow is one-dimensional so that the vertical components of velocity and acceleration are negligible.
iii. The pressure in the vertical cross section is hydrostatic.
iv. Boundary friction and turbulence can be accounted for by introduction of a resistance term that is the same as at a corresponding uniform flow depth.
v. The velocity distribution in the vertical cross section is the same as the distribution in steady flow.

Each term in the momentum equation corresponds to a component of the energy gradient as

$\frac{1}{g}\frac{\partial u}{\partial t}$, the slope due to the velocity variation with time (acceleration),

$\frac{1}{g}u\frac{\partial u}{\partial x}$, the slope due to velocity variation with distance in the direction of flow,

$\frac{\partial h}{\partial x}$, the slope of the water surface,

$\frac{q}{g}\cdot\frac{u}{h}$, the slope due to lateral inflow,

and S and S_f are slopes as defined previously.

Lighthill and Whitham (1955), Henderson (1963), and Woolhiser and Liggett (1967) have reported on conditions where the gravity and friction components dominate the other terms of the momentum equation. These two components reach an approximate equilibrium so that the momentum equation can be reduced to

$$S = S_f \quad . \qquad (3\text{-}3)$$

This simplification is known as the kinematic wave approximation to the momentum equation.

Kinematic Equations for a Plane

Equation (3-3) can be used to write a parametric equation for the local velocity as

$$u = \alpha h^{N-1} \qquad (3\text{-}4)$$

where h is the local mean depth, and α and N are parameters related to surface roughness and geometry. Chezy's turbulent flow formula is

$$u = C\sqrt{RS_f} \qquad (3\text{-}5)$$

where R is the hydraulic radius and C is the Chezy

friction factor of flow resistance. For planes and wide channels, $R \approx h$. This approximation and the substitution of Eq. (3-3) into Eq. (3-5) results in Eq. (3-4) with $\alpha = C\sqrt{S}$, and $N = 3/2$.

For laminar flow, the Darcy-Weisbach friction factor is

$$f = \frac{k}{R_e} \tag{3-6}$$

where k is a dimensionless friction parameter and R_e is the Reynolds number. The Darcy-Weisbach formula

$$S_f = \frac{f}{4R}\frac{u^2}{2g} \tag{3-7}$$

can be rewritten upon substitution of Eq. (3-3) as

$$S = \frac{f}{8g}\frac{u^2}{h} \quad . \tag{3-8}$$

The Reynolds number is

$$R_e = \frac{uh}{\nu} \tag{3-9}$$

where ν is the kinematic viscosity. Substituting Eq. (3-9) and (3-6) into Eq. (3-8) yields

$$S = \frac{fR_e\nu u}{8gh^2} \tag{3-10}$$

or

$$u = \frac{8gSh^2}{k\nu} \quad . \tag{3-11}$$

Equation (3-11) has the form of Eq. (3-4) with $\alpha = \frac{8gS}{k\nu}$ and $N = 3$.

Equation (3-4) can be substituted into Eq. (3-1) and yields

$$\frac{\partial h}{\partial t} + \frac{\partial(\alpha h^{N-1} \cdot h)}{\partial x} = q \tag{3-12}$$

$$\frac{\partial h}{\partial t} + \alpha N h^{N-1}\frac{\partial h}{\partial x} = q \quad . \tag{3-13}$$

The total differential of $h[x,t]$ is

$$dh = \frac{\partial h}{\partial t} \cdot dt + \frac{\partial h}{\partial x} \cdot dx \quad . \tag{3-14}$$

Equations (3-13) and (3-14) can be solved simultaneously. The matrix form of the equations is written

$$\begin{bmatrix} 1 & \alpha N h^{N-1} \\ dt & dx \end{bmatrix}\begin{bmatrix} \frac{\partial h}{\partial t} \\ \frac{\partial h}{\partial x} \end{bmatrix} = \begin{bmatrix} q \\ dh \end{bmatrix} \quad . \tag{3-15}$$

Equating the determinant of the square matrix to zero defines the path of the characteristic in the x-t plane

$$\frac{dx}{dt} = \alpha N h^{N-1} \quad . \tag{3-16}$$

Substituting the column vector of the right hand side of Eq. (3-15) into the second column of the square matrix and equating the determinant to zero defines the rate of change of depth with respect to time along the characteristic

$$\frac{dh}{dt} = q \quad . \tag{3-17}$$

Equations (3-16) and (3-17) are the characteristic equations. Equation (3-17) can be integrated for constant q, to find the depth along the characteristic as

$$h = h_o + q(t-t_o) \tag{3-18}$$

where h_o is the initial depth at time t_o. The uniform flow equation can be written

$$Q = \alpha h^N \tag{3-19}$$

where Q is the discharge rate. Equations (3-16), (3-18), and (3-19) can be used to compute the entire outflow hydrograph for a single plane segment from a constant lateral inflow rate of q. This development of dimensional kinematic flow equations for a single plane is analogous to the equations for a wide channel and the development for the channels will not be repeated here. Discussion of the equations for a wide channel will follow in a later section.

Finite Difference Method of Solution

Equation (3-13), the kinematic flow equation, can be solved analytically for many initial and boundary conditions, if shocks are not present. Such solutions become cumbersome for realistic situations so it is convenient to use a finite difference method of numerical solution. Kibler and Woolhiser (1970) investigated several different methods of numerical solutions including: (1) an upstream differencing scheme, (2) a four-point implicit scheme, and (3) the Lax-Wendroff explicit scheme. These finite difference schemes were compared with the method of characteristics for evaluation of their performance. The Lax-Wendroff scheme was found to give the most satisfactory results. The method has second-order accuracy but because it is explicit, it requires a limitation of the time step size to maintain numerical stability. The implicit scheme is unconditionally stable which permits fewer time steps than the Lax-Wendroff scheme, but requires an iterative process for solution which under some circumstances may negate the time step advantage. Figure 3-2 shows the notation for the Lax-Wendroff scheme.

The strategy of solving the kinematic equation is to find the depth at the advanced time step, $h[x,t+\Delta t]$, in terms of known values. Expand $h[x,t+\Delta t]$ in a Taylor's series

$$h[x,t+\Delta t] = h[x,t] + \frac{\partial h}{\partial t}\Delta t + \frac{\partial^2 h}{\partial t^2}\frac{\Delta t^2}{2} + 0(\Delta t)^3 \tag{3-20}$$

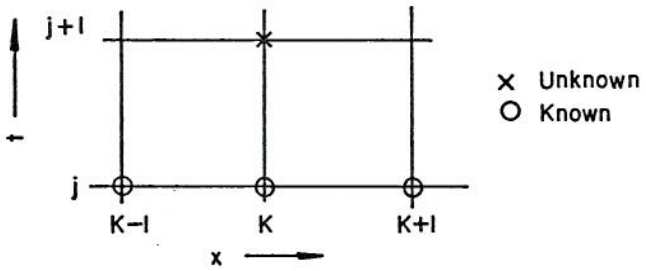

Fig. 3-2 Lax-Wendroff Finite Difference Scheme

where $0(\Delta t)^3$ is the order of the truncation error. Equation (3-12) can be written as

$$\frac{\partial h}{\partial t} = -[\frac{\partial (\alpha h^N)}{\partial x} - q] \; ; \qquad (3\text{-}21)$$

then

$$\frac{\partial^2 h}{\partial t^2} = - \frac{\partial}{\partial t} [\frac{\partial (\alpha h^N)}{\partial x} - q] = - \frac{\partial}{\partial x} [\frac{\partial (\alpha h^N)}{\partial t}] + \frac{\partial q}{\partial t} \quad . \qquad (3\text{-}22)$$

Completing the differentiation with respect to t, Eq. (3-22) becomes

$$\frac{\partial^2 h}{\partial t^2} = - \frac{\partial}{\partial x} [\alpha N h^{N-1} \frac{\partial h}{\partial t}] + \frac{\partial q}{\partial t} \quad . \qquad (3\text{-}23)$$

Now, substitute Eq. (3-21) into Eq. (3-23), then

$$\frac{\partial^2 h}{\partial t^2} = \frac{\partial}{\partial x} [\alpha N h^{N-1} (\frac{\partial (\alpha h^N)}{\partial x} - q)] + \frac{\partial q}{\partial t} \quad . \qquad (3\text{-}24)$$

Equations (3-21) and (3-24) can now be substituted into the Taylor's series expansion which results in

$$h[x,t+\Delta t] = h[x,t] - \Delta t[\frac{\partial (\alpha h^N)}{\partial x} - q]$$

$$+ \frac{\Delta t^2}{2} [\frac{\partial}{\partial x}(\alpha N h^{N-1}[\frac{\partial (\alpha h^N)}{\partial x} - q]) + \frac{\partial q}{\partial t}] \; . \qquad (3\text{-}25)$$

This second order approximation for $h[x,t+\Delta t]$ provides the basis for the Lax-Wendroff finite difference formulation as follows:

$$h_k^{j+1} = h_k^j - \Delta t[\frac{\alpha (h_{k+1}^{jN} - h_{k-1}^{jN})}{2\Delta x} - \frac{(q_{k+1}^j + q_{k-1}^j)}{2}]$$

$$+ \frac{\Delta t^2 \alpha N}{4\Delta x} \{(h_{k+1}^{jN-1} - h_k^{jN-1}) [\frac{\alpha (h_{k+1}^{jN} - h_k^{jN})}{\Delta x} - \frac{(q_{k+1}^j + q_k^j)}{2}]$$

$$+ (h_k^{jN-1} - h_{k-1}^{jN-1}) [\frac{\alpha (h_k^{jN} - h_{k-1}^{jN})}{\Delta x} - \frac{(q_k^j + q_{k-1}^j)}{2}]$$

$$+ \frac{2\Delta x}{\Delta t \alpha N} (q_k^{j+1} - q_k^j)\} \; . \qquad (3\text{-}26)$$

This finite differencing formulation permits the evaluation of depths interior of the upstream and downstream boundaries.

The solution for the entire length of flow can be established when the initial and boundary conditions are established. The initial condition must be specified as

$$h[x,0] \begin{cases} 0 \\ \text{or, for all } x \\ > 0 \end{cases} \; . \qquad (3\text{-}27)$$

The upstream boundary depth is determined by the position of the plane in a cascade. Consider a cascade of planes where i is the order of the plane in the cascade (for the uppermost plane, $i = 1$), ℓ is the length of a plane, and w is the width. Then,

$$h[0,t]_i = \begin{cases} 0, \text{ if } i = 1 \\ f(h[\ell,t]_{i-1}, w_{i-1}, w_i), \text{ if } i > 1 \end{cases} \; . \qquad (3\text{-}28)$$

The discharge from an upper plane is assumed to be modified as the ratio of the upper width to the lower width. The upstream boundary depth for the i^{th} plane which receives inflow from the $(i-1)^{th}$ plane is found by

$$h[0,t]_i = [(Q[\ell,t]_{i-1} \cdot \frac{w_i}{w_{i-1}}) \cdot \frac{1}{\alpha_i}]^{1/N_i} \quad . \qquad (3\text{-}29)$$

Equation (3-29) defines the upstream boundary depth. The downstream boundary depth cannot be obtained from the finite difference scheme because of the nature of the scheme. However, the characteristic equations can be used to obtain the depth at the downstream boundary. Equation (3-18) with $t_o = 0$, can be substituted into Eq. (3-16) to obtain

$$dx = \alpha N (h_o + qt)^{N-1} \, dt \quad . \qquad (3\text{-}30)$$

Integration of this equation yields

$$x = \frac{\alpha}{q}(h_o + qt)^N + c \qquad (3\text{-}31)$$

where c is a constant of integration. At $x = x_o$ and $t = t_o$, the initial location and time, the constant can be evaluated as

$$c = x_o - \frac{\alpha}{q}(h_o + qt_o)^N \quad . \qquad (3\text{-}32)$$

Equation (3-32) can be substituted into Eq. (3-31) with the result

$$x = x_o + \frac{\alpha}{q}[(h_o + qt)^N - (h_o + qt_o)^N] \qquad (3\text{-}33)$$

but because $h = h_o + qt$ and if $t_o = 0$, Eq. (3-33) becomes

$$x - x_o = \frac{\alpha}{q}(h^N - h_o^N) \quad . \qquad (3\text{-}34)$$

Defining $\Delta x = x - x_o$ and solving Eq. (3-34) for h,

$$h = (h_o^N + \frac{q}{\alpha}\Delta x)^{1/N} \quad . \qquad (3\text{-}35)$$

Figure 3-3 shows the path of the characteristic from the NK-1 node to the downstream boundary, node NK.

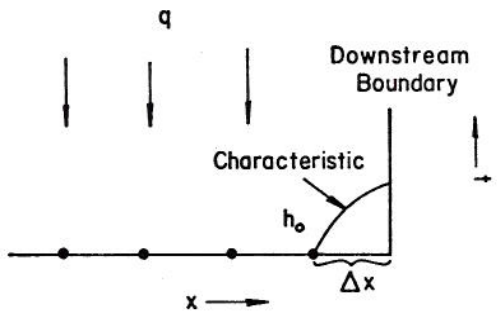

Fig. 3-3 Path of Characteristic at Downstream Boundary

This section has presented a means of routing a lateral inflow over a series of cascading planes using the Lax-Wendroff finite difference scheme for the interior depths with specified initial and upstream boundary conditions. The downstream boundary depth was found by integrating the characteristic equations of the kinematic equation.

Numerical Stability

A disadvantage of the Lax-Wendroff scheme, when compared with the implicit scheme that was analyzed by Kibler and Woolhiser (1970), is that a numerical stability criterion must be maintained, while the implicit scheme is unconditionally stable. A numerically stable finite difference scheme is one that does not allow a small perturbation in the solution to grow without limit until it destroys the calculation. The stability criterion for the Lax-Wendroff finite difference scheme can be derived by an approximate method. For complete details the reader is referred to Kibler and Woolhiser (1970).

The results of this derivation can be summarized by noting the numerical solution, h_k^j, is equal to the true solution, $h(j\Delta t, k\Delta x)$, plus an error term, $\tilde{h}_k^j$, that is

$$h_k^j = h(j\Delta t, k\Delta x) + \tilde{h}_k^j \quad . \tag{3-36}$$

A numerically stable scheme is one in which the ratio of successive error terms is less than or equal to unity, i.e.,

$$|\tilde{h}_k^{j+1}/\tilde{h}_k^j| \leq 1 \quad . \tag{3-37}$$

The stability criterion for this finite difference scheme is

$$\alpha N h^{N-1} \cdot \frac{\Delta t}{\Delta x} \leq 1 \tag{3-38}$$

so that for a fixed length increment, Δt, and the largest depth on the surface at time t, h_{max},

$$\Delta t \leq \frac{\Delta x}{\alpha N h_{max}^{N-1}} \tag{3-39}$$

insures that stability exists at all points on the surface. This method of deriving the stability criterion is only approximate since it is based upon a linear analysis. Presently, there is not a general way of analyzing nonlinear problems for numerical stability. However, Eq. (3-39) does indicate an appropriate time step for the Lax-Wendroff scheme.

3.2 Channel Routing

Free surface flow in channels can be computed using the kinematic approximation to the equations of unsteady, gradually varied flow. The difference between routing runoff over planes and through channels is that upstream inflow to a plane is given in discharge per foot of width of the plane, while upstream inflow to a channel is the total discharge from the previous segment. For watershed area computation, a channel is assumed to have negligible width. Therefore, rainfall does not fall directly onto the channel. The lateral inflow to a channel is the discharge per foot of width received from an adjacent plane.

The two general geometrical shapes that are considered in this study are a trapezoidal and a circular cross-section, as shown in Fig. 3-1. The trapezoidal shape can be used to simulate geometry from nearly rectangular to very broad swale-like channels, including triangular, by specifying the proper geometric parameters. The circular cross-section can be used to simulate the geometry of urban storm drains.

Trapezoidal Open Channels

The continuity equation for a channel with lateral flow is

$$\frac{\partial A}{\partial t} + \frac{\partial Q}{\partial x} = q \tag{3-40}$$

where A is the cross-sectional area; Q is the channel discharge; and q is the lateral inflow per foot of length. Assuming that Q can be expressed as a function of A, Eq. (3-40) can be rewritten in the form

$$\frac{\partial A}{\partial t} + \frac{dQ}{dA}\frac{\partial A}{\partial x} = q \quad . \tag{3-41}$$

A Taylor's series expansion of Eq. (3-41) can be performed analogous to that of Eq. (3-20). (A complete derivation of the finite difference equation will not be carried out here.) The result of the expansion is

$$A_k^{j+1} = A_k^j - \Delta t \left(\frac{Q_{k+1}^j - Q_{k-1}^j}{2\Delta x} - q^j\right) + \frac{\Delta t^2}{2}\left(\left[\frac{\frac{dQ^j}{dA_{k+1}} + \frac{dQ^j}{dA_k}}{2}\right] \cdot \left(\frac{Q_{k+1}^j - Q_k^j}{\Delta x} - q^j\right) - \left[\frac{\frac{dQ^j}{dA_k} + \frac{dQ^j}{dA_{k-1}}}{2}\right]\left(\frac{Q_k^j - Q_{k-1}^j}{\Delta x} - q^j\right)\right)/\Delta x + \frac{q^{j+1} - q^j}{\Delta t}\right) , \tag{3-42}$$

which is the Lax-Wendroff finite difference scheme for a channel with lateral inflow. The kinematic approximation is entered into the calculation through the discharge relationship. If the Chezy formula is used, then

$$Q = \alpha R^{N-1} A \qquad (3\text{-}43)$$

where $\alpha = C\sqrt{S}$; R is the hydraulic radius; A is the cross-sectional area; and N is 3/2. Hydraulic radius is A/P where P is the wetted perimeter. Than Q is related to the cross-sectional area by

$$Q = \alpha \frac{A^N}{P^{N-1}} \quad . \qquad (3\text{-}44)$$

The functional relationship of dQ/dA terms in Eq. (3-42) can be found from the set of geometrical relationships found in Table 3-1.

The downstream boundary solution is found by a first-order finite difference scheme based on Eq. (3-40)

$$A_{NK}^{j+1} = A_{NK}^{j} + \Delta t\left[\frac{q^{j+1} + q^{j}}{2} - \left(\frac{Q_{NK}^{j} - Q_{NK-1}^{j}}{\Delta x}\right)\right] \qquad (3\text{-}45)$$

where the subscript NK denotes the downstream boundary node.

Table 3-1 Elements of a Trapezoidal Channel from Geometry of Fig. 3-1

Geometric or Hydraulic Element	Variable Name	Relationship
Wetted perimeter at depth H	P	B·CO1 + H·CO2
---	CO1	1/ZL + 1/ZR
---	CO2	$\sqrt{1 + 1/ZL^2}$ + $\sqrt{1 + 1/ZR^2}$
Discharge at depth H	GAF(H)	$\alpha(H\cdot CO1\cdot(B+H/2))^N/(B\cdot CO1+H\cdot CO2)^{N-1}$
Area at depth H	AFH(H)	H·CO1·(B+H/2)
---	HF(H)	$(H\cdot CO1\cdot(B+H/2))^{N-1}/(B\cdot CO1+H\cdot CO2)^N$
dQ/dH	DGH(H)	α HF(H)·[CO1·(B+H)·N·(B·CO1 + H·CO2)-(N-1)·CO2·(H·CO1·(B+H/2))]
Depth at area A	HFA(A)	$-B+\sqrt{B^2 + (2\cdot A/CO1)}$
dQ/dA	DGA(H)	DGH(H)/(CO1·(B+H))

Circular Closed Conduits

The problem of routing discharge through circular conduits is important in the urban environment where many watersheds contain storm sewers. The problem can also be extended to those watersheds with combined sanitary and storm sewers. The limitation of the kinematic approximation is that it cannot account for any backwater effect. Any user of this model must apply it cautiously and avoid applications where free outfall conditions do not exist. The conduits are assumed to maintain free surface conditions at all times. This assumption may not deviate from many storm sewer designs because the greatest carrying capacity occurs at about 90 percent of full pipe flow. Fig. 3-4 shows the hydraulic characteristics of a partially full circular conduit. Storm sewer inlets are often designed to intake less than full pipe flow. In many areas the topography is such that runoff greater than the design capacity of sewers can be routed through the gutter system to some lower point on the watershed.

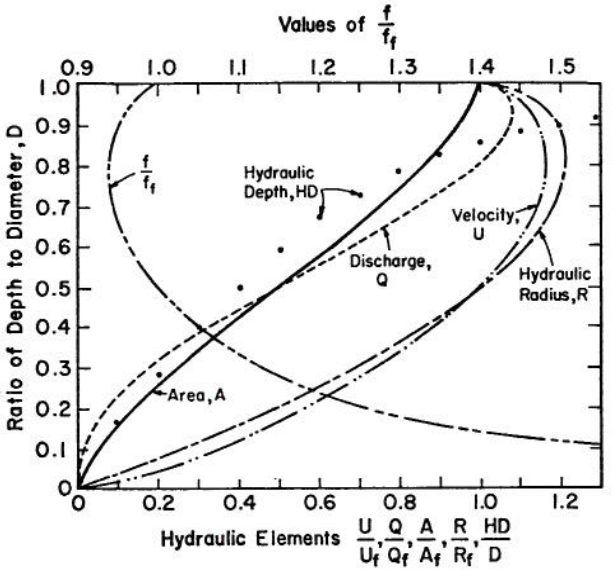

Fig. 3-4 Hydraulic Elements of a Circular Conduit (after Water Pollution Control Fed., 1969)

The equation of continuity for a closed conduit is

$$\frac{\partial A}{\partial t} + \frac{\partial Q}{\partial x} = 0 \quad . \qquad (3\text{-}46)$$

This differs from the open channel equation because lateral inflow is zero for a closed conduit. The input to the channel is at the upstream end either in the form of an outflow hydrograph from a previous channel or conduit or the inlet hydrograph from overland flow. Table 3-2 gives the relationship of several geometric parameters to the diameter of a pipe and the interior angle to the water surface for a circular cross-section as shown in Fig. 3-1. The kinematic assumption of bed slope being equal to the friction slope is entered into the calculation by the parametric relationship for discharge. The most general discharge relationship and the one often used for flow in pipes is the Darcy-Weisbach formula

$$S_f = \frac{f}{4R}\frac{u^2}{2g} \qquad (3\text{-}47)$$

where f is the Darcy-Weisbach friction factor. The kinematic assumption allows substitution of S for S_f into Eq. (3-47) and by solving for velocity, Eq. (3-47) is rewritten as

Table 3-2 Geometric Elements of a Partially Full Circular Conduit from Geometry of Fig. 3-1

Element	Relationship
Depth, H	$D(1 - \cos(\theta/2))/2$
Area, A	$D^2(\theta - \sin\theta)/8$
Hydraulic Radius, R	$D(1 - \sin\theta/\theta)/4$
Wetted Perimeter, P	$D(\theta)/2$
Hydraulic Depth, HD	$D(\frac{\theta - \sin\theta}{\sin\theta/2})/8$

$$u = \sqrt{\frac{8g}{f}\, RS} \quad . \tag{3-48}$$

Discharge is computed using Eq. (3-48) and the cross-sectional area by

$$Q = \alpha \frac{A^N}{P^{N-1}} \tag{3-49}$$

where α is $\sqrt{\frac{8g}{f}}\, S$ and $N = 3/2$. Equation (3-49) is the same as Eq. (3-44) for trapezoidal channels, except for α and geometrical relationships for A and P .

Equation (3-46) can be rewritten as

$$\frac{\partial A}{\partial t} + \frac{dQ}{dA}\frac{\partial A}{\partial x} = 0 \quad . \tag{3-50}$$

This equation is nonlinear, as were the kinematic equations for overland flow and flow in trapezoidal channels. Equation (3-50) is solved by a finite-difference scheme that is different from the Lax-Wendroff explicit scheme previously used. The general form of the numerical stability criterion for explicit finite difference methods is

$$c \frac{\Delta t}{\Delta x} \leq 1 \tag{3-51}$$

where c is the wave celerity. Equation (3-51) is known as the Courant condition. Because the velocities in storm drains can be rather high, the time step required for a specified length increment may be quite small so that stability be maintained. The finite difference scheme used for the evaluation of Eq. (3-47) is a four-point implicit scheme with the form

$$\frac{(A_k^{j+1} - A_k^j) + (A_{k-1}^{j+1} - A_{k-1}^j)}{2\Delta t} + \omega\left(\frac{dQ}{dA}^{j+1} \cdot \left(\frac{A_k^{j+1} - A_{k-1}^{j+1}}{\Delta x}\right)\right)$$

$$+ (1 - \omega)\left(\frac{dQ}{dA}^{j} \cdot \left(\frac{A_k^j - A_{k-1}^j}{\Delta x}\right)\right) = 0 \,, \tag{3-52}$$

where ω is a weighting factor for the space derivative at the current and the past time step. The possible range of values for ω and the importance of it will be investigated in Chapter 5. A property of this implicit scheme is that the value of the unknown, A_k^{j+1} , must be solved by an iterative technique, like Newton's method of finding roots of an equation. Also, a means of evaluating the terms dQ/dA must be established before Eq. (3-52) can be solved. The functional relationship between Q and A depends upon the discharge formula which is used, i.e., Chezy, Darcy-Weisbach, or Manning's equation. It is apparent from Table 3-2 that any relationship between Q and A will involve trigonometric functions. Trigonometric functions are evaluated by a series approximation on a computer, and if evaluated many times, the computational time for a simulation is large. An alternative to this procedure is to create a table of A vs. Q values at the beginning of computations for each circular conduit. For any value of A computed, linear interpolation can be used to find the corresponding Q value. This procedure is used to evaluate dQ/dA .

A method for routing flows through free surface channels has been developed in the past two sections. To apply this method to a specific channel, we need to know the length, slope cross-sectional geometry, and a roughness coefficient for the conduit. With this information, we can compute the outflow hydrograph from a channel for a specified inflow hydrograph.

3.3 Infiltration

Smith (1972) reported on extensive numerical experiments based on Richard's equation for a range of soils from fine clay with swelling properties to a moderately uniform sand. The infiltration model as shown in Fig. 3-5 resulted from analysis of simulation

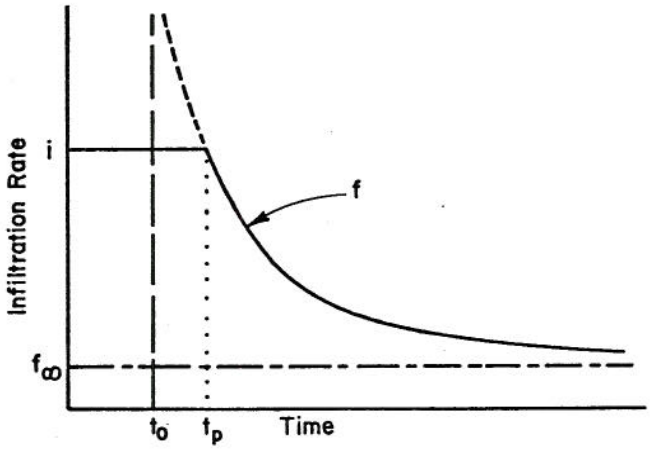

Fig. 3-5 General Infiltration Response Curve (after Smith, 1972)

using a uniform rainfall rate for six soils. Initially, the infiltration rate is limited by the rainfall rate, i . Then, soil surface capillary potential goes to zero and surface runoff begins at the time denoted t_p in Fig. 3-5. This time marks the beginning of the infiltration decay-type function that has the form:

$$f = f_\infty + A(t - t_o)^{-\alpha} \tag{3-53}$$

where f is the infiltration rate; f_∞ is the steady-state infiltration rate; t is time; t_o is the vertical asymptote of infiltration decay function; and A and α are parameters unique to a soil, initial moisture, and rainfall rate.

For instantaneous ponding at $t = 0$, Eq. (3-53) also applies, since this condition represents the case where $i \to \infty$, and consequently $t_o = 0$. Smith found that use of dimensionless variables would result in a single normalized infiltration equation; the dimensionless variables are defined as

$$i_* = \frac{i}{f_\infty}, \text{ dimensionless rainfall}$$

$$f_* = \frac{f}{f_\infty}, \text{ dimensionless infiltration}$$

$$t_* = \frac{t}{T_o}, \text{ dimensionless time}$$

where f, f_∞, i, t are defined previously, and T_o is designated as a normalizing time.

The normalizing time is defined as

$$\int_o^{T_o} As^{-\alpha} ds = f_\infty T_o \qquad (3\text{-}54)$$

where s is the time variable of integration. For sudden ponding, this normalizing time is the time at which one-half of the total accumulated infiltration is due to the constant infiltration rate, f_∞, and one-half of the accumulated infiltration is due to the variable infiltration rate. The solution of Eq. (3-54) is

$$T_o = \left[\frac{A}{(1-\alpha)f_\infty}\right]^{1/\alpha} . \qquad (3\text{-}55)$$

A graphical presentation of T_o, as defined by Eq. (3-54) for a ponded initial condition, is shown in Fig. 3-6. Equation (3-53) which can be normalized

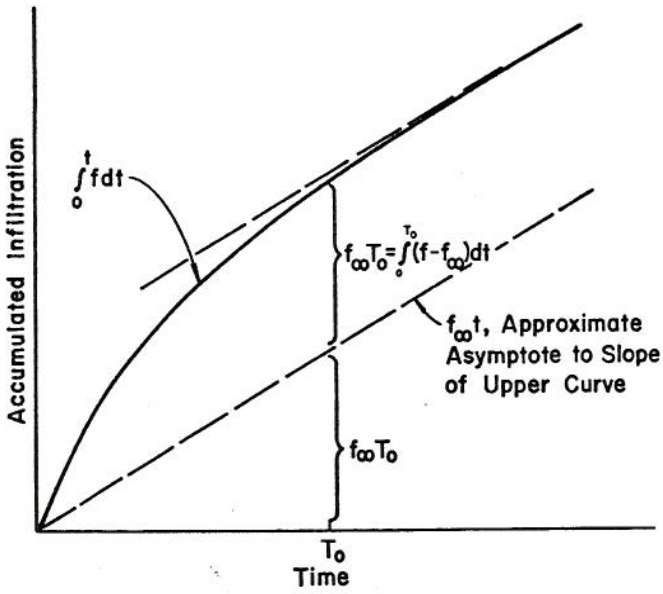

Fig. 3-6 Normalizing Time, T_o (after Smith, 1972)

by using the above dimensionless variables for infiltration and time, results in

$$f_* = 1 + (1-\alpha)(t_* - t_{o*})^{-\alpha} \qquad (3\text{-}56)$$

where A has been incorporated into T_o by utilizing Eq. (3-55).

The value of the non-dimensionalization procedure is that parameter T_o is much more nearly a constant for a wide range of i_* than is parameter A. This is demonstrated in the experimental results of Smith (1972) reproduced in Fig's. 3-7 and 3-8. Clearly the wider variations of A are significantly reduced by using Eq. (3-56) with T_o from Eq. (3-55).

Figure 3-7 shows the variation of T_o with rainfall rate for the six soils that Smith tested. There was very little variation of T_o with i_* greater than 5 for any soil. The loams and clays showed little variation of T_o at any rainfall rate. Figure 3-8 shows the variation of A and α for the soils tested for a range of rainfall rates under constant initial moisture conditions, and indicates that the value of α approaches a constant at higher rates of i_*.

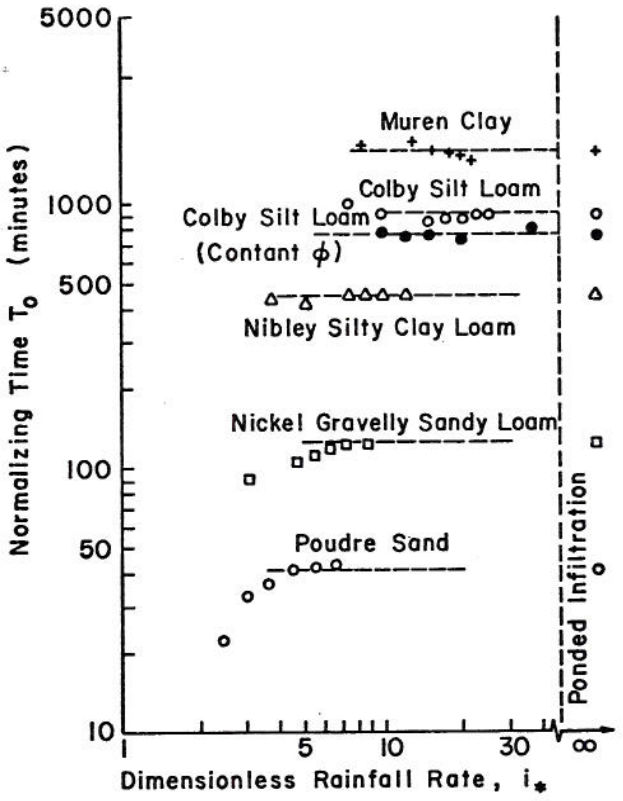

Fig. 3-7 Variation of T_o With Rainfall Rate, i_* (after Smith, 1972)

Use of Eq. (3-56) to describe rainfall infiltration implies determination of four parameters; f_∞,

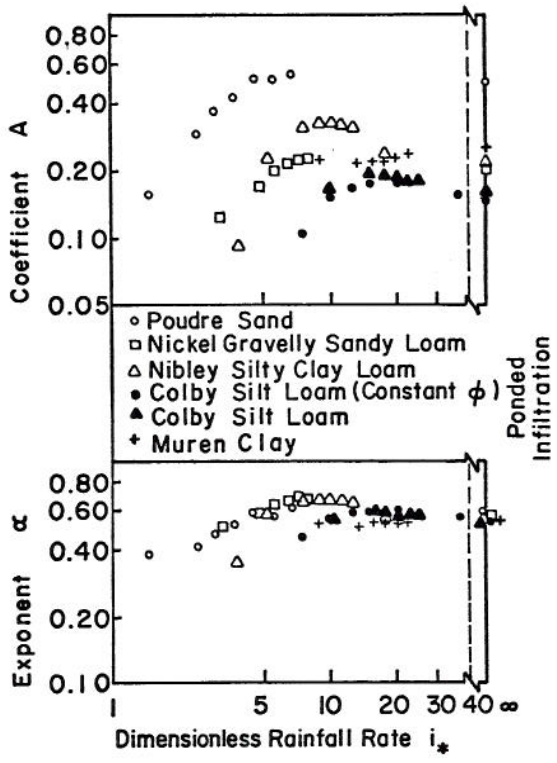

Fig. 3-8 Range of Values for A and α (after Smith, 1972)

α , T_o , and t_{o*} . Alternately, Eq. (3-53) requires values for f_∞ , A , α , and t_o . Appendix A illustrates the estimation of the four dimensioned parameters from infiltrometer data. The term f_∞ is considered a basic soil parameter. Clearly, T_o may be calculated by Eq. (3-55), once A and α are found.

Parameter t_o is related to time of ponding, t_p , which is an important value needed in rainfall infiltration simulation. Clearly, one point on the infiltration curve in Fig. 3-5 is (i, t_p) . Thus, from Eq. (3-53),

$$t_o = t_p - [\frac{A}{i-f_\infty}]^{1/\alpha} \qquad (3\text{-}57)$$

or, in dimensionless terms, from Eq. (3-56),

$$t_{o*} = t_{p*} - [\frac{1-\alpha}{i_*-1}]^{1/\alpha} \qquad (3\text{-}58)$$

Time of ponding has been studied extensively in various approximations and numerical solutions to the basic soil water flow equations (Eq. (2-5)). Smith (1972) demonstrated that an excellent approximation for t_{p*} under a wide range of patterns of $i_*(t)$, $t < t_p$, could be obtained by predicting accumulated infiltration at ponding, F_p . For uniform i_* , F_{p*} is $i_* t_{p*}$, but for any pattern, numerical simulation indicates (Smith and Chery, 1973)

$$F_{p*} = \gamma(i_{p*}-1)^{1-\beta} \qquad (3\text{-}59)$$

Parameters γ and β may be found by logarithmic plotting of F_p vs. $i_{p*}-1$, as shown in Fig. 3-9.

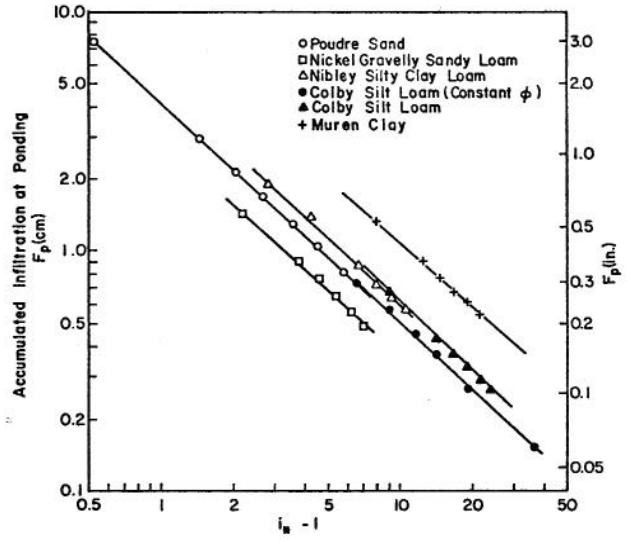

Fig. 3-9 Relation of Infiltrated Volume at Ponding, F_p , to Dimensionless Rainfall Rate i_*

Experiments are required to determine values for γ and β for a particular soil; however, β was found to be very close to 2.0 for six selected soils (Parlange and Smith, 1976). Then, one infiltrometer run could provide data for estimating γ from Eq. (3-59).

A second method to estimate F_p may be taken from Parlange and Smith (1976), who devised a method to predict t_{p*} with only one parameter, which is related by theory directly to soil physical properties. Figure 3-10 indicates a proportionality between $\ln(i_*/i_*-1)$ and F_p . This figure uses the same data (Parlange and Smith, 1976) as Fig. 3-9. In equation form, $F_p \propto \ln(i_*/i_*-1)$. Having determined T_o and f_∞ , we may also write, in dimensionless terms,

$$F_{p*} = B_p \ln(\frac{i_*}{i_*-1}) \quad . \qquad (3\text{-}60)$$

B_p , the dimensionless slope of each line in Fig. 3-10, becomes the dimensionless ponding coefficient, one of the basic infiltration model parameters.

Either Eq. (3-59) or (3-60) may be used to determine t_p for a rainfall pattern composed of rain rate pulses. A simple accounting procedure is used, whereby at the end of the k^{th} rain pulse, the accumulated infiltration is:

$$F_k = \sum_{j=1}^{k} t_j i_j \qquad (3\text{-}61)$$

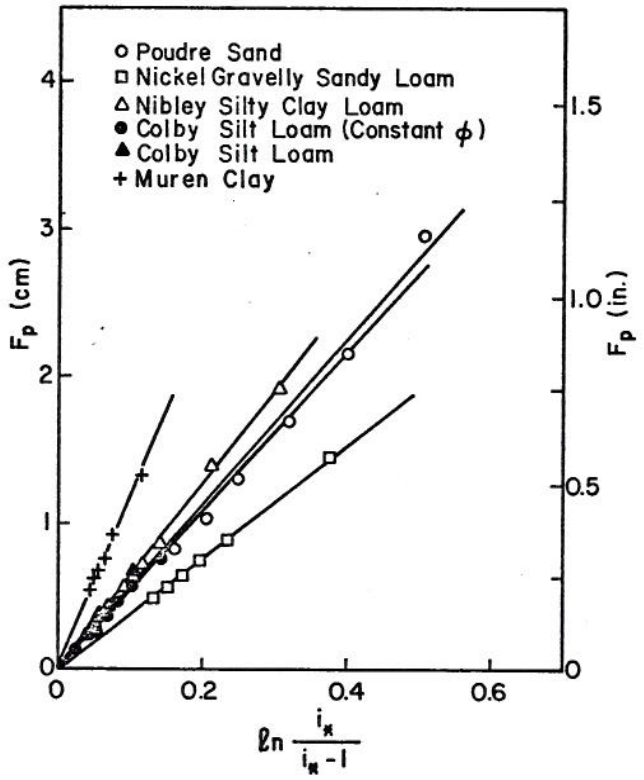

Fig. 3-10 Parlange's Derived Relation Between Infiltrated Volume at Ponding, F_p, and Dimensionless Rainfall Rate, i_*, Demonstrated for Six Soils

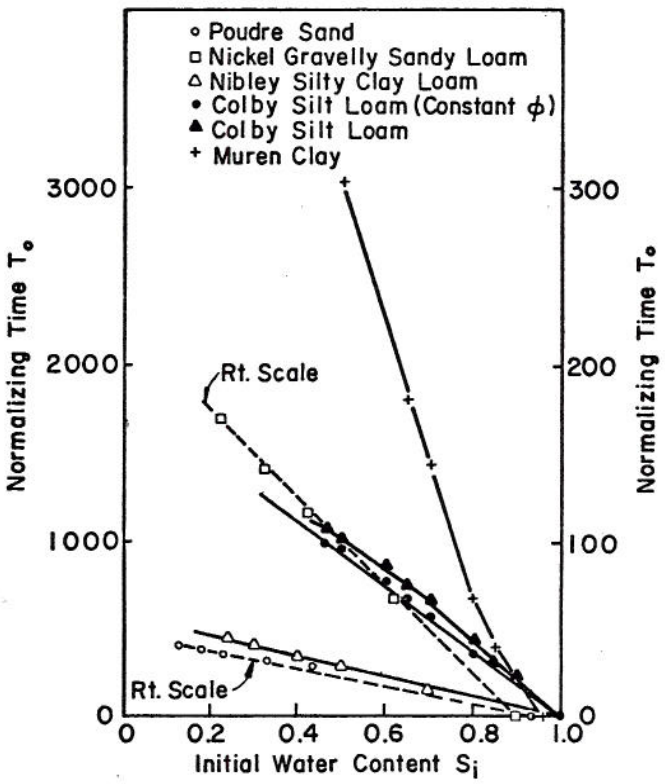

Fig. 3-11 Variation of T_o with Initial Soil Water Content, S_i, (after Smith, 1972)

Ponding occurs when $F = F_p(i_k)$, which may be in the middle of a pulse. Thus, if $F_{k-1} < F_p(i_{k-1})$ but $F_k > F_p(i_k)$, we find $\Delta t = t_p - t_{k-1}$ such that

$$F_{*k-1} + \frac{i_k \Delta t}{f_\infty T_o} = B_p \ln\left(\frac{i_k}{i_k - f_\infty}\right) = F_p(i_k) \quad . \qquad (3\text{-}62)$$

For $t > t_p$, infiltration decay proceeds as for uniform rainfall rate, as long as $i \geq f_\infty$. Having determined t_{p*}, t_{o*} may be determined from Eq. (3-58).

The procedure discussed above permits calculation of infiltration based upon dimensionless Eq. (3-56), under conditions of constant, uniform, initial soil water. To be applicable to most field problems of infiltration, the procedure should have the capability of handling variable initial soil water conditions as well.

Results of numerical experiments, using a wide range of initial relative saturation, S_i, show a nearly linear relationship with the normalizing time, T_o, except for swelling soils, as shown in Fig. 3-11 (Smith, 1972). The data indicate the S_i intercept occurs very close to the maximum relative saturation, S_o, which was 0.90 to 0.95 for the soil data used. Using the linear relationship of Fig. 3-11, T_o can be described as a parameter for a given soil by the equation:

$$T_o = C_1(S_o - S_1) \qquad (3\text{-}63)$$

where C_1 is a constant, to be experimentally determined for each soil. Figure 3-12 illustrates the variation of t_{p*} with initial relative saturation for all soils tested and indicates that a good first approximation for non-swelling soils is to consider <u>dimensionless</u> ponding time, t_{p*}, to be independent of S_i. This results from the variation of T_o with S_i, which scales t_p to account for variations in S_i.

Finally, simulation of infiltration for soils, where the total available pore volume has been reduced by large rocks in the soil (Smith, unpublished) has shown that the basic scaling parameter, T_o, is proportionally reduced by an increasing proportion of rock volume. If we define relative rock content, v_r, as volume of rock per unit volume, we may expand Eq. (3-63) on the basis of numerical simulation with Eq. (2-5), to

$$T_o = C_1(S_o - S_i)(1 - v_r) \quad . \qquad (3\text{-}64)$$

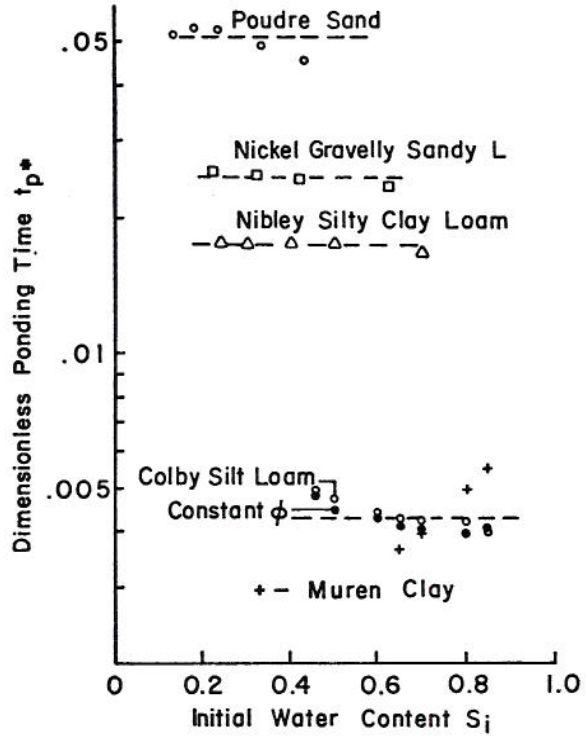

Fig. 3-12 Variation of Ponding Time, t_{p^*}, with S_i (after Smith, 1972)

3.4 Computer Program KINGEN

KINGEN is a computer program based upon the mathematical model developed in this chapter. The model can compute flow for the following geometrical segments: overland flow over a rectangular impervious surface, overland flow over a rectangular pervious surface with an infiltration component to compute rainfall excess, open channel flow in a trapezoidal-shaped channel, and free surface flow in a circular conduit. Watershed geometry is represented by combinations of the segments just mentioned. Computer model parameters are estimated from available information about the watershed. This information may be obtained from topographic maps, aerial photographs, soil surveys, property development records, watershed reconnaissance, or any other source that may contain hydrologic information. Input data are utilized by the computer model to sequentially compute the outflow hydrograph from each segment. The computation begins on the segment at the highest elevation of the watershed and continues down slope to the lowest point on the watershed. Figure 3-13 is a flow chart of KINGEN and provides a brief outline of the computational logic utilized in the model.

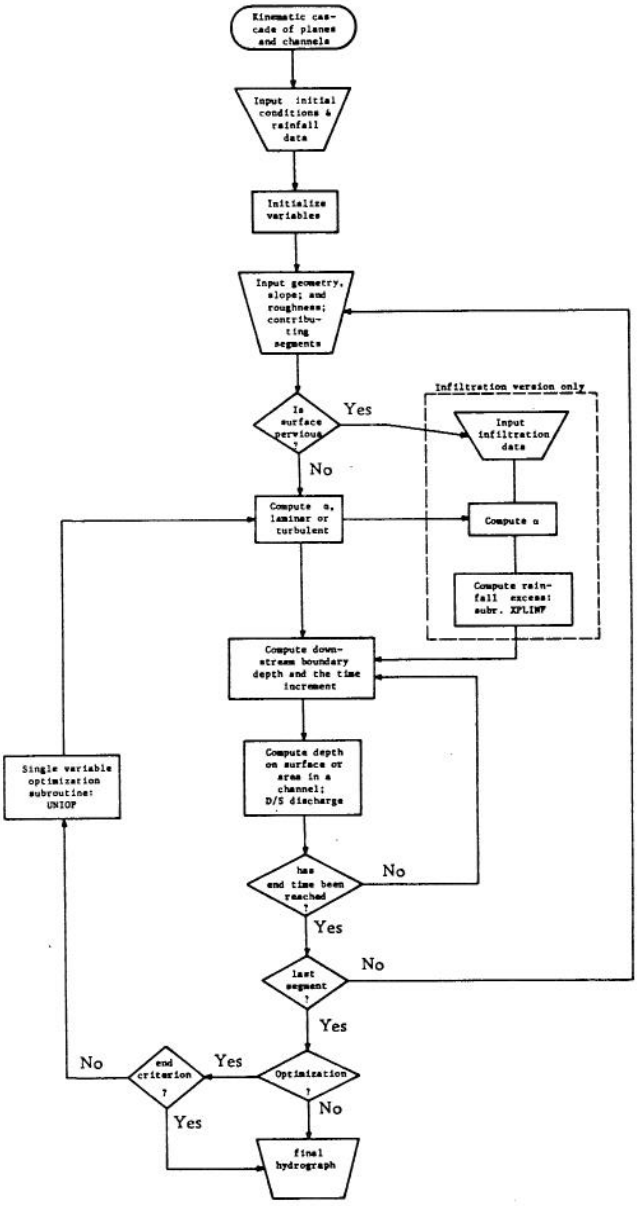

Fig. 3-13 Flowchart of Program KINGEN

Chapter 4
EXPERIMENTAL DATA

The data used in this investigation are from three watersheds: a) the Rainfall-Runoff Experimental Facility at Colorado State University, hereafter called RREF, b) an experimental agricultural watershed at Edwardsville, Illinois, and c) an urban area near Denver, Colorado, that has been selected as an experimental watershed by the United States Geological Survey. These watersheds represent a variety of conditions. The geometry of RREF is simple and the surface is impervious. The agricultural watershed geometry is more complex than the geometry of RREF but although the surface is still relatively uniform, the area is pervious. The geometry of the urban watershed is quite complex and there is a mixture of impervious and pervious area.

4.1 Colorado State University Rainfall-Runoff Experimental Facility

Dickinson, Holland, and Smith (1967) described the original concepts and initial experiments with an experimental watershed composed of two planes contributing laterally to a triangular-shaped channel with a segment of a cone at the upstream end of the channel. Fawkes (1972) gives details of the watershed as it has evolved as shown in Fig. 4-1. The one-half acre watershed is designed to be large enough to avoid the problem of scaling in laboratory hydrologic models but the size is not so large that good control of the input and output cannot be maintained. The simulated rainfall is supplied by a grid of lawn sprinklers supported 10 ft above the surface and centrally controlled for simultaneous operation. The input rate can be varied as 0.5, 1, 2, and 4 in/hr. Since these rates are only approximate, the exact input is calculated by allowing an event to run until an equilibrium discharge is reached. This equilibrium rate is the input rate for a set of partial equilibrium events.

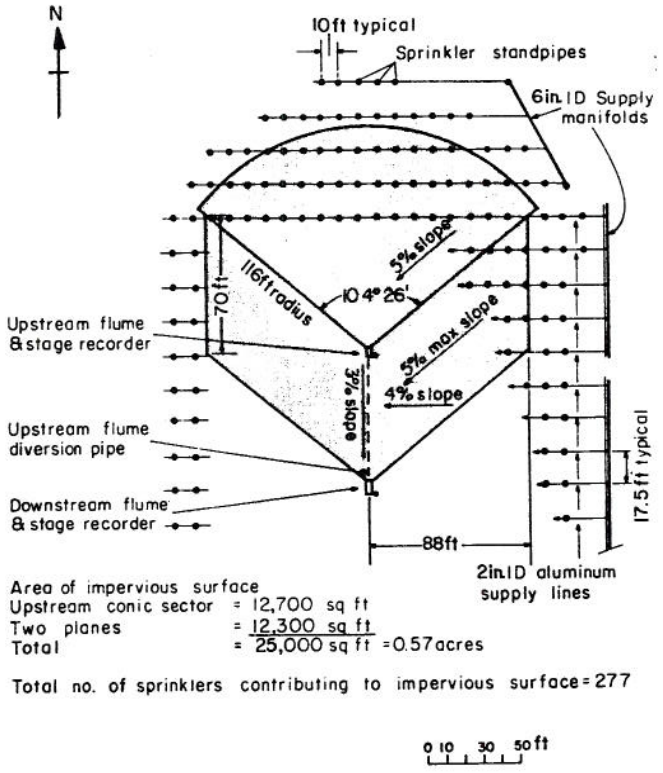

Fig. 4-1 Colorado State University Rainfall-Runoff Experimental Facility (after Fawkes, 1972)

Discharge is gaged by two H-flumes equipped with FW1 water stage recorders. The FW1 recorders have been modified to give a time resolution of 5 sec per smallest chart division. The stage is converted to discharge by the rating curve for the appropriate size flume. Runoff from the watershed can be gaged at two points; discharge from the converging section is measured before it flows into the channel, and the total discharge is measured at the lowest point on the watershed.

The watershed is impervious butyl rubber laid over sand that has been graded to a constant slope of 5% on the converging section, 5% on the planes and 3% on the channel. Experiments have been conducted with the rubber surface or with additional material placed on top of the rubber to increase the resistance to flow. Gravel spread at 0.75 in. uniformly over the surface is the most commonly used material for increasing the surface roughness. Varying densities of gravel as well as different spatial distribution of the gravel on the watershed surface have been used.

4.2 Edwardsville, Illinois, Watershed

From 1940 to 1943, extensive hydrologic field investigations were conducted on several small agricultural watersheds near Edwardsville, Illinois (Holtan and Minshall, 1968)(see Fig. 4-2). These

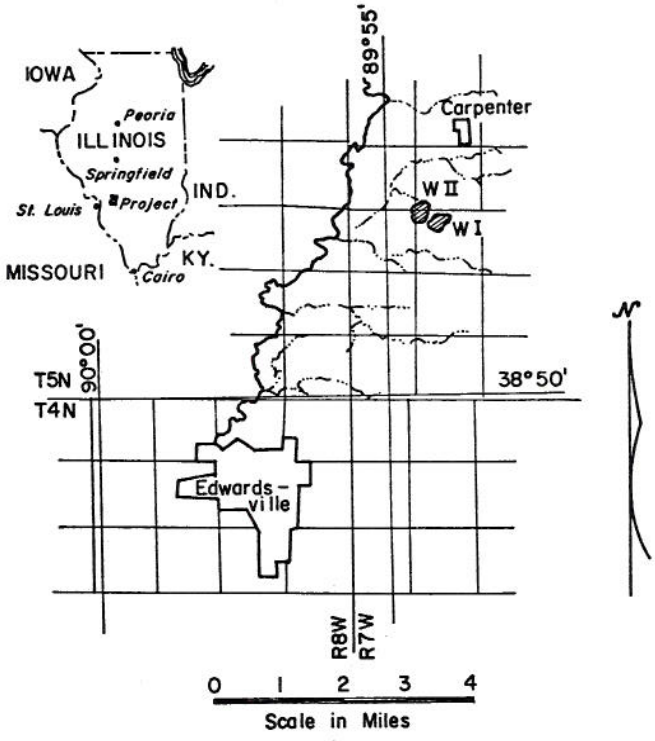

Fig. 4-2 Experimental Watersheds Near Edwardsville, Illinois

watersheds had previously been equipped with rain gages and weirs for recording rainfall and runoff. The investigations recorded information about soil moisture, soil temperature, soil structure, vegetative cover, and infiltration characteristics of test plots. This study is confined to the smallest watershed which is designated W-I, a 27.2-acre fan-shaped area.

Description of the Watershed

Watershed W-I is a cultivated area with a range in elevation of about 20 ft and nearly two-thirds of the area having slope of about 1%, except near the waterways where the slope may be near 10%. There are about 1600 ft of waterways on the watershed, as shown in Fig. 4-3, with average channel slope of about 2%. From 1940 to 1943, the watershed cover was 100% alfalfa (Minshall, 1962). The soils on this watershed are Alma and Bogota silt loams, which are of loessial origin and overlie glacial till with a claypan layer at depths of 10 to 20 in. When these soils are dry and protected with a good vegetative cover, they take in precipitation rapidly until the surface is saturated. After surface saturation, additional precipitation results in a high percentage of runoff. The mean annual precipitation in the area is about 40 in. distributed throughout the year. April, May and June have slightly higher amounts of rainfall than other months. The type of precipitation varies from snow and sleet in winter to short-duration convective thunderstorms in summer. Figure 4-3 also shows a schematic representation of a kinematic cascade model for Watershed W-I.

Infiltration and Rainfall-Runoff Data

The infiltration surveys were conducted using a type "F" infiltrometer on 6- by 12-ft rectangular plots at representative locations over the watershed. Soil moisture samples were taken before each experiment. The simulated rainfall rate was calibrated by measuring the runoff rate from the plot; the infiltration was computed as the difference between the rainfall and runoff rates. This procedure, which neglects the surface storage lag, can lead to errors in computed infiltration rate (Smith, 1976). These infiltration experiments were used to aid in calibrating the infiltration component of the watershed model.

Precipitation was measured with a recording rain and snow gage capable of a time resolution of 30 sec. Runoff from the watershed was measured at the outlet by a 30-in. broad-crested, concrete, weir with a 2:1 side slope continuously monitored with a water stage recorder.

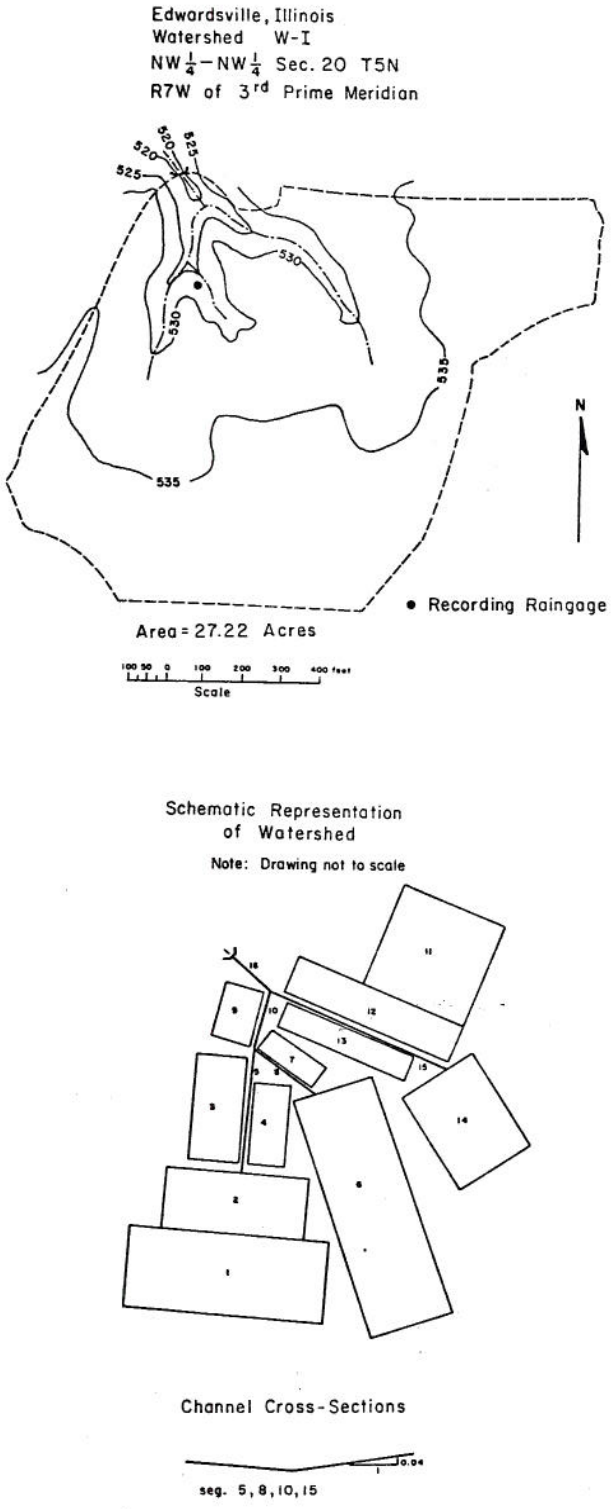

Fig. 4-3 Watershed W-I and Possible Schematization for Input to Program KINGEN

4.3 Urban Watershed near Denver, Colorado

Early in 1968, the U. S. Geological Survey began a cooperative study with the Denver Regional Council of Governments and the Urban Drainage and Flood Control District to collect and analyze rainfall-runoff data from small drainage basins in the Denver metropolitan area. By 1972, 30 urban stations had recorded rainfall-runoff data. These watersheds were selected to provide a wide range of values in drainage area, percentage of impervious cover, slope and length of main channel. This present study is restricted to a single, arbitrarily chosen watershed in Northglenn, a suburb of Denver. Figure 4-4 shows the relative location of Hillcrest Drain, USGS Station No. 06720300. Figure 4-5 is a map of the Hillcrest Drain watershed.

Rainfall-Runoff Data

Detailed records of rainfall and water stage are collected at each station by simultaneous operation of two digital recorders that code data on a 16-channel

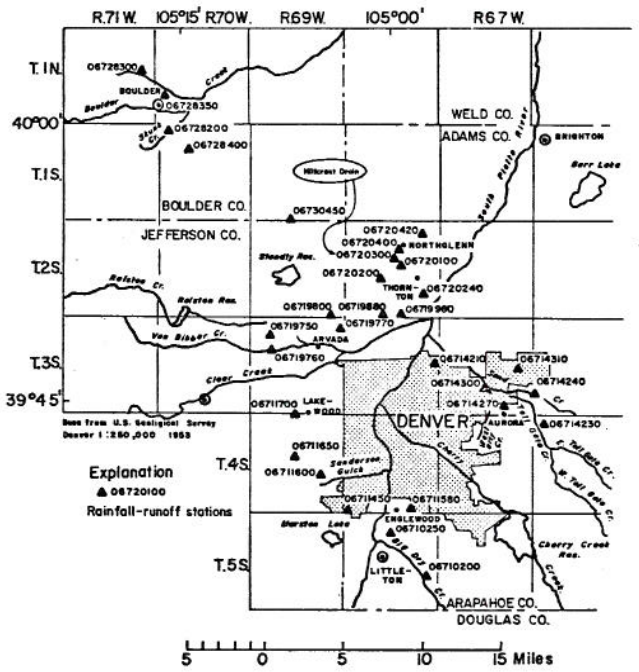

Fig. 4-4 U.S.G.S. Rainfall-Runoff Stations near Denver (after Ducret and Hodges, 1972)

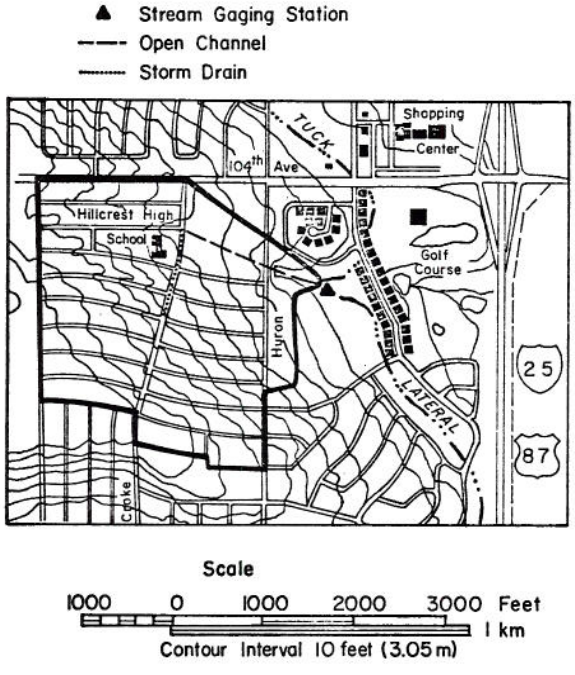

Fig. 4-5 Hillcrest Drain Watershed near Northglenn, Colorado

paper tape at 5-min. intervals. A single timer provides synchronous actuation of both recorders, which eliminates timing discrepancies that may occur when separate timing mechanisms are utilized for two recorders. The stage-discharge relationship at Hillcrest Drain has been determined by the step-backwater method because the flow is controlled by the resistance in the reach of channel downstream from the gage.

The rainfall-runoff data through 1971 from the Colorado small basins were published by Ducret and Hodges (1972). Rainfall is printed as interval depths for time increments of 5 min. or more. The tabulation of precipitation intervals does not begin until the precipitation in a 5-min. interval exceeds 0.015 in. The runoff data are printed as stage height in feet with 10 ft. representing the bottom of the gage; this stage height has been converted to discharge (in cubic feet per second).

Watershed Characteristics

The Denver area has a mean annual precipitation of about 13 in. unevenly distributed throughout the year. Winter precipitation is snow; there is a pronounced rainy season between April and September when most of the rainfall results from short-duration, high-intensity thunderstorms.

The Hillcrest Drain area was rural before 1955. Early development began slowly but during the 1960's, urbanization occurred very rapidly. Figure 4-6 shows

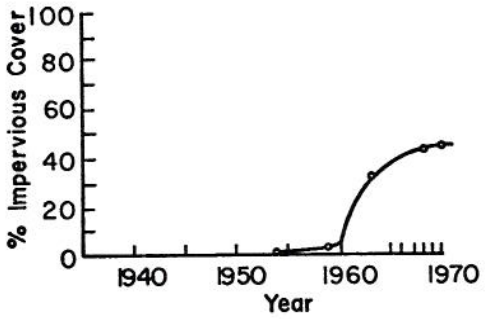

Fig. 4-6 Urbanization of Hillcrest Drain Watershed

the sequential urbanization of the area as measured by the percent of impervious cover on the watershed. The watershed is comprised of single-family dwellings, one school and adjacent grounds plus the playground of another school, and a small area of businesses at the northern edge of the watershed.

The soils on this watershed are Fort Collins clay and clay loam with a moderate to heavy texture. These soils developed from alluvial material carried from the mountains to the west and deposited on top sandstone and shale formations (Harper, et. al., 1932). The soil is well developed and infiltrates water moderately if the surface is protected by a vegetative cover and not compacted. Most of the pervious area is covered with thick bluegrass that is maintained as well watered lawns.

The land surface slopes gradually to the northeast at a 1 to 2% grade. The surface geometry and storm sewer information was obtained from drawings and specifications filed with the city of Northglenn by the developers of the area; the watershed was field-checked to verify the physiographic features.

4.4 Data Evaluation and Limitations

The analysis of data used in this investigation is difficult because each of the three groups of data

has been observed and recorded in a different manner. The two natural watersheds, Edwardsville and Hillcrest Drain, have a common problem that results from observing, or at least reporting the continuous processes of rainfall and runoff by a series of discrete points of time and rate. Use of the RREF minimizes this problem by designing the experiments so that rainfall occurs in discrete pulses.

The timing and variability of natural rainfall is a feature that is difficult to precisely define but is important when a watershed model is used for predicting the runoff. Use of the RREF eliminates some of these problems because the control system is designed so that the beginning and ending of the rainfall or a change in the rate occurs with negligible delay from the system command. The spatial variability of rainfall on the RREF is minimized by having the sprinkler grid properly located and adjusted. The RREF data have been corrected for small discrepancies that may result when the computed rainfall volume is compared with the observed runoff volume. The beginning of rainfall on a natural watershed is often subjectively defined, as is the case of the Hillcrest Drain urban area. The start of rainfall is defined as at least 0.015 in. in a 5-min. period. For example, if a rainfall event begins very slowly, e.g., 0.02 in. in a 10-min. period, this would not be recorded as the beginning of the event, because it is less than the minimum specified amount; however, this 0.02 in. could have a significant effect on infiltration and detention storage in the watershed. If a significant rain pulse begins after the 10-min. interval, the rain gage records this as the beginning of rainfall, instead of the actual beginning 10-min. earlier. The problem of defining the rainfall beginning is not so clear on the Edwardsville watershed because no minimum criterion is stated for the start. Generally, the start is defined by an observer who scans the rainfall record until a response is perceived; this may introduce a bias by the observer. The problem of defining the time rainfall begins can be minimized by selecting a period when most rainfall events begin very quickly with high intensities. This is generally true of convective storms during the summer in both the Edwardsville, Illinois, and Denver, Colorado, areas.

The spatial variability of rainfall over a natural watershed is another problem that can cause difficulties in interpretation. Often, a watershed has no more than one precipitation gage on or near the area. This single point rainfall is sometimes assumed to occur uniformly over the area, whereas, actually, the storm can be moving or changing intensities differently throughout the watershed. Even if more than one precipitation gage is available, it is difficult to determine the area of the watershed that a raingage represents. One means of alleviating the spatial variability problem is to restrict the analysis to small watersheds where the assumption of uniform rainfall is justified. All of the watersheds in this study are less than 180 acres in size.

Discharge measurements can be another possible source of errors for any of the three watersheds in the investigations. However, the RREF and Edwardsville watershed are equipped with a flume or weir that has been laboratory tested and is believed to be accurate within a few percent. The step-backwater rating at Hillcrest Drain may be susceptible to significant errors if good control is not maintained in the measured section. The largest source of error may result from the data being discretized, as is done at Hillcrest Drain for 5-min. intervals. There can be a significant variation of discharge during a 5-min. period.

In the previous section, problems that may exist in the observed data used in this study have been discussed. These possible errors must be considered whenever one attempts to draw conclusions from results that utilize observed data for input to the model, e.g., rainfall, or for comparison to computed results, e.g., outflow hydrograph.

Chapter 5
RESULTS

5.1 Flow Routing in Circular Conduits

The mathematical equations to route flows in an open channel of circular cross section with no lateral inflow were presented in the section on *Circular Closed Conduits*. The parametric equation for discharge was based on the Darcy-Weisbach formula. Many engineers are accumstomed to using Manning's discharge formula for flows in storm sewers. A large portion of published data concerning storm sewers gives Manning's n as the resistance factor. These facts warrant the use of Manning's n for flow resistance in storm sewers in this study. The relationship of f and n is given by

$$f = \frac{8g}{(1.49^2)} \frac{n^2}{R^{1/3}} \qquad (5\text{-}1)$$

Equation (5-1) indicates f varies according to the hydraulic radius for a constant n . Figure 3-4 shows how the ratio of f divided by the full pipe f varies as a function of depth for circular cross sections.

Initial numerical experiments were conducted utilizing a second order Lax-Wendroff finite difference scheme similar to that developed for the trapezoidal channel with the appropriate changes made for circular geometry. The time step for computation was based upon an approximation of Eq. (3-51) and is

$$\Delta t \leq \frac{\Delta x}{dQ/dA} \qquad (5\text{-}2)$$

The experiments indicated that small time steps were required to maintain stability for gradually varied flow of small magnitude. Large flows would have required very small time increments and made the computational cost of calculating flows too high for practical use. The decision was made to test an implicit finite difference scheme so that the problem of small time steps could be eliminated. The four point implicit scheme was presented in the section on *Circular Closed Conduits* and is illustrated in Fig. 5-1. The

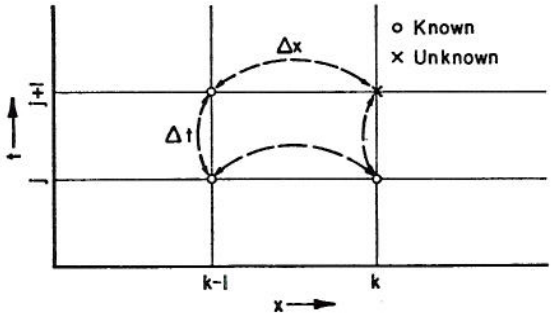

Fig. 5-1 Implicit Finite Difference Grid

figure shows the point at which the value for cross sectional area is unknown. The dashed arrows show the pairs of nodal points that are used when computing derivatives in the time and space directions.

The kinematic wave-routing technique was tested on data published by Harris (1970). Harris developed a computer program to route flows through storm drains using the method of characteristics to solve the complete equations of continuity and momentum. This program was verified utilizing data from tests conducted at Colorado State University on a 3-ft. diameter pipe, 824 ft. long. The program accurately reproduced the measured flows. The shortcomings of the method of characteristics is the relatively large computational time and computer storage required. Harris needed a method to route flows in real time, i.e. while the event was still occurring, on a small computer. He concluded that the method of characteristics did not meet his requirements. However, the method of characteristics did provide an accurate method with which Harris could verify simplified methods. In this study, the results of the method of characteristics as developed by Harris also serves as the criterion to evaluate the performance of the kinematic flood routing model. Harris conducted some numerical experiments with a circular conduit with the following characteristics:

Pipe diameter = 6 ft.
Length = 14,000 ft.
Slope = 0.001%
Manning's n = 0.012

The variable ω of Eq. (3-52) was defined as a weighting factor for the space derivatives and acts as a damping coefficient. It can theoretically have a range of values from 0 to 1. However, for $\omega < 1/2$ the scheme is unstable. When $\omega = 1/2$ equal weight is given to the space derivatives at time levels j and j + 1 . This value of ω corresponds to no damping being introduced from the finite difference scheme; however, some artificial damping may be beneficial when using a finite difference scheme. Figure 5-2 illus-

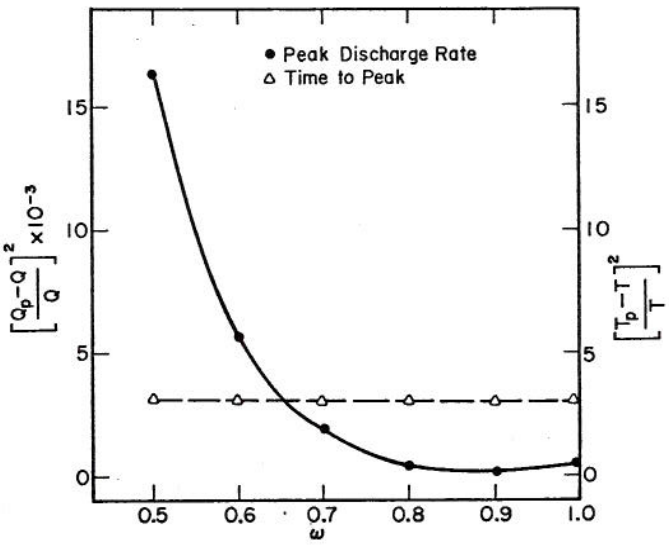

Fig. 5-2 Variation of Peak Discharge and Timing with Weighting Factor, ω

trates the effect of a variable ω on peak discharge and the timing of the peaks. The computed peak discharge and time to peak are denoted Q_p and T_p ,

respectively, and the observed peak discharge and time to peak are denoted Q and T, respectively. The minimum value of the deviation in discharge is about $\omega = 0.9$, but within the range $0.7 \leq \omega \leq 1.0$ the deviation is very small and not sensitive to the value of ω. As ω approaches 0.5, the deviation increases rapidly. The artificial damping effect of ω can often be used beneficially to suppress the minor perturbations that may be introduced into the computation due to the numerical scheme. Precaution must be observed when ω is allowed to approach the value of 1, because the resulting damping may be sufficient to obscure a feature of the model that could be important in the calculated flows. Figure 5-2 shows that the deviation in timing of the peak is not affected by variation of ω. This relationship of timing and ω is the condition that is expected because ω influences only the space derivative and not the time derivative.

Figure 5-3 shows the results of sensitivity tests of the time increment, ΔT, and the length increment,

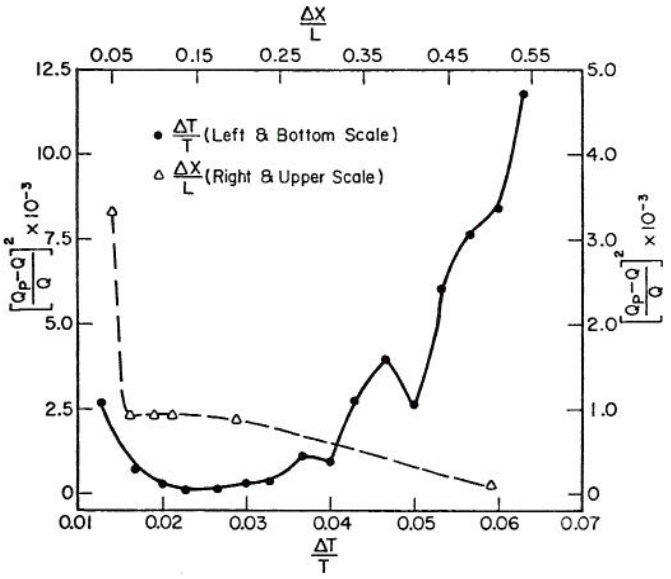

Fig. 5-3 Variation of Peak Discharge with Length and Time Increments

ΔX. Because the finite difference scheme is implicit, the ΔT is specified and not changed through the flow computation. The results indicate that for $\Delta T/T$, where T is the total duration of the event, in the range of values 0.01 to 0.05, the peak discharge is not very sensitive. However, for values of $\Delta T/T$ greater than 0.05, the peak response is sensitive to the time increment. Choice of a ΔT increment should be related to the time characteristics of the system response. If the inflow hydrograph varies significantly during a period of time, the model time increment must be capable of accounting for the variations. The results of tests on the length increment indicate that it is not necessary to choose very small ΔX increments; in fact, the smallest ΔX tested resulted in the largest error.

Hydrographs computed with the kinematic routing technique were compared with Harris' numerical experiments. Figures 5-4a, b and c show the results of routing three inflow hydrographs through the circular

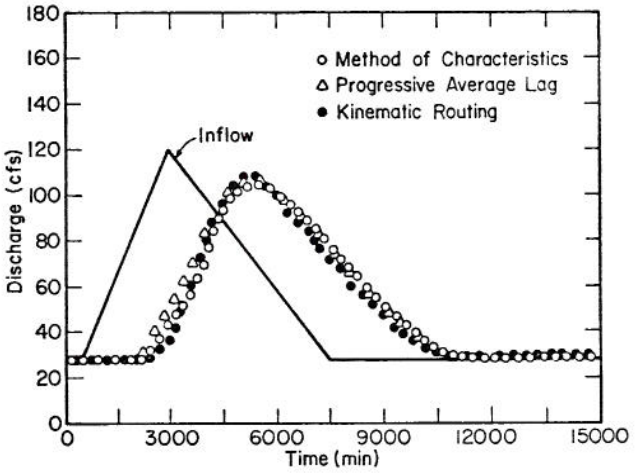

Fig. 5-4(a) Comparison of Flow Routing Techniques for Circular Conduits

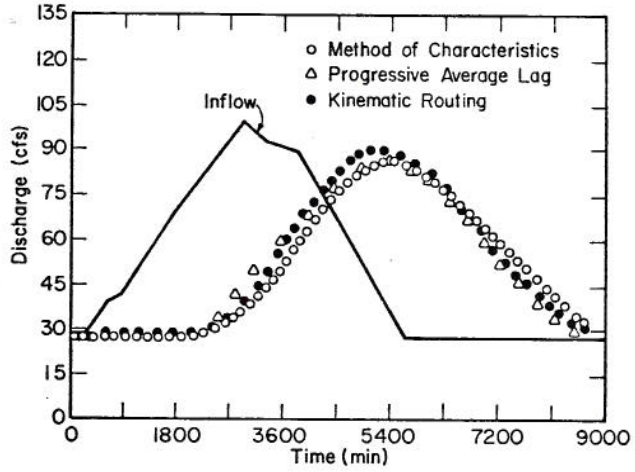

Fig. 5-4(b) Comparison of Flow Routing Techniques for Circular Conduits

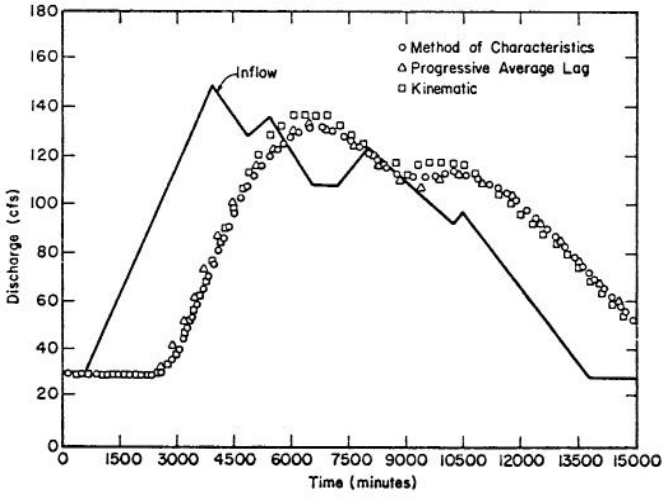

Fig. 5-4(c) Comparison of Flow Routing Techniques for Circular Conduits

conduit previously described in this section. The kinematic hydrographs fit the hydrographs computed by the method of characteristics very well. It is shown that kinematic routing consistently overpredicts the peak discharge by a small amount and slightly underpredicts the recession hydrograph. Harris' simplified routing technique, called progressive-average lag, is also plotted in Fig. 5-4a, b, and c. This technique uses a group of averages of the inflow hydrograph to offset and reduce the upstream input. The kinematic routing and progressive-average lag technique compare very closely at most points on the hydrograph. The advantage the kinematic technique has over the lag technique is the kinematic routing, based upon the hydraulics of the flow, while the lag routing requires at least three observed hydrographs to calibrate routing constants.

In this section, a kinematic routing procedure for flows in circular conduits has been analyzed. The technique was shown to give good results as compared with a routing technique using the method of characteristics to solve the complete equations of continuity and momentum. The kinematic routing procedure has the advantage over a simplified lagging technique in that kinematic routing can be used for design studies in areas without data because no historical hydrographs are required to evaluate any routing constants as is required for the lagging technique.

5.2 Incorporation of Infiltration Component

Smith's (1972) infiltration model was presented in Section 3.3. A computer subroutine, called XPLINF, based upon the mathematics of that section was developed by Smith, modified, and incorporated with the kinematic surface runoff model, KINGEN. Infiltration rate is computed in the XPLINF algorithm, with rainfall assumed to be constant over the time interval. Rainfall excess, the difference between precipitation and infiltration, is provided interactively to each node of the surface runoff component. A few modifications have been made to the original infiltration model to reduce computation time.

The original method of finding the time to ponding was to iterate through the rainfall hyetograph by some small time step until the accumulated rainfall volume equalled or exceeded the infiltration volume, predicted by Eq. (3-61). A modification to the subroutine was made so that Eq. (3-62) is now used to solve for the time to ponding. If Δt_k exceeds the length of the k^{th} rainfall increment, the infiltrated volume is increased by the amount of accumulated rainfall for the k^{th} increment and Eq. (3-62) is solved for the $(k+1)^{th}$ increment. These steps are repeated until the time to ponding is found.

The infiltration subroutine was also modified so that it would not be necessary to compute infiltration at each time interval required to maintain numerical stability for surface routing. Figure 3-5 shows how the infiltration rate changes rapidly just after time t_p but then the rate of change of the infiltration rate decreases and ultimately approaches zero as the steady-state infiltration rate, f_∞, is approached. The shortest time intervals to compute infiltration should occur just after t_p with the time intervals increased as f_∞ is approached. However, the time interval computed by the surface runoff component has the opposite proportionate size as required for the infiltration component. At t_p, runoff begins but the depth on the surface is quite small and, consequently, a rather large time-interval is calculated. As the infiltration rate decreases, the lateral inflow increases, resulting in an increase of the depth. This increase results in a smaller time interval being required to maintain numerical stability. The dilemma of the conflicting time intervals for the surface and infiltration components is solved by developing an empirical time interval as defined by

$$\Delta t = CF(TI_i - TI_{i-1}) \left(\frac{f_\infty}{f}\right) \qquad (5\text{-}3)$$

where CF is a coefficient greater than unity; TI is the time at the beginning of a rainfall increment; f is the infiltration rate for the past time interval; and f_∞ is the steady-state infiltration rate. Equation (5-3) defines a time increment that is small when f is large in comparison with f_∞ but as f approaches f_∞, the time increment increases. The range of values of the coefficient CF that have been used in this study are from 1.25 to 3.0. The lower value corresponds to studies on one or two planes, while the higher value corresponds to complex geometry of a cascade of multiple planes and channels. Figure 5-5 shows

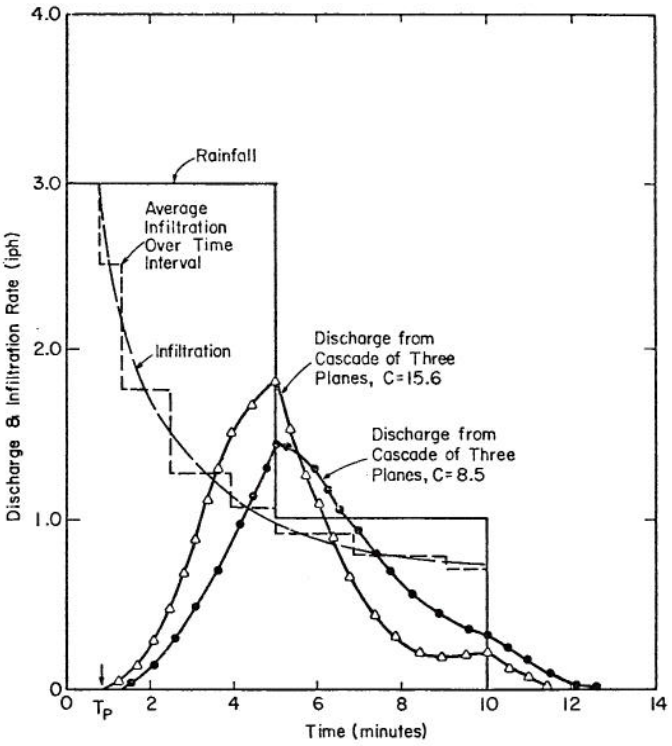

Fig. 5-5 Infiltration and Runoff from a Pervious Plane

an example of pulsed rainfall input onto a cascade of three infiltrating planes, the infiltration function and the resulting outflow hydrograph from the rainfall excess. Besides the continuous infiltration function, Fig. 5-5 shows the step-like function of infiltration that results when the subroutine XPLINF is called once for each time interval as defined by Eq. (5-3). Two outflow hydrographs are shown where one is the response to the rainfall excess routed over a smooth surface

with a Chezy coefficient of friction, C = 15.6 . The other hydrograph is the response to the rainfall excess routed over a roughened surface with a Chezy C = 8.5 . These two hydrographs demonstrate how the response is related to the surface characteristics and also the infiltration characteristics.

Testing the Infiltration Model

The infiltration component was tested on some infiltrometer experiments from the Edwardsville, Illinois, watershed described in Section 4.2. Recorded data from the infiltrometer experiments along with a soil survey of the watershed were used to estimate the model parameters. The Alma and Bogota silt loams of the watershed corresponded closely with the Colby silt loam (constant ϕ) with which Smith (1972) conducted experiments. Table 5-1 lists the values of the

Table 5-1 Infiltration Parameters of Edwardsville Infiltrometer Tests

Parameter	Value of Parameter
α	0.58
γ	0.90
S_o	0.95
C_i^*	Estimated from infiltrometer experiment
S_i	do.
f_∞	do.

*this constant is related to the normalizing time by Eq. (3-63)

model parameters as estimated from Smith's work. The normalizing time for each infiltrometer test was estimated by the technique illustrated in Fig. 3-6 of plotting the accumulated infiltration vs. time. The normalizing time is then estimated from the plot to be that time at which half of the total infiltration volume is due to f_∞ and half to the variable infiltration rate. The parameters S_i and f_∞ were measured directly for each infiltrometer experiment. Figures 5-6 to 5-8 show the computed and observed results of the infiltrometer tests. The infiltrometer tests show a wide range of infiltration responses. The slope of these plots varies from 11% to less than 1% and seems to affect infiltration rates. Plots 1 and 2 have the highest slope and the lowest minimum infiltration rates. It would have been possible to obtain a much better fit of the observed hydrograph for individual experiments by adjusting for hydrograph lag or by optimizing the infiltration parameters. However, the primary objective was to test the infiltration component of the model using only a priori information that was obtained from soil characteristics and field tests.

Infiltration Sensitivity

The sensitivity of the infiltration component was analyzed by a series of tests utilizing parameter perturbation. So that errors in the data did not influence the tests, the "observed" response was generated by the model for a selected set of parameters. The parameters were then varied about the original set. The "observed" parameters are given in Table 5-2. The

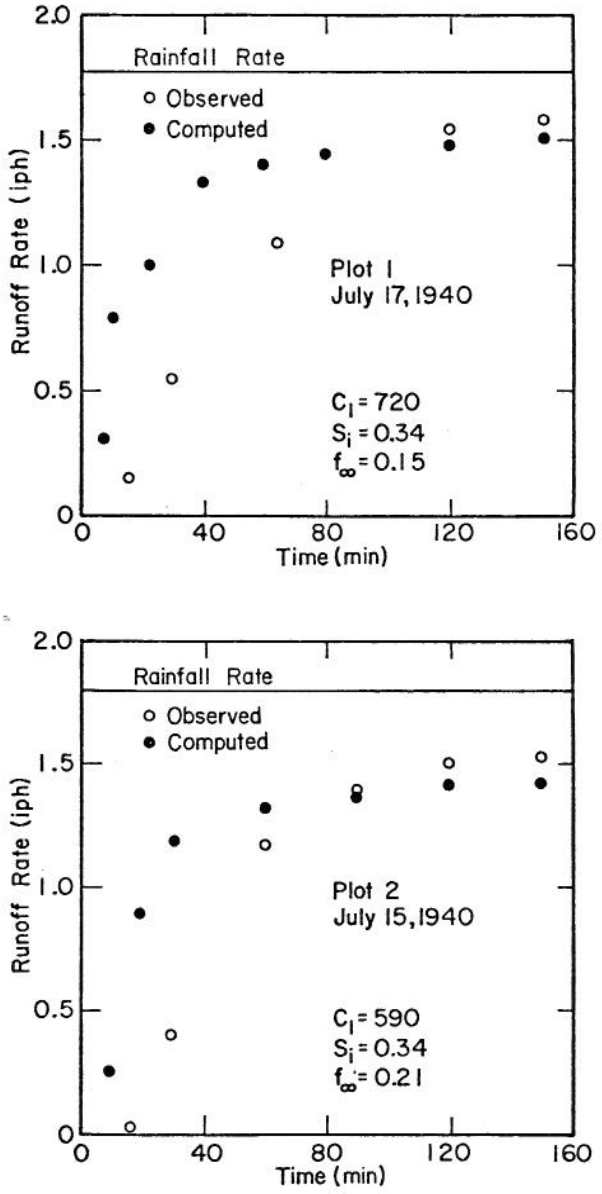

Fig. 5-6 Plots 1 and 2 Infiltrometer Tests

value of S_o has been held constant at 0.95 throughout this analysis. The results of the sensitivity analysis are presented in Figs. 5-9 and 5-10.

The objective function for the sensitivity analysis is

$$O.F. = \left(\frac{F-F_p}{F}\right)^2 \qquad (5\text{-}4)$$

where F is the total "observed" accumulated infiltration and F_p is the predicted infiltration. This objective function was compared to the sum of deviations for a set of points along the entire infiltration curve. The distribution is similar, except the magnitude is different. Therefore, the simpler objective function is used. The "O" subscripted parameters in Figs. 5-9 and 5-10 refer to those values

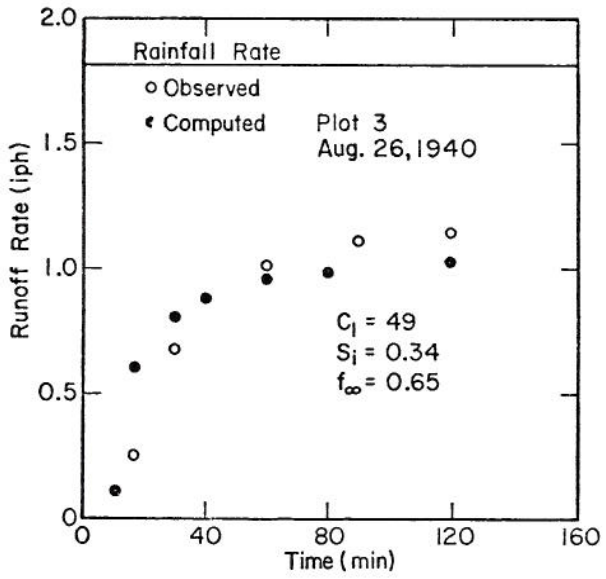

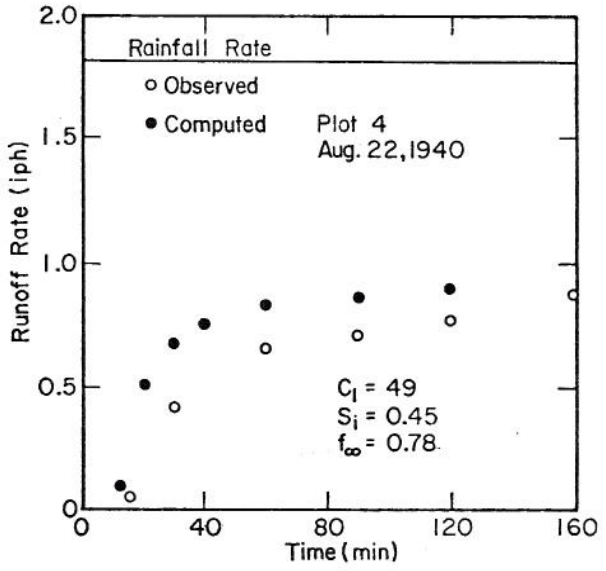

Fig. 5-7 Plots 3 and 4 Infiltrometer Tests

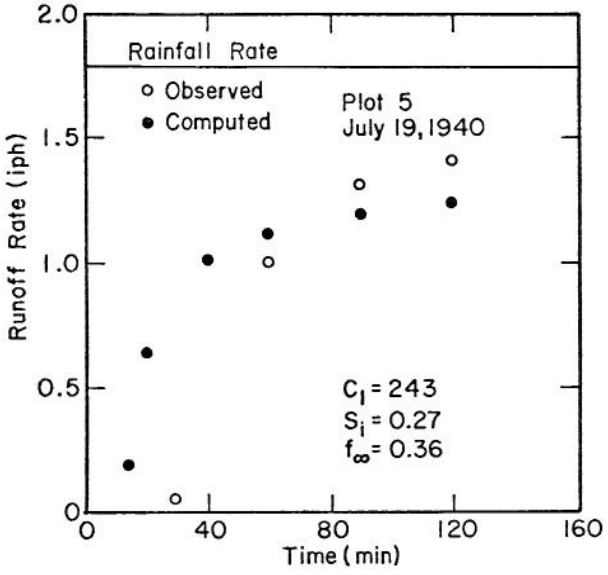

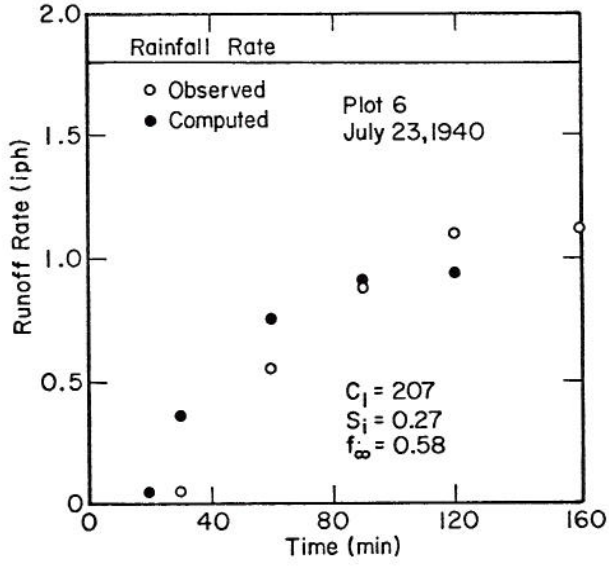

Fig. 5-8 Plots 5 and 6 Infiltrometer Tests

Table 5-2 "Observed" Infiltration Parameters for Sensitivity Tests

Parameter	Value of Parameter
α	0.58
γ	1.35
C_l	873
S_i	0.50
f_∞	0.40

from Table 5-2. Figures 5-9 and 5-10 are arranged so that each succeeding figure has the normalized deviation scale reduced by a factor of 10 from the previous figure. From these plots, one concludes that minimum infiltration is the most sensitive parameter for infiltration with the initial water content and the constant relating water content and normalizing time being somewhat less sensitive. The most sensitive parameters are fortunately those that have the most physical significance and can be estimated from field experiments if they are available. The parameters α and γ are the most difficult to estimate from field measurements but also least affect the computed infiltration.

5.3 Testing the Watershed Model

The previous two sections of this chapter have involved the development and verification of components of the computer model. These components have been incorporated with the surface water model and

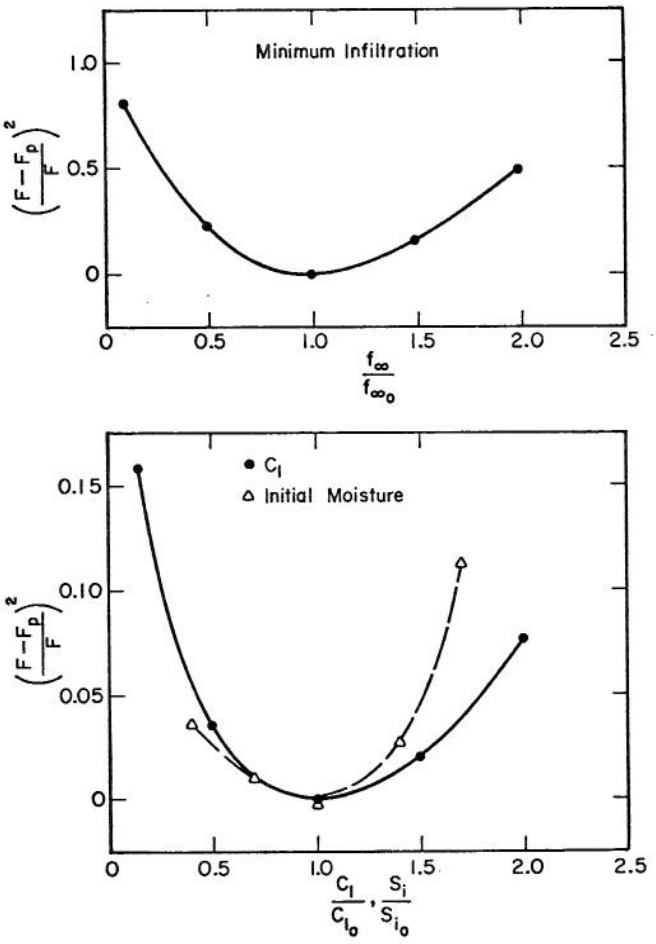

Fig. 5-9 Infiltration Sensitivity of f_∞, C_l and S_i

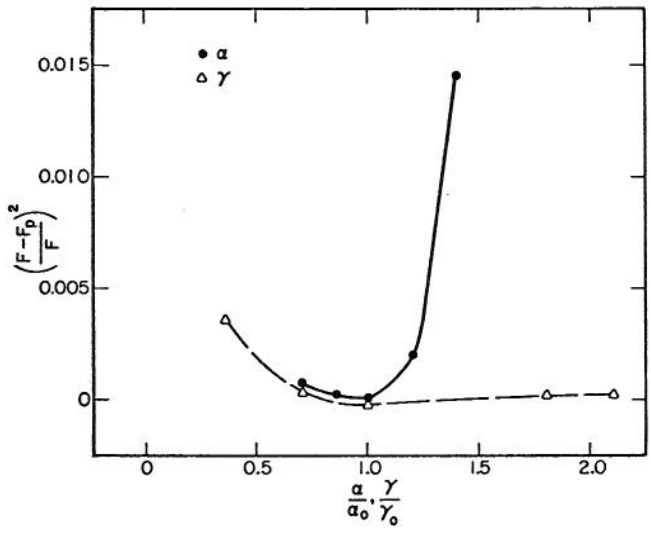

Fig. 5-10 Infiltration Sensitivity of α and γ

together they form a complete watershed model of rainfall and associated runoff. The remainder of this chapter is devoted to testing the model on several experimental watersheds that vary in surface characteristics, pervious and impervious areas, and degree of precision with which the rainfall-runoff process is measured.

Colorado State University Rainfall-Runoff Experimental Facility

Past studies of the data from this facility have concentrated on the upstream conic section that accounts for slightly more than half the area. This study is concerned with analyzing data for the entire watershed so that the composite effect of a conic section, planes, and a triangular-shaped channel can be studied. Simulation tests were conducted on two types of surface configurations, a butyl rubber surface over the entire watershed and a butyl rubber surface covered with 20-lb. of gravel/yd^2 over the lower one-third of the conic section and one-third of the two planes. The conic section was represented by a series of cascading planes. Kibler and Woolhiser (1970) present a procedure to determine the appropriate width of planes to approximate a conic section while maintaining the correct area.

The first hypothesis to be tested is that a constant friction relationship is sufficient to describe the flow regime. Detailed investigations of the mechanics of overland flow (Woo and Brater, 1962; Yu and McNown, 1964; and Fawkes, 1972) indicate that flow begins as laminar and then becomes turbulent as the Reynolds number increases. Thus, a more precise friction relationship would be variable, with the highest roughness when depth is small and roughness decreasing as the depth of flow increases. However, the hypothesis of constant friction is formulated on the assumption that the composite geometry and finite difference approximation would mask the laminar-turbulent effect. A constant value for the Chezy C friction coefficient was obtained from Singh's (1974) study of the data from the RREF. He obtained values for the kinematic wave coefficient α by optimizing on the peak discharges for rainfall-runoff events from the conic section. Values of α were obtained for each event. Average α's for a set of events from the same surface configuration were used to estimate a constant friction factor. Chezy's C was obtained by relating α and C by the equation

$$C = \frac{\alpha}{\sqrt{S}} \quad . \tag{5-5}$$

After the initial runs were made, the conclusion was drawn that a constant friction factor was adequate to match peak rates but in some cases the rising limb of the hydrograph was not well simulated. The results of some of these tests are presented in Figs. 5-11 and 5-12.

An alternative to the constant friction relationship is one of the types of variable friction laws used by Fawkes (1972) on the CSU facility. This type of friction relationship accounts for laminar-turbulent flow regime and also has the capability of accounting for flow resistance due to the impact of rain drops on the surface. Figure 5-13 shows the variable friction relationship. The parameters of the friction relationship are k, a constant; R_{e_T}, a transitional Reynolds number; and IC, an intensity coefficient.

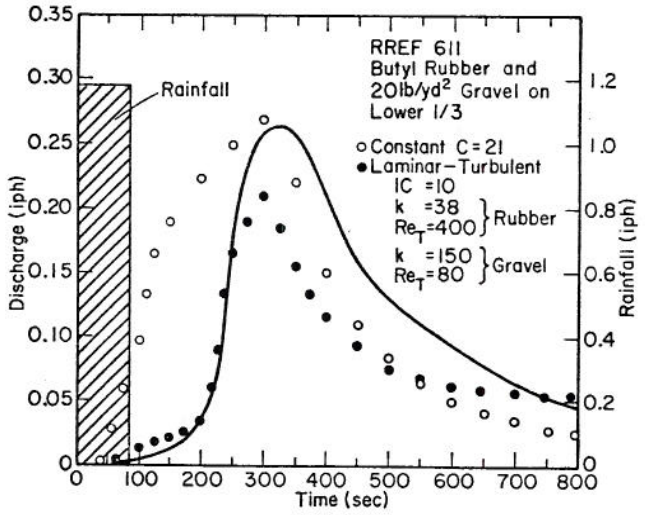

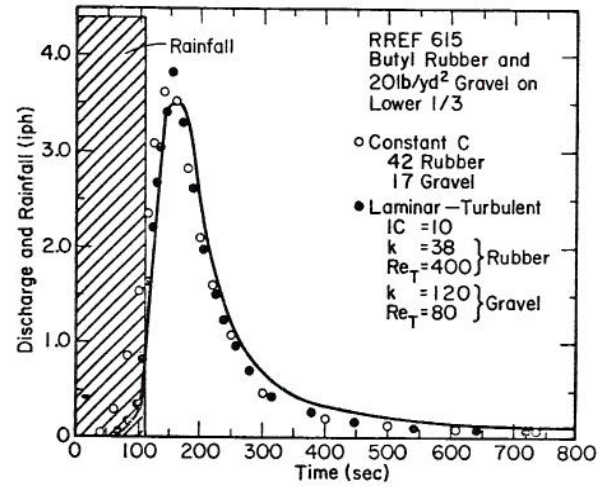

Fig. 5-11 RREF Hydrographs from Butyl Rubber and Gravel Surface

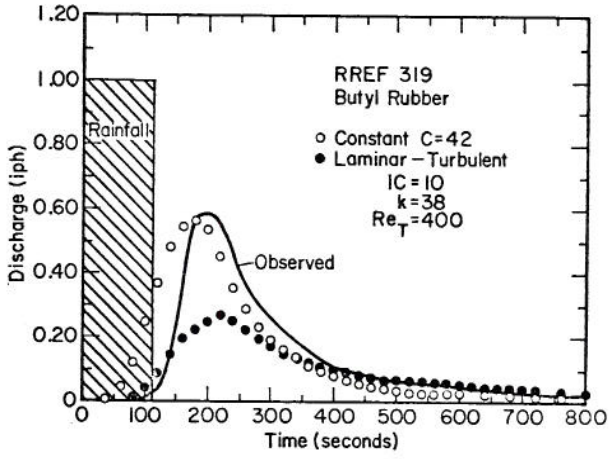

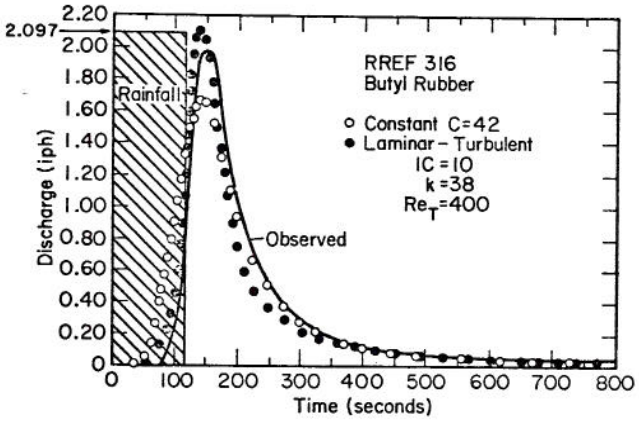

Fig. 5-12 RREF Hydrographs from Butyl Rubber Surface

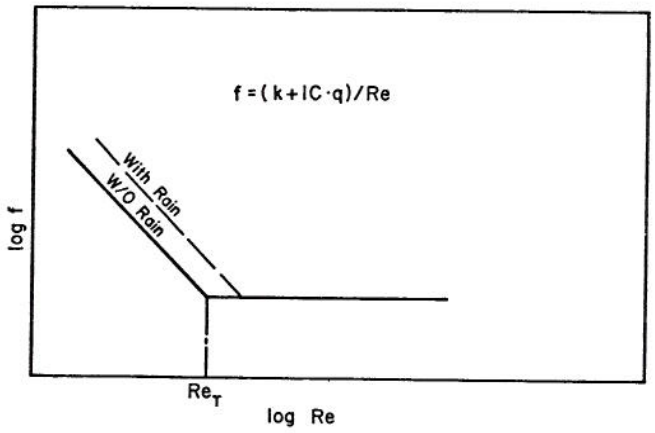

Fig. 5-13 Laminar-Turbulent Friction Relationship

The q variable is the rainfall rate. These parameters were estimated from Fawke's (1972) study of runoff from butyl rubber and graveled surfaces for the conic section. The best results were obtained by using k values that were about 50% higher than the average k value as computed by Fawkes. The results of simulations using a laminar-turbulent friction relationship are plotted in Figs. 5-11 and 5-12, along with the simulations using a constant friction relationship. These figures allow comparison of the two friction relationships that have been used in the watershed model. In three of the four cases, the peak discharge is more closely approximated by the constant Chezy C relationship, while the laminar-turbulent relationship consistently matches the rising limb of the hydrographs, especially for the surface of a combination of butyl rubber and gravel. Before drawing conclusions about which of the friction relationships is best, we must consider the technique by which the parameters were estimated. Singh optimized only on the peak discharge rates, while Fawkes optimized the parameters based upon the entire hydrographs. This choice of objective functions is reflected in the performance of the model, as use of Singh's C values results in a better fit of peaks, while use of Fawke's relationship gives a better overall fit of the hydrograph.

Schaake's Urban Watershed

Schaake (1965, 1970) reported the results of computer simulations of runoff from a small urban catchment that has been studied by the Johns Hopkins University Storm Drainage Research Project. The results

are used in this study to provide an independent verification of the surface water routing portion of the watershed model that has been developed in previous sections. Schaake (1965) presented results from a deterministic runoff model based on the complete unsteady flow equations for channel routing and overland flow routing. Schaake (1970) presented results of the simulation of an event, where the computer model was based upon kinematic routing for both channel and overland flow. This event had also been reported in the 1965 publication. There is very little difference in the computed results from these two different models. The storm designated 3SPL1, and the 0.39-acre watershed, designated SPL1, have been described in detail in Schaake's 1970 publication. A diagram of the watershed and the geometry of Schaake's computer segments are shown in Fig. 5-14. Schaake specified

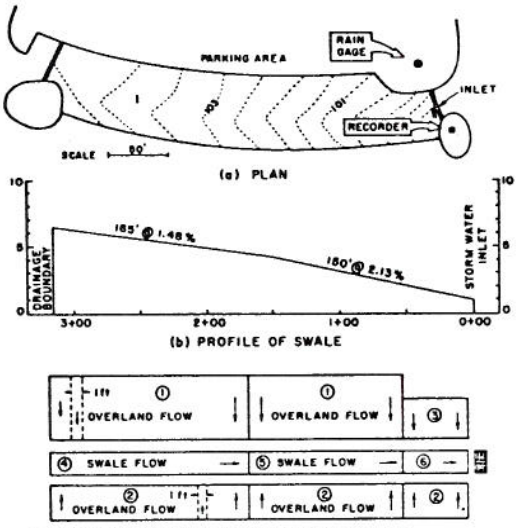

Component	Length (ft)	Width or Dia (ft)	Slope (ft/ft)	Side Slope	Inflow to Component: Lateral Inflow	Inflow to Component: Upstream Inflow
①	36	1	.019	–	Rainfall	—
②	20	1	.0167	–	Rainfall	—
③	25	1	.019	–	Rainfall	—
④	165	–	.0148	113:1	① and ②	—
⑤	100	–	.0213	113:1	① and ②	④
⑥	50	–	.0213	113:1	② and ③	⑤

(d) PHYSICAL CHARACTERISTICS OF COMPONENTS IN THE SCHEMATIC REPRESENTATION

Fig. 5-14 Geometric Characteristics of Small Urban Area (after Schaake, 1970)

that overland flow for the watershed should be computed by a laminar flow relationship. His roughness parameter for laminar overland flow was given a value of 10; this parameter is theoretically equivalent to the parameter k (shown in Fig. 5-13) divided by four. The swale shown in Fig. 5-14 was represented by a triangular-shaped channel where turbulent flow is assumed to exist throughout the entire runoff event. A roughness parameter similar to Manning's n with a value of 0.02 was assigned by Schaake to the swale area.

The strategy of the independent test of the computer model KINGEN is to use the geometric segments, just as Schaake had represented the watershed as well as the same number of Δx increments for each segment. These selections avoid bias by using another's representation of the watershed. Schaake used a specified time increment in the explicit finite difference form of the kinematic equations. The model KINGEN computes the necessary Δt to maintain numerical stability as defined by Eq. (3-39). Since the geometric characteristics of the watershed have been determined, the test of the model is the selection of the roughness parameters. The laminar-turbulent friction relationship, described in the section on *Colorado State University Rainfall-Runoff Experimental Facility*, is used to model the surface roughness. The transition Reynolds number is selected as 300 and the intensity coefficient as 10. This leaves the parameter k to be chosen. Two simulation tests were made with storm 3SLP1 as the input. The first test was with the lower extreme value of k for concrete or asphalt, as reported by Woolhiser (1974). The other test was with the upper extreme value of k . The results of these two test computations are shown in Fig. 5-15 along with the measured

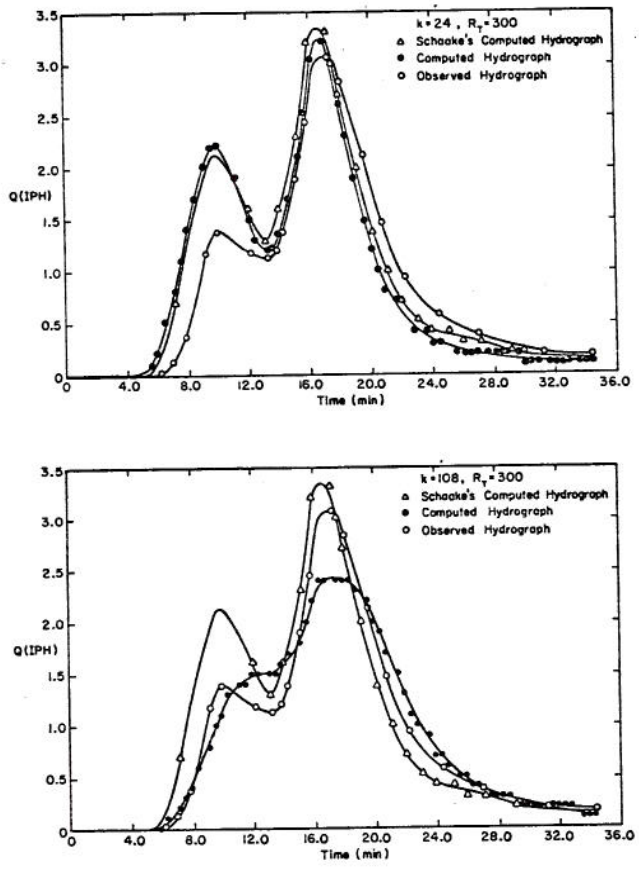

Fig. 5-15 Comparison of Measured and Synthesized Runoff Hydrographs--Urban Area

runoff hydrograph and Schaake's computed hydrograph. This figure shows the results of the computer simulation bracket the observed results by using the extreme values as reported in the engineering literature. These results are encouraging because they indicate that a watershed engineer could exercise some judgment about the physical characteristics of the watershed and estimate an appropriate roughness parameter that would result in reasonable predictions of runoff, as long as

the roughness parameter was within the reported limits. Comparison of the computed results from program KINGEN and Schaake's work reveals very little difference between the two for the lowest value of k . Both simulations overpredicted the first peak by substantial amounts. The higher value of k resulted in a better estimation of the first peak but the estimation of the second peak was then poorer for the lower k value.

Hillcrest Drain, Colorado Urban Watershed

The watershed model is used in the section on *Schaake's Urban Watershed* to simulate runoff from a small urban catchment with a uniform surface cover of asphalt. In this section, the model is used to simulate runoff from a large urban watershed that is a mixture of pervious and impervious area. A description of the Hillcrest Drain watershed was given in Section 4.3. The complexity of the watershed features, natural and man-made, requires an extremely large number of computer segments to represent the physiographic features with any degree of completeness. The computer storage required to accommodate such a large number of geometric segments may not exist on any standard computer that is available to watershed engineers. The computational cost of such a complete representation is prohibitive even for research. Another possibility of representing the watershed geometry is to use only two or three computer segments, i.e. one or two planes and a channel, and optimize the watershed parameters by matching computed and measured results. However, physical interpretation of parameters obtained by this type of technique becomes very difficult, if not impossible. Also, transferability of results from the Hillcrest Drain watershed to other watersheds may not be possible. The solution to the dilemma of representing the watershed by a very large number of segments or a very few segments is a compromise of the two extremes. The watershed is represented by enough segments to maintain a resemblance of the physiographic features, but the number is limited to keep the computer storage and computation time to an acceptable level. Even with severe simplifications of the geometry, the number of computer segments used to represent the Hillcrest Drain watershed exceeds 150 and for the most detailed representation used, the number is slightly more than 200. Figure 5-16 shows the computer segments, indicated by dashed lines, used to represent a typical block of the watershed. Each segment is numbered in the same order that computations occur. The computer segments, their corresponding physical significance, and the sources of inflow are listed in Table 5-3. This schematization of the urban watershed is the most complete representation that is used.

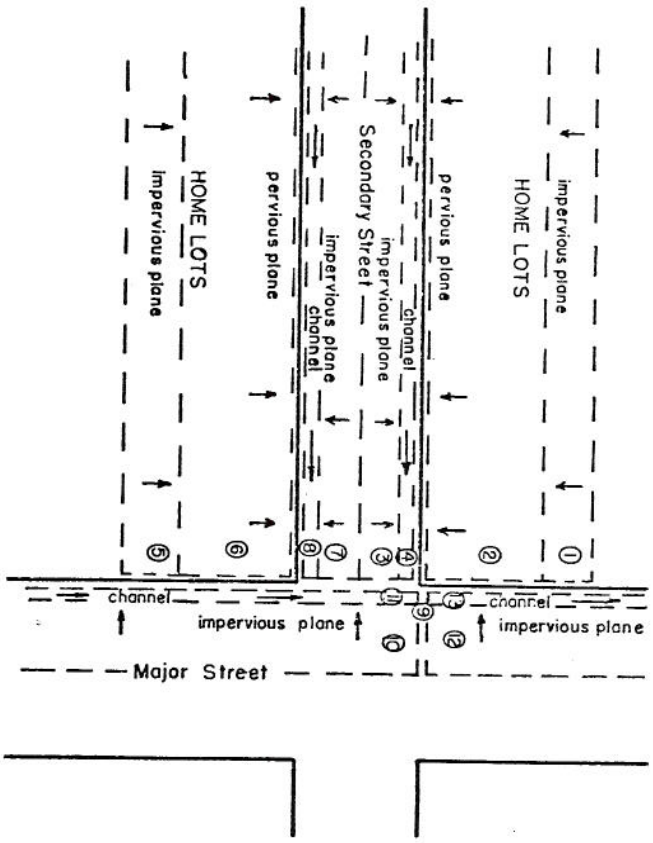

Fig. 5-16 Geometric Segments for a Typical Block in an Urban Watershed

Table 5-3 Computer Segments Used to Represent Geometry Shown in Fig. 5-16

Segment Number	Physical Significance	Lateral Inflow	Upstream Inflow	
			Plane	Channel
1	Roof	Rainfall	-	-
2	Lawn	Rainfall	1	-
3	Street	Rainfall	-	-
4	Gutter	2, 3	-	-
5	Roof	Rainfall	-	-
6	Lawn	Rainfall	5	-
7	Street	Rainfall	-	-
8	Gutter	6, 7	-	-
9	None (add channels)	-	-	4, 8
10	Street	Rainfall	-	-
11	Gutter	12	-	-
12	Street	Rainfall	-	-
13	Gutter	12	-	9, 11

Parameter Estimation

The dimensions of the computer segments were estimated from an enlarged topographic map of the watershed. Summation of the area of all the computer segments is within 2% of the total area of the watershed as measured from the topographic map. The soil characteristics of the watershed were described in Section 4.3. These characteristics represent the conditions when the area was cultivated for agricultural purposes. Changes in some of the soil characteristics are expected to have occurred when the area was urbanized. The clayey subsurface material that is excavated for basements is often spread atop or mixed with the topsoil, which reduces the infiltration rate of the soil. Also the soil is compacted during the movement of construction equipment and the planting of lawns. The model parameters for the pervious sections of the watershed were obtained by comparison of the measured and adjusted soil characteristics to the

range of soils that Smith (1972) used to conduct infiltration experiments. The comparison revealed the characteristics of the watershed soils to be closest to those of Muren clay soil. Table 5-4 lists the model parameters for the infiltration component of the urban watershed. Preliminary test results showed that runoff did not occur from the pervious area, when the C_1 value for Muren clay was used for the short duration storms, as observed on the watershed. The C_1 value was lowered to that value in Table 5-4 and corresponds nearly to the C_1 for Nibley silty clay loam.

Table 5-4 Infiltration Parameters for Hillcrest Drain Soil

Parameter	Value of Parameter
α	0.53
γ	0.45
S_o	0.95
C_1	400
f_∞	0.2*
S_i	0.4**

*after initial tests, this was lowered to 0.1 in/hr.

**minimum moisture content because of watered lawns, events preceded by precipitation estimated at higher content.

The surface roughness characteristics were modeled by constant Chezy C friction factors. These friction factors were estimated by comparison of the surface type being considered with the types of surfaces that have been studied extensively for surface runoff and reported in the literature. The constant friction factors were estimated for five types of surfaces: streets, gutters, lawns, roofs, and storm sewers. Table 5-5 lists the values of the roughness coefficient for these surfaces.

Table 5-5 Roughness Factors for Hillcrest Drain Watershed

Type of Surface	Chezy C Friction Factor
Street	50
Roof	50
Lawn	4.2
Gutter	85
Storm Sewer	Manning's n = 0.013

The storm sewer roughness is listed in terms of Manning's n for reasons that are outlined in Section 5.1. The friction factor for storm sewers has the value that is often recommended for concrete pipe. The Chezy C values are within the values reported by Woolhiser (1974). The geometric, infiltration, and flow resistance parameters are estimated for the urban watershed. With this information, simulation experiments are conducted using measured rainfall events as input to the model. Information about the watershed as a hydrologic system is obtained by making modifications to the parameters, as described in this section.

Effects of simplifications to watershed representation

The importance of runoff from the pervious area is analyzed by postulating that runoff is coming from only the directly connected impervious areas, i.e., streets contributing to the gutters and storm sewers. This assumes that all lateral inflow to the lawns, either rainfall or runoff from roofs, is infiltrated and none flows into the gutter. Simulation experiments, based upon this assumption, are compared with the observed hydrographs. Results of these simulations are used to judge the importance of the runoff from pervious areas of the urban watershed. Figure 5-17 shows

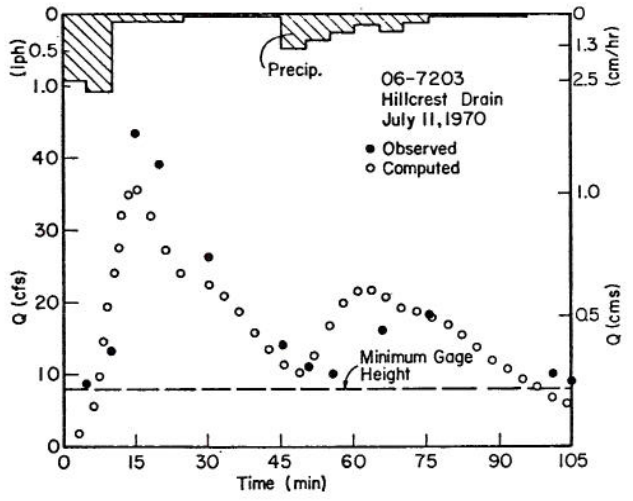

Fig. 5-17 Runoff Simulation from Hillcrest Drain, No Contribution from Pervious Area

the results of a typical example assuming no contribution of flow from the pervious area. Four storms were simulated with this assumption. Three of the four events showed results similar to Fig. 5-17, i.e., underprediction of the volume and peak rates. The fourth simulation resulted in overprediction of the volume and peak by more than 50%. Further investigations of the fourth event revealed that it was the first event recorded at the gaging station and the possibility of errors in the data because of faulty calibration is great. No plausible explanation other than this one could be formulated about the event. Since overprediction occurs when only the streets and gutters are assumed to be contributing flow, greater overprediction occurs when the more realistic assumption is used that all areas contribute flow. The underprediction of the

majority of events is what is expected when only a limited area of the watershed contributes to the runoff process. The conclusion is drawn that runoff from the pervious portion of urban watersheds is important even for moderate storms and is not to be ignored when simulating the runoff events.

Further simulation tests were conducted with the entire area of the watershed contributing flow. The infiltration parameters used in these tests are shown in Table 5-4. The results of this simulation are an increase of the peak discharge rate and of the total volume of runoff. However, the results are still an underprediction of the observed peaks and volumes. The minimum infiltration rate, f_∞, was lowered to 0.1 IPH and further simulations were conducted. This parameter modification results in a better approximation of the peak flow rates but the recession hydrograph is again underpredicted. The problem of underprediction of the recession portion of the hydrographs is similar to that reported by Smith (1970). Representation of overland flow as runoff from a plane surface results in the implicit assumption that the entire surface is covered by water if there is any depth whatsoever present. The real situation is that the surface is covered by a series of depression and undulations. When rainfall ceases, only a portion of the surface is covered by water; the remainder of the surface protrudes above the water surface. Thus, infiltration computed for a plane surface is too large during recession as compared with the natural situation where infiltration is occurring on only the submerged portion of the surface. It is necessary to limit the amount of infiltration that occurs on the recession portion of hydrographs so that computed recessions not consistently underpredict the observed recession. An empirical factor was developed that was used to limit the amount of negative lateral inflow (precipitation and surface water is less than infiltration). The factor is

$$F' = 1 - e^{-k'h} \qquad (5\text{-}6)$$

where k' is a constant with value 75, and h is the depth of water on the surface in feet. The parameter F' ranges in value from zero to unity. When h is zero, F' is zero and when h is 0.75 in., F' is 0.99. Thus, recession infiltration is limited by the exponential factor as given in Eq. (5-6) whenever the mean water depth is below 0.75 in. (This feature is not included in the program KINGEN 75, which is listed in Appendix B).

Simulations using the final watershed representation

Multiple storms from the urban watershed are simulated with the computer parameters, as shown in Table 5-4, for infiltration with f_∞ lowered to 0.1 IPH. Roughness parameters and surface geometry are as shown in Table 5-5 and Fig. 5-16, respectively. The results of these simulations are plotted in Figs. 5-18 through 5-20. The results show an overestimation of runoff volume in some of the cases but an underestimation of the volume in other cases. The peak discharges show a similar distribution of the predictions. The major problem lies in the estimation of rainfall excess. This problem is divided into two sub-problems. One is the amount of infiltration on pervious areas and the other is the geometric representation of the watersheds in terms of the percentage of pervious and impervious area as compared with the actual amount of these areas.

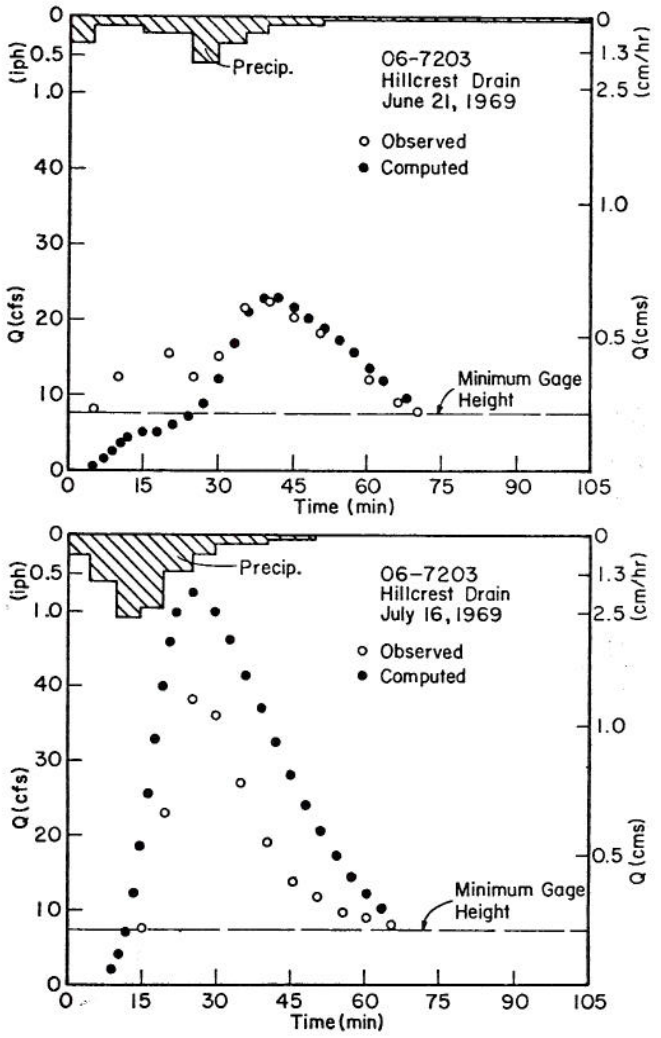

Fig. 5-18 Hillcrest Drain, June 21 and July 16, 1969

The ratio of impervious areas to the total watershed area was measured by Root and Miller (1971) and was nearly constant during the study period at a value of about 42%. The ratio of impervious to total area of the computer segments is 40%. A consistent underestimation of runoff volume is expected as a result of this bias in the amount of impervious area. The distribution of the impervious area and the amount that is directly connected to the gutter and storm sewer systems is not precisely known. Its importance requires further investigation.

One problem that is likely to cause the variations of overprediction and also underprediction is the estimation of infiltration for each storm. The infiltration parameters have been held constant for each event, except for the initial water content, S_i. This variable was altered when recorded data was sufficient to indicate that rainfall events or lack of them occurred so as to affect the antecedent moisture condition. The record of rainfall at Hillscrest Drain is not published for each day, but only when there is a runoff event. This lack of rainfall data and the unpredictable times of lawn watering present a problem when attempting to estimate the antecedent

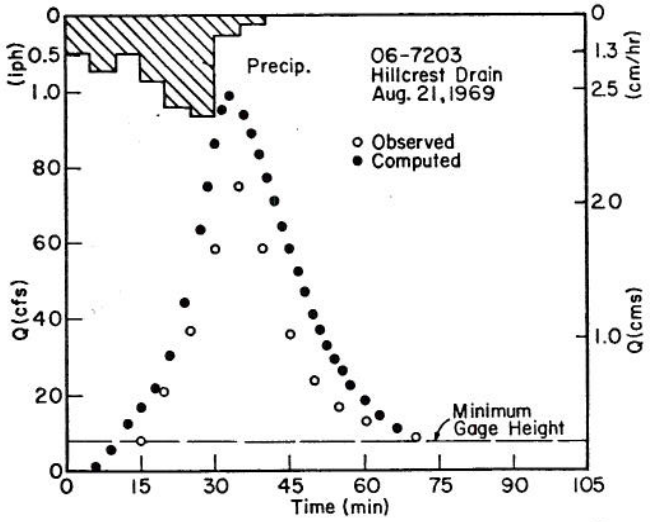

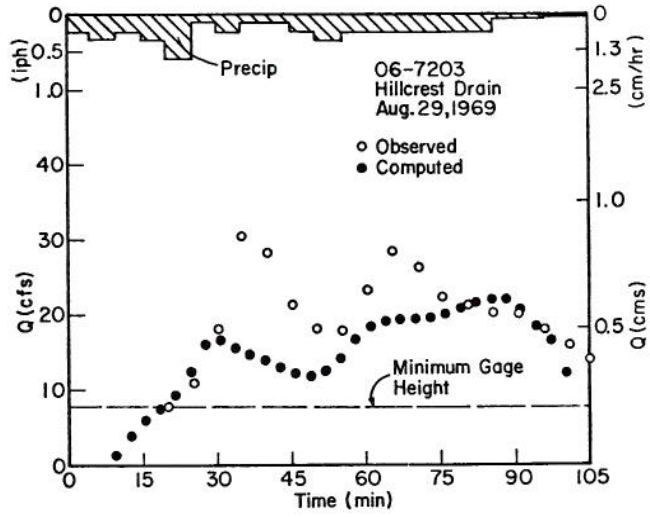

Fig. 5-19 Hillcrest Drain, August 21 and 29, 1969

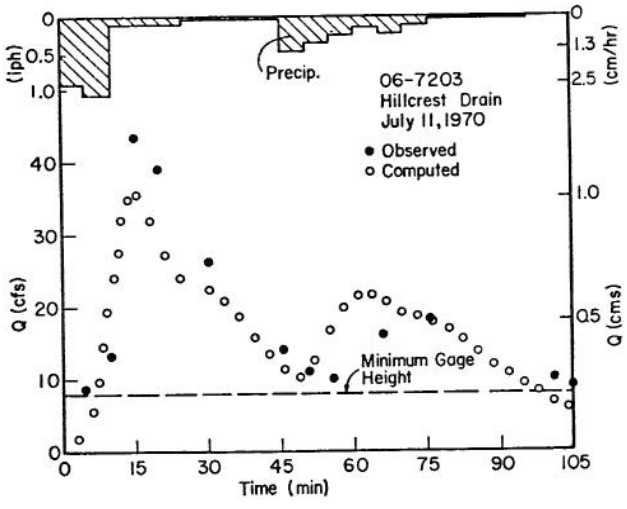

Fig. 5-20 Hillcrest Drain, July 11, 1970

moisture. Because the usual rainfall event is the localized thunderstorms in this area, the use of precipitation records from some other measuring station is not adequate to define the conditions on the Hillcrest Drain watershed. The computed results indicate the surface runoff model is adequate to simulate the outflow hydrograph, even for this complex system, if the rainfall excess is accruately estimated. The problem of infiltration estimation is the greatest problem that must be overcome before the model can be widely used as a means of estimating the runoff from such a complex hydrologic system as the Hillcrest Drain watershed.

Agricultural Watershed near Edwardsville, Illinois

The watershed model has been used in the past three sections to simulate runoff from watersheds that are partially or totally impervious. The W-I watershed near Edwardsville, Illinois is an entirely pervious area and was described in Section 4.2. Simulation of runoff from this watershed is the most severe test in this study of the infiltration component of the watershed model. The infiltration parameters are determined from the infiltrometer experiments, soil survey, and comparison to the parameters reported in Section 3.3. The infiltration characteristics are assumed to represent the entire watershed. That is, one set of infiltration parameters is assigned to all the pervious segments of the watershed. There is sufficient information from the soil survey to allow a more detailed representation of the watershed infiltration characteristics. However, the objective of testing the infiltration component of the model is to determine its applicability to an agricultural watershed in which detailed information on infiltration characteristics other than the predominant soil type is normally not available. Thus, a watershed engineer generally assumes that uniform infiltration conditions exist over the entire watershed.

Parameter estimation

Figure 4-3 shows a topographic map of watershed W-I and a schematic representation of the geometry. The computer segments are chosen from the map to conserve the watershed area and channel flow length. Details of the geometric segments are shown in Table 5-6. The choice of geometric representation for the

Table 5-6 Geometry of Watershed Segments at Edwardsville, Illinois W-I

Segment Number	Type	Length (ft)	Width (ft)	Slope	Contributing Inflow
1	plane	312	663	.01	Rainfall
2	plane	275	519	.015	Rainfall,1
3	plane	205	327	.039	Rainfall
4	plane	143	265	.035	Rainfall
5	channel	385	-	.018	2,3,4
6	plane	785	282	.017	Rainfall
7	plane	140	276	.043	Rainfall
8	channel	245		.016	6,7
9	plane	150	203	.07	Rainfall
10	channel	195	-	.021	5,8,9
11	plane	465	380	.009	Rainfall
12	plane	165	573	.042	Rainfall,11
13	plane	125	492	.056	Rainfall
14	plane	395	270	.013	Rainfall
15	channel	675	-	.018	12,13,14
16	(add channels)	-	-	-	10,15

computer model user is subjective. There are several reasons the geometric representation is maintained as simple as possible. Computer time is saved with a simple representation because fewer calculations are made than for a very detailed representation. There is also a savings of time for processing input data. However, there is a trade-off in the accuracy of simulation and cost of computations. Further investigation is required to adequately define the detail of representation that is required to obtain a desired degree of accuracy.

Results of infiltrometer tests were presented in Section 5.2 These tests were conducted on sample plots of the W-I watershed. The range of steady state infiltration rates of the infiltrometer experiments is .15 to .78 IPH. The upper values of this range are quite high for the silt loam soil of the watershed. Several rainfall-runoff events of extended duration were analyzed for infiltration losses. Rainfall events of duration of 12 hours or more are assumed to have reached a steady-state condition of infiltration. Pulses of moderate intensity rainfall that occur late in a storm are used to estimate the minimum infiltration rate by calculating the difference between rainfall and runoff for a period of time. The difference between rainfall and runoff is the infiltration. The analysis of extended events shows the f_∞ rate was about .10. Chow (1964) described a soil type within which the Alma and Bogota soils are classes as having a minimum infiltration rate from 0.05 to 0.15. Thus, the results of the infiltrometer tests show substantially higher infiltration rates than other analyses of similar soil types. The minimum infiltration rate for the W-I watershed is estimated to be 0.12. The infiltration parameters, as determined by comparison to the Colby silt loam described in Section 3.3, are listed in Table 5-7.

Table 5-7 Infiltration Parameters for W-I Runoff Simulation

Parameter	Value of Parameter
α	0.58
γ	0.90
S_o	0.95
C_1^*	5000
S_i	Estimated for each storm
f_∞	0.12

The watershed area was planted entirely with alfalfa during the study period. One roughness parameter is assumed to describe flow resistance for the entire overland flow portion of the watershed. The Chezy C friction factor estimated for the watershed is 5.1. This value is within the range of Chezy C values reported by Woolhiser (1974) for short-grass prairie. The value is slightly higher than those reported by Woolhiser (1974) for bluegrass sod. The swale-like areas of the watershed are represented as channel segments. The flow in these areas is deeper than over the plane segments. Often there is little or no vegetation established in the lowest portion of the swales. These two factors result in lower effective flow resistance in the swales than in the overland areas. The Chezy C value assigned to the channel segments is 35. The determination of the geometric, infiltration, and flow resistance parameters permits simulation of runoff from the W-I watershed.

Simulation of runoff from watershed W-I

The results of some of the runoff simulations are shown in Figs. 5-21 and 5-22. The results indicate

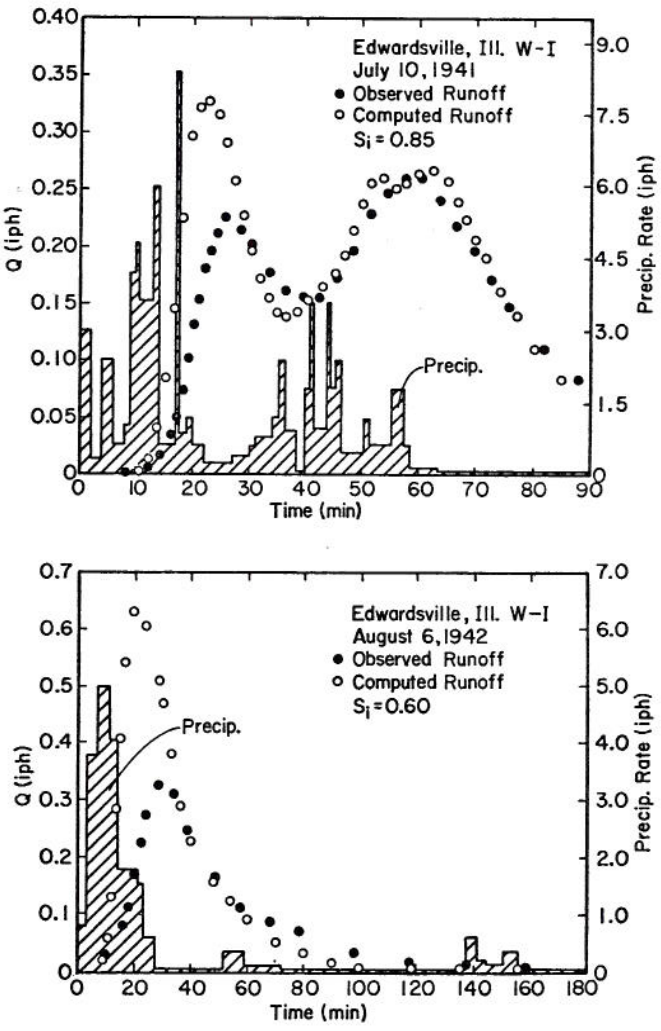

Fig. 5-21 Hydrographs from Watershed W-I, July 10, 1949 and August 6, 1942

that the observed and computed hydrographs are closely matched when the rainfall excess is properly estimated. Rainfall excess during the early portion of each event is the quantity least adequately simulated by the watershed model. The constant friction relationship is adequate to approximate flow resistance during the rising limb, peak discharge rates, and the recession portion of the runoff events. More comprehensive

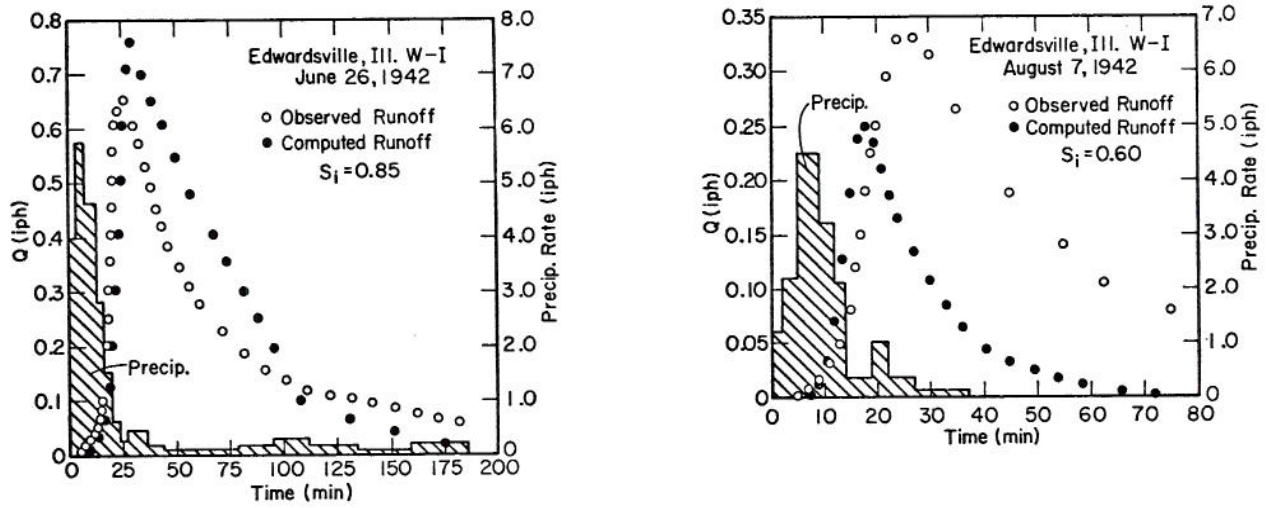

Fig. 5-22 Hydrographs from Watershed W-I, June 26, 1942 and August 7, 1942

friction relationships are unwarranted unless more precise means of estimating rainfall excess are developed. The inability to use information directly from the infiltrometer experiments when estimating infiltration parameters for the entire watershed is somewhat disappointing. A possible explanation of the variation of infiltrometer experiments and the natural infiltration is the difference between the infiltrometer and natural surfaces. The 6 by 12 foot plots of the infiltrometer experiments were probably chosen where the surface was uniform and had few depressions. This results in the surface water covering the ground area uniformly. The natural surface may consist of significant undulations and depressions. Except during the higher intensities of rainfall, surface runoff may quickly form into rivulets and not cover the entire surface uniformly. Thus, infiltration is restricted to less than the entire watershed surface. It is encouraging that infiltration parameters estimated by comparison of the watershed soil to the soil types discussed in Section 3.3 resulted in as good of estimations of runoff as indicated by the results.

Chapter 6
CONCLUSIONS AND RECOMMENDATIONS

6.1 Conclusions

Kinematic routing of flow in circular conduits is applicable within the limitations of kinematic wave theory. Kinematic routing cannot account for backwater effects; applications must be limited accordingly. This study shows that kinematic routing performs as well as a hydrograph lag method for predicting outflows. The kinematic method has the advantage that no observed hydrographs are needed to estimate parameters.

Computation of infiltration on pervious surfaces is based upon a parametric decay-type function. Field measurements are used to estimate parameters for simulation of infiltrometer experiments. The three most sensitive parameters of the five computer infiltration parameters have physical significance. A previous study of the infiltration component lists appropriate parameters for a wide range of soil types. It is possible to estimate infiltration parameters of a soil by comparison of type and characteristics to results of the previous study.

A variable friction relationship that accounts for both laminar and turbulent flow regimes gives a better overall fit to the hydrograph than a constant friction relationship. However, the constant relationship may give a better fit of the peak discharge rate based on a priori estimates of flow resistance. The variable friction relationship is warranted only on a totally impervious area. When a watershed is partially or totally pervious, the estimation of rainfall excess is more important than the type of friction relationship used. On pervious watersheds, the constant friction relationship is adequate.

The watershed model is used to simulate runoff from two urban watersheds. Results from the small impervious watersheds show good agreement between observed and predicted hydrographs. Results from the large, complex urban watershed are good when the rainfall excess is properly estimated. Results from both watersheds indicate that a priori estimates of friction parameters are adequate to define flow resistance. The watershed model can be applied to complex urban systems, to predict runoff rates for sizing storm drains and conveyance structures. However, the current form of the model may be too complex for widespread use as a design tool. It does have application in further research and also as a comparative tool for the more simplified methods of flow calculations, like the unit hydrograph.

6.2 Recommendations

Further research should be undertaken to make a more extensive study of kinematic routing in circular conduits by testing the technique on observed data.

The infiltration component of the watershed model should be extensively tested on field data for a variety of soil and cover conditions. Initial soil moisture content should be estimated using daily models that account for drainage and evapotranspiration.

REFERENCES

1. Acker, P. and J. Harrison, Attenuation of flood waves in part-full pipes. Proc. of Institute of Civil Engrs., London, Vol. 28, pp. 361-382, 1964.

2. ASCE Urban Hydrology Research Council, Systematic study and development of long-range programs of urban water resources research. First Year Report. Cambridge, Massachusetts, 1968.

3. Biswas, Asit K., History of hydrology. North-Holland Publ. Co., Amsterdam, 336 p., 1970.

4. Brakensiek, D. L., Kinematic flood routing. Trans. ASAE, Vol. 10, No. 3, pp. 340-343, 1967a.

5. Brakensiek, D. L., A simulated watershed flow system for hydrograph prediction; a kinematic application. Proc. International Hydrology Symposium, Fort Collins, Colorado, pp. 18-24, 1967b.

6. Chow, V. T., editor, Handbook of applied hydrology. McGraw-Hill, Inc., New York, pp. 12-1 to 12-30, pp. 20-1 to 20-45, 1964.

7. Committee on Flood Control, Task Force on Effect of Urban Development on Flood Discharges, Effect of urban development on flood discharges--current knowledge and future needs. Proc. ASCE, Vol. 95, No. HY1, 1969.

8. Dawdy, D. R., Considerations in evaluating mathematical modeling of urban hydrologic systems. U. S. Geological Survey Water-Supply Paper 1591-D, 1969.

9. Denver Regional Council of Governments, Urban storm drainage criteria manual. Vol. 1, prepared by Wright-McLaughlin Engineers, Denver, Colorado, 1969.

10. Dickinson, W. T., M. E. Holland, and G. L. Smith, An experimental rainfall-runoff facility. Hydrology Paper No. 25, Colorado State University, Fort Collins, Colorado, 81 p., 1967.

11. Ducret, G. L., Jr., and H. E. Hodges, Rainfall-runoff data from small watersheds in Colorado, June, 1968 through September, 1971. Colorado Water Resources Basic-Data Release No. 27, 1972.

12. Eagleson, P. S., Dynamic hydrology. McGraw-Hill Book Co., New York, 462 p., pp. 331-367, 1970.

13. Fawkes, P. E., Roughness in a model of overland flow. M.S. Thesis, Colorado State University, Fort Collins, Colorado, 1972.

14. Foster, G. R., L. F. Huggins, and L. D. Meyer, Simulation of overland flow on short field plots. Water Resources Res., Vol. 4, No. 6, pp. 1179-1187, 1968.

15. Gonzalez, D. D. and G. L. Ducret, Jr., Rainfall-runoff investigations in the Denver metropolitan area, Colorado. U. S. Geological Survey Colorado Dist. Water Res. Div. Open-File Report 71003, 1971.

16. Harper, W. G., L. Acott, and E. Frahm, Soil survey of the Brighton area, Colorado. U. S. Dept. of Agriculture, Bureau of Chemistry and Soils, Series 1932, No. 1, 1932.

17. Harris, G. S., Real time routing of flood hydrographs in storm sewers. Proc. ASCE, Vol. 96, No. HY6, pp. 1247-1260, 1970.

18. Henderson, F. M., Flood waves in prismatic channels. Proc. ASCE, Vol. 89, No. HY4, pp. 39-69, 1963.

19. Henderson, F. M. and R. A. Wooding, Overland flow and groundwater flow from a steady rainfall of finite duration. J. of Geophysical Res., Vol. 69, No. 8, pp. 1531-1540, 1964.

20. Hicks, W. I., A method of computing urban runoff. Trans. ASCE, Vol. 109, pp. 1217-1253, 1944.

21. Holtan, H. N. and N. E. Minshall, Plot samples of watershed hydrology. Agricultural Research Service publ. ARS 41-133, 1968.

22. Horner, W. W. and F. L. Flynt, Relations between rainfall and runoff from small urban areas. Trans. ASCE, Vol. 101, pp. 140-183, 1936.

23. Horton, R. E., An approach toward a physical interpretation of infiltration capacity. Proc. Soil Sci. Soc. Am., Vol. 5, pp. 399-417, 1940.

24. Ibbit, R. P., Systematic parameter fitting for conceptual models of catchment hydrology. Ph.D. dissertation, University of London, London, England, 1970.

25. Iwagaki, Yuichi, Fundamental studies on the runoff analysis by characteristics. Disaster Prevention Research Institute Bulletin No. 10, Kyoto University, Kyoto, Japan, 1955.

26. Izzard, C. F., Hydraulics of runoff from developed surfaces. Proc. of Highway Research Board, Vol. 26, pp. 129-146, 1946.

27. Kibler, D. F., A kinematic overland flow model and its optimization. Ph.D. dissertation, Colorado State University, Fort Collins, Colorado, 1968.

28. Kibler, D. F. and D. A. Woolhiser, The kinematic cascade as a hydrologic model. Hydrology Paper No. 39, Colorado State University, Fort Collins, Colorado, 1970.

29. Langford, K. J. and A. K. Turner, An experimental study of the application of kinematic wave theory to overland flow. J. of Hydrology, Vol. 18, No. 2, pp. 125-145, 1973.

30. Licthy, R. W., D. R. Dawdy, and J. M. Bergmann, Rainfall-runoff model for small basin flood hydrograph simulation. Symposium of International Assoc. of Scientific Hydrology, Publ. No. 81, Tucson, Arizona, 1968.

31. Lighthill, M. H. and G. B. Whitham, On kinematic waves, I. Flood movement in long rivers. Proc. Royal Soc. of London, Ser. A., Vol. 229, pp. 281-316, 1955.

32. Linsley, R. K., M. A. Kohler and J. H. Paulhus, Applied hydrology. McGraw-Hill Book Co., Inc., New York, 1949.

33. Lopez, O. G., Response time in urban Colorado basins. M.S. Thesis, Colorado State University, Fort Collins, Colorado, 1973.

34. McCuen, R. H., The role of sensitivity analysis in hydrologic modeling. J. of Hydrology, Vol. 18, No. 1, pp. 37-53, 1973.

35. Minshall, N. E., Predicting storm runoff on small experimental watersheds. Trans. ASCE, Vol. 127, Paper No. 3333, pp. 625-659, 1962.

36. Morgali, J. R., Laminar and turbulent overland flow hydrographs. Proc. ASCE, Vol. 96, No. HY2, pp. 441-460, 1970.

37. Morgali, J. R. and R. K. Linsley, Computer analysis of overland flow. Proc. ASCE, Vol. 91, No. HY3, pp. 81-100, 1965.

38. Overton, D. E. and D. L. Brakensiek, A kinematic model of surface runoff response. IASH Symposium, Wellington, New Zealand, 1970.

39. Papadakis, C. and H. Preul, University of Cincinnati urban runoff model. Proc. ASCE, Vol. 98, No. HY10, 1972.

40. Parlange, J.-Y. and R. E. Smith, Ponding time for variable rainfall rates. Canadian J. Soil Science, Vol. 56, pp. 121-123, 1976.

41. Philip, J. R., Theory of infiltration. Advances in Hydroscience. (ed. by V. T. Chow), Academic Press, New York, Vol. 5, pp. 215-296, 1969.

42. Root, R. R. and L. D. Miller, Identification of urban watershed units using remote multispectral sensing. Environmental Resources Center, Colorado State University, Completion Report Series No. 29, 1971.

43. Schaake, J. C., Synthesis of the inlet hydrograph. Technical Report No. 3, Storm Drainage Research Project, The Johns Hopkins University, 1965.

44. Schaake, J. C., Deterministic urban runoff model. Institute on Urban Water Systems, Fort Collins, Colorado, 1970.

45. Schulz, E. F., Recent development in urban hydrology. Paper presented to the Chinese Society of Civil Engineers, Taipei, Taiwan, 1971.

46. Singh, V. P., A nonlinear kinematic wave model of surface runoff. Ph.D. dissertation, Colorado State University, Fort Collins, Colorado, 1974.

47. Smith, F. M., A volumetric-threshold infiltration model. Ph.D. dissertation, Colorado State University, Fort Collins, Colorado, 1971.

48. Smith, R. E., Approximations for vertical infiltration rate patterns. Transactions of the ASAE, Vol. 19, No. 3, pp. 505-509, 1976.

49. Smith, R. E., Mathematical simulation of infiltrating watersheds. Ph.D. dissertation, Colorado State University, Fort Collins, Colorado, 1970.

50. Smith, R. E., The infiltration envelope: results from a theoretical infiltrometer. J. of Hydrology, Vol. 17, No. 1/2, pp. 1-21, 1972.

51. Smith, R. E. and D. L. Chery, Jr., Rainfall excess model from soil water flow theory. J. of the Hydraulics Division, ASCE, Vol. 99, No. HY9, Proc. Paper 9990, pp. 1337-1351, 1973.

52. Smith, R. E. and D. A. Woolhiser, Mathematical simulation of infiltrating watersheds. Hydrology Paper No. 47, Colorado State University, Fort Collins, Colorado, 44 p., 1971.

53. Tholin, A. L. and C. J. Kiefer, The hydrology of urban runoff. Trans. ASCE, Vol. 125, pp. 1308-1355, 1960.

54. Viessman, W. and J. C. Geyer, Characteristics of the inlet hydrograph. Proc. ASCE, Vol. 88, No. HY5, pp. 245-268, 1962.

55. Water Pollution Control Federation, Design and construction of sanitary and storm sewers. Manual of Practice No. 9, 1969.

56. Woo, D. and E. F. Brater, Spatially varied flow from controlled rainfall. Proc. ASCE, Vol. 88, No. HY6, pp. 31-56, 1962.

57. Wooding, R. A., A hydraulic model for the catchment-stream problem, I. Kinematic wave theory. J. of Hydrology, Vol. 3, No. 3, pp. 254-267, 1965.

58. Woolhiser, D. A., Overland flow on a converging surface. Trans. ASAE, Vol. 12, No. 4, pp. 460-462, 1969.

59. Woolhiser, D. A., Simulation of unsteady overland flow. Chapter 12, Institute on Unsteady Flow, Fort Collins, Colorado, 1974.

60. Woolhiser, D. A., C. L. Hanson, and A. R. Kuhlman, Overland flow on rangeland watersheds. J. of Hydrology (N.Z.), Vol. 9, No. 2, pp. 336-356, 1970.

61. Woolhiser, D. A. and J. A. Liggett, Unsteady, one-dimensional flow over a plane--the rising hydrograph. Water Resources Res., Vol. 3, No. 3, pp. 753-771, 1967.

62. Yevjevich, Vujica, Bibliography and discussion of flood-routing methods and unsteady flow in channels. U. S. Geological Survey Water-Supply Paper No. 1690, 1960.

63. Yevjevich, Vujica and A. H. Barnes, Flood routing through storm drains, Part I. Hydrology Paper No. 43, Colorado State University, Fort Collins, Colorado, 107 p., 1970.

64. Yu, Y. S. and J. S. McNown, Runoff from impervious surfaces. J. of Hydraulic Research, Vol. 2, No. 1, pp. 3-23, 1964.

APPENDIX A

PROGRAM KINGEN 75

GENERAL DESCRIPTION

The program KINGEN described in the main portion of this report was developed for research purposes over a period of several years. Consequently, the program became progressively more complicated and difficult to understand. A new program KINGEN 75 is described and documented in the following pages. The approach used is similar to that described in the main part of this report but the program has been subdivided into several subroutines and some of the numerical methods used are different. Friction law options have been added and a subroutine to check the input for errors has also been included.

KINGEN 75 consists of program MAIN and 18 subroutines listed below. The principal function of each subroutine is indicated here and is also indicated in the comments cards in the Program Listing, Appendix B.

PROGRAM MAIN: Calls subroutines READER, PLANE and CHANNL.

SUBROUTINES:

1. READER: Reads in model parameters, watershed geometry data and rainfall data. Called from MAIN.
2. INSPEC: Inspects input data for errors and prints out an error message, if one is detected.
3. RESET: Places input data read by SUBROUTINE READER into appropriate arrays. This is done so that no subscripts are necessary on the data cards.
4. CONVERT: Converts units of time and length in input data to units used internally and reconverts to desired units in output.
5. PLANE: Finite difference solution for overland flow on a plane. A four-point implicit method is used.
6. CHANNL: Implicit finite difference solution for unsteady flow in channels with trapezoidal or circular cross sections.
7. XPLINF: Computes infiltration rates. Called only from PLANE.
8. ADD: Adds specified discharges (lateral flow, channel junctions), and computes upstream boundary values (depth, area, or intersection angle θ in conduits).
9. RESLAW: Calculates the parameters for the hydraulic resistance law selected in the input.
10. CHGLAW: Changes the hydraulic resistance laws at the transition Reynolds number if Laminar-Turbulent option has been selected.
11. UNIF: Uses linear interpolation to convert a list of discharge values at irregular time increments into a list with regular time increments.
12. IMTHUB: Calculates a residual function for an assumed value of the independent variable θ in the iterative solution of upper boundary area of a circular conduit, given an upstream discharge Q from ADD. Called from ADD thru ITER.
13. IMPLCT: Four-point implicit finite difference scheme. Called from subroutines PLANE and CHANNL.
14. ITER: Newton-Raphson iteration scheme to solve general nonlinear equations of the form $F(x) = 0$. Called from subrouting IMPLCT.
15. IMPOCF: Calculates a residual function for an assumed depth h in the iterative solution of depth along a plane. Called from IMPLCT thru ITER.
16. IMPCHA: Calculates a residual function for an assumed area in the iterative solution for cross-sectional area in a trapezoidal channel. Called from IMPLCT thru ITER.
17. IMPCIR: Calculates a residual function for assumed value of the independent variable θ in the iterative solution for cross-sectional area in a circular channel. Called from IMPLCT thru ITER.
18. IMPAUB: Calculates a residual function for an assumed area in the iterative solution for the upper bound area of a trapezoidal channel, given an upstream discharge. Called from ADD thru ITER.
19. ERROR: Prints appropriate error messages.

PROGRAM INPUT

The watershed is first divided into cascades of rectangular planes contributing to a network of triangular, trapezoidal, or circular channels, as described in the main portion of this report.

Input data are read by SUBROUTINE READER in an order specified by NAMELIST and DATA declarations.

Example 1. As an example, consider the input cards for the hypothetical watershed shown in Fig. A-1. In this example, the plane, element number 1, contributes lateral inflow to a trapezoidal channel, element number 2.

Identification Card. From the comment cards in SUBROUTINE READER, we find that the data cards are preceded by a card, which may contain up to 80 columns of alphanumeric identifying information. For this example, the information card will be as shown below:

Col.	1	. . . . .
	b*	EXAMPLE 1 IMPERVIOUS PLANE AND TRAPEZOIDAL CHANNEL

*b indicates a blank column

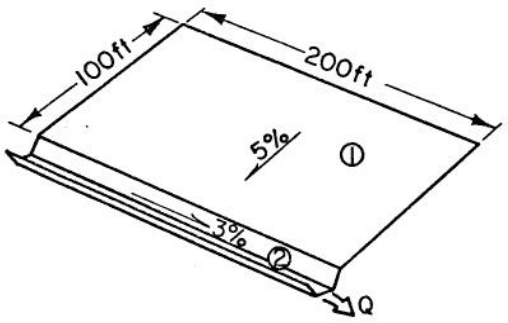

Fig. A-1 Hypothetical Watershed

Card 1. From the comment cards in the program listing, Appendix B, we find that the first data card contains the variables for NAMELIST BEGIN, where: NELE is the number of elements in the system (in this case, 2). The maximum NELE allowable in this program is 20. This can be increased by modifying COMMON and DATA statements and part of subroutine INSPEC. NRES is a resistance law code that allows considerable freedom in choosing the hydraulic resistance law to be used. From the comments in SUBROUTINE PLANE, we find that we have the following four choices for a plane:

NRES = 1: a Manning Law will be used,
NRES = 2: a Laminar Law will be used until the Reynolds number exceeds a certain value, then Manning's Law will be used,
NRES = 3: a Laminar Law will be used until the Reynolds number exceeds a given value, then the Chezy Law will be used,
NRES = 4: the Chezy Law will be used.

For plane 1, let us assume that we will use the Laminar-Manning Law, therefore, NRES = 2. The Manning Law will automatically be used for channels with this option.

CLEN is a characteristic length that is used within the program to choose the length of Δx increments in the finite difference solutions. It should normally be set equal to the sum of the lengths of the longest cascade of planes in the system or the longest single channel, whichever is greatest. The number of Δx increments is then:

NK = MAX1(15*XL(J)/CLEN,3)

For this example, CLEN = 200 ft.

TFIN is the desired maximum duration of the runoff event (in seconds, minutes or hours). Assume for this example that we wish the program to stop after it has computed a runoff hydrograph with a duration of 60 min. from the beginning of the rain.

DELT is the desired time increment for computations and for print-out of the hydrograph. The choice of DELT depends on the time resolution of the rainfall input data and the response time of the system. For this example, choose DELT = 2 min.

THETA is the weighting factor in the implicit numerical solution. When THETA = 0.5 the x-derivatives are computed by an average of the derivatives at time steps i and i+1 . If THETA = 1, the x-derivatives are computed entirely from the derivatives at time i+1 . We will use THETA = 0.8.

TEMP is the water temperature in degrees Fahrenheit, used to compute the kinematic viscosity for laminar flow computations. If TEMP is not entered, a default value of 65° is used. We will use the default value.

Card 1 will be as shown below:

Cols.	1	2 . . . . .
	b	$ BEGIN NELE = 2, NRES = 2, CLEN = 200., TFIN = 60., DELT = 2., THETA = 0.8 $

Card 2. Card 2 contains the variables and parameters for NAMELIST OPTION where: NØPT is a code reserved to allow an optimization subroutine to be added. When NØPT = 0 the program is in the prediction mode. When NØPT = 1 the reading sequence includes observed time-discharge data, which can be used to calculate an objective function. The friction parameters could be optimized by including a new subroutine. THIS OPTION IS NOT OPERATIVE IN KINGEN 75 SO NØPT = 0.

NTIME is a time units code referring to the time units of input and output data.

$$\text{NTIME} = \begin{cases} 1 - \text{seconds} \\ 2 - \text{minutes} \\ 3 - \text{hours.} \end{cases}$$

In this case, the input data were in minutes so NTIME = 2.

NUNITS is a code referring to input units (all internal calculations are done in English units).

$$\text{NUNITS} = \begin{cases} 1 - \text{English} \\ 2 - \text{Metric.} \end{cases}$$

Rainfall rates in English units are in inches per hours and all lengths are in feet. Metric rainfall rates assume centimeters per minutes, and all lengths must be in meters. Input data for this example are in English units so NUNITS = 1. Card 2 is shown below:

Cols.	1	2. . . . .
	b	$ OPTION NØPT = 0, NTIME = 2, NUNITS = 1 $

Card 3. Card 3 contains the data for NAMELIST ORDER.

NLØG(I), I = 1, NELE contains the index number assigned to planes and channels in the order in which computations should proceed. It is not necessary that NLØG(I+1) = NLØG(I)+1; however, the outflow hydrographs of all elements contributing as lateral inflow or upstream inflow to the element J must be computed before the computations can proceed for element J . Card 3 is shown below:

Cols.	1	2. . . . .
	b	$ ORDER NLØG(1) = 1,2, $

Note that the index (1) is required for this array.

Card 4. Card 4 contains data describing an element of the cascade as specified by NAMELIST FIRST.

J is the index number of the element for the plane in the example J = 1 .

NU is the number of the plane element contributing to the upstream boundary of element J . If element J is the uppermost in a cascade of planes, NU = 0 .

NR is required for channels and is the number of the plane contributing lateral inflow to the right side of the channel. NR is omitted for a plane element.

NL refers to the plane contributing to the left side of the channels. NL is omitted for a plane element.

NC1 and NC2 refer to the numbers of channels contributing at the upstream boundary of a channel. For this example, they may be omitted for element 1.

NCASE is a code to indicate the type of channel cross section. NCASE may be omitted for element 1.

NPRINT is a code used to obtain or suppress print-out of output from any element.

NPRINT = 1 - No print-out
2 - Outflow hydrograph and interim computational data will be printed.

We will select the no print-out option for plane 1. NPRINT = 1. Card 4 is shown below:

```
Cols.  |1| 2. . . . . .
       |b| $ FIRST J = 1, NU = 0, NPRINT = 1 $
```

Card 5. Card 5 contains element geometry and hydraulic roughness data as specified by NAMELIST SECOND.

J is the element number.

XL is the length of the plane in appropriate units. For this example, XL = 100 ft.

W is the width of the element. For element 1, W = 200 ft.

S is the slope. S = 0.05.

ZR , ZL , A , and DIAM are not required for plane elements.

R1 is the turbulent law roughness parameter (Manning's n in this case). If we assume that plane 1 is covered with asphalt, an appropriate Manning's n is 0.013.

R2 is the laminar law parameter (K in the expression $f = \frac{K}{R}$ where f is the Darcy-Weisbach friction factor and R is the Reynolds number). A K value of 80 is within the range shown in Table A-1. R2 is omitted if only a turbulent law is used. Friction parameters listed in Table A-1 were obtained from experiments reported in the literature and are generally representative of very small areas. If a plane is used to represent a section of watershed larger than about two acres, the friction parameter must be adjusted (see Lane, Woolhiser and Yevjevich, 1975).

FMIN is the minimum (steady state) infiltration rate for a plane. We will assume that the asphalt plane is impervious.

Table A-1 Resistance Parameters for Overland Flow[1/]

Surface	Laminar Flow K_o	Turbulent Flow Manning's n	Turbulent Flow Chezy C ($ft^{1/2}/sec$)
Concrete or Asphalt	24 - 108	.01 - .013	73 - 38
Bare Sand	30 - 120	.01 - .016	65 - 33
Graveled Surface	90 - 400	.012 - .03	38 - 18
Bare Clay-Loam Soil (eroded)	100 - 500	.012 - .033	36 - 16
Sparse Vegetation	1000 - 4,000	.053 - .13	11 - 5
Short Grass Prairie	3000 - 10,000	.10 - .20	6.5 - 3.6
Bluegrass Sod	7000 - 40,000	.17 - .48	4.2 - 1.8

Card 5 is shown below:

```
Cols.  |1|2. . . . . .
       |b|$ SECOND  J = 1, XL = 100., W = 200., S = 0.05, R1 = 0.013,
       | |R2 = 80., FMIN = 0. $
```

Card 6. Card 6 normally contains the infiltration parameters for a plane as specified by NAMELIST THIRD. FOR THIS EXAMPLE, the plane is impervious (FMIN = 0) so NAMELIST THIRD is omitted. An example with infiltration will be considered subsequently. The plane element has been completely described, so Card 6 will contain data describing the channel, element 2.

As described for Card 4, J = 2 , NU = 0 , and NR = 0 . In this example, plane 1 contributes lateral inflow to the left side of channel 2 so NL = 1 . NC1 and NC2 are omitted because no channels contribute to the upstream boundary of channel 2.

From the comments in subroutine CHANNL, the code NCASE indicates the type of channel cross section.

NCASE = 1 Trapezoidal cross section.
NCASE = 2 Circular cross section.
NCASE = 3 Has been reserved for input of irregular cross sections. IT IS NOT OPERATIVE IN KINGEN 75.

Use of NCASE = 3 will result in a programmed stop. In this example, NCASE = 1.

We will select the print-out option for the channel so NPRINT = 2.

Card 6 is shown below:

```
Cols.  |1|2. . . . . .
       |b|$ FIRST  J = 2,  NU = 0,  NR = 0,  NL = 1,  NC1 = 0,
       | |NC2 = 0,  NCASE = 1,  NPRINT = 2 $
```

[1/] From Woolhiser, D. A. "Simulation of Unsteady Overland Flow." Chapter 12 in Unsteady Flow in Open Channels. Water Resources Publication, Fort Collins, Colorado, 1975.

Card 7. Card 7 contains element geometry and hydraulic roughness data for channel 2 as specified by NAMELIST SECOND.

As described for Card 5, J = 2 and XL = 200.. The width W is set equal to zero, indicating that this element is a channel. S = 0.03. ZL, ZR and A are defined in Fig. A-2.

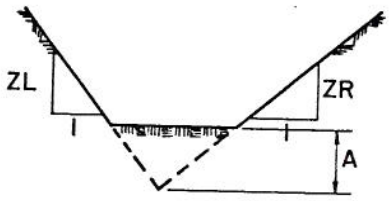

Fig. A-2 Trapezoidal Channel Geometry. (Looking downstream)

For this example, we will assume that ZR = ZL = 1. and that A = 1. Thus, we have a trapezoidal channel with 1:1 side slopes and a 2-ft. bottom width. If the channel is triangular, A should be set equal to a very small number rather than zero to avoid problems in a function subroutine. DIAM is the diameter of a circular channel and may be omitted for this case.

R1 is the turbulent law roughness parameter for the channel. Because we have chosen the Laminar-Manning Law, it will be Manning's n. Choose R1 = 0.013 for this example. R2 may be omitted for the channel and FMIN = 0.0 for a channel.

Card 7 is shown below:

Cols.	1	2 . . . . .
	b	$ SECOND J = 2, XL = 200., W = 0, S = 0.03, ZL = 1.0, ZR = 1.0, A = 1.0, R1 = 0.013, FMIN = 0.0 $

Card 8. All of the geometric data and parameters for the watershed itself have now been provided. Card 8 contains rainfall data as specified by NAMELIST RAIN. Let us assume that the rainfall intensity histogram for the event of interest is shown in Fig. A-3.

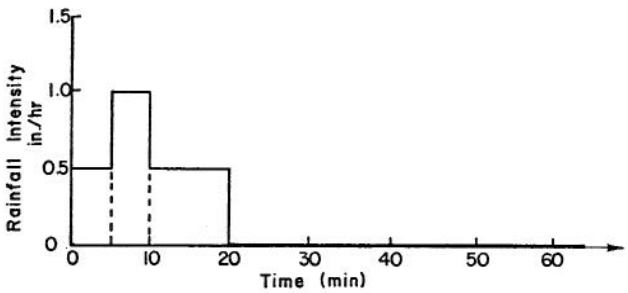

Fig. A-3 Rainfall Intensity Histogram

QI(I) is the rainfall rate (iph or cm/min). TI(I) is the time at which the corresponding rainfall rate begins. ND is the number of rainfall data pairs.

Card 8 is shown below:

Cols.	1	2. . . . .
	b	$ RAIN QI(1) = 0.5, 1.0, 0.5, 0.0, 0.0, TI(1) = 0.0, 5.0, 10.0, 20.0, 65., ND = 5 $

Note that the subscript 1 (one) is required for arrays QI and TI . TI(ND) should be greater than TFIN shown on Card 1 so that the rainfall rate is defined throughout the event.

Because the optimization option is inoperative in KINGEN 75, NAMELIST RAIN is the last item of input.

Example 2. WATERSHED WITH INFILTRATION, BRANCHED CHANNELS AND CIRCULAR CONDUIT. In this example, use of an infiltrating plane, branched channels, and a circular conduit will be illustrated. The seven element model is shown schematically in Fig. A-4. The impervious plane-channel pair of the previous example will be used as elements 1 and 2. Necessary data cards will be shown and comments given where the options are different from those explained in the previous example.

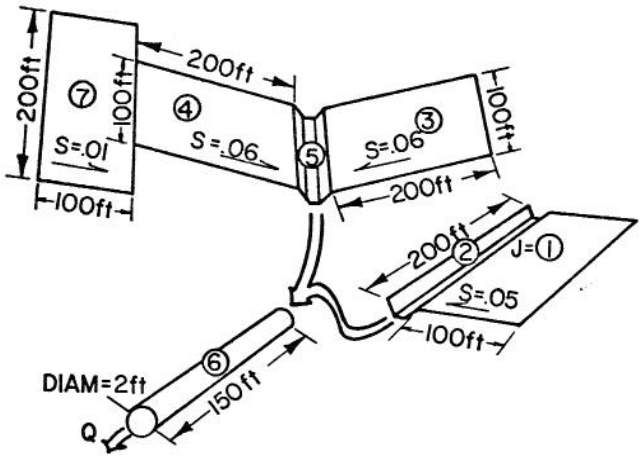

Fig. A-4 Elements Used in Example 2

Identification Card.

Cols.	1	2. . . . .
	b	EXAMPLE 2. INFILTRATING PLANE AND BRANCHED CHANNEL CASE WITH CIRCULAR CONDUIT

Card 1.

Col.	1.	. . . . .
	b	$ BEGIN NELE = 7, NRES = 2, CLEN = 300., TFIN = 90., DELT = 2., THETA = 0.8 $

TFIN has been increased in anticipation of longer recession from a hydraulically rougher, grassed surface, and a larger watershed.

Card 2. Same as in previous example.

Card 3. As indicated in Fig. A-4, the order would proceed as shown:

Col.	1	. . . . .
	b	$ ORDER NLOG(1) = 1, 2, 3, 7, 4, 5, 6 $

Card 4. Same as in previous example.

Card 5. Same as in previous example.

Card 6.

Cols.	1	2. . . . .
	b	$ FIRST J = 2, NU = 0, NR = 0, NL = 1, NC1 = 0, NC2 = 0, NCASE = 1, NPRINT = 1 $

We have deleted printout as this is now an intermediate output.

Card 7. Same as in previous example.

Card 8. The second channel (element 5) drains two infiltrating planes, (elements 3 and 4) each 100 ft. wide, and 200 ft. long. The right plane is the element 3, and Card 9 will be the same as Card 4 (except J = 3), since this plane also is the most upstream element and contributes to a channel.

Cols.	1	2. . . . .
	b	$ FIRST J = 3, NU = 0, NPRINT = 1 $

Card 9. The data on this card specify the geometry for plane three, and asymptotic ($t \to \infty$) infiltration rate FMIN (as an indicator of whether this surface is impervious or pervious). FMIN must be in the same units as the rainfall, given later, as indicated on Card 2 by parameter NUNITS. Its value is found in this example, from an infiltrometer experiment as explained below. R1 and R2 have been chosen from Table A-1 to approximately represent a sparsely vegetated rangeland watershed.

Cols.	1	2. . . . .
	b	$ SECOND J = 3, XL = 200., W = 100., S = 0.06, R1 = 0.05, R2 = 2000., FMIN = 0.2362 $

Card 10. The infiltration parameters for the model outlined by Eqs. (3-56), (3-60), and (3-64) in Chapter 3 are specified by data in NAMELIST THIRD. Table A-2 summarizes the parameters describing infiltration from Chapter 3 and their corresponding computer names. To illustrate the determination of these parameters from field data, we shall here assume that an infiltrometer experiment has been performed on the same soil type, and the data shown in Table A-3 have been obtained.

The basic model parameters are obtained from this infiltrometer data in the following manner. First, a log-log plot of $t - t_o$ vs. $f - f_\infty$ is made with initial estimates of t_o and f_∞. This is essentially a graphical fitting of the data to Eq. (3-53), and is demonstrated in Fig. A-5. From Table A-2, apparently $2 < \hat{t}p < 3$, and a reasonable first estimate for t_o is $1/2\ t_p$. Apparently, f_∞ is less than .028 cm/min. and t_o and f_∞ are varied to obtain a reasonably straight line. The process is aided by noting that estimates of f_∞ that are too large or too small affect the curve at the lower end (t large) of the data, and, conversely, the curve is sensitive to estimates of t_o at the opposite (t small) end. The user is cautioned that large infiltrometer plots incorporate considerable storage delay into measurements of the plot outflow, which will bias the infiltration parameters, unless this is corrected. This as well as natural soil variability cause response curves typically not to exhibit the sharp break at $t = t_p$ shown in Fig. 3-5.

As shown in Fig. A-5, a line has been fitted to the data of Table A-2 using $t_o = 1.3$ and $f_\infty = 0.01$ cpm. The intersection of this line with the horizontal line representing $i = 0.1596$ cpm is at $t_p - t_o \simeq 1.45$, or $t_p = 2.75$ min. The slope of the line is $\alpha = -0.51$, and A is the value of $f - f_\infty$ when $t - t_o = 1.0$, here found to be 0.185 cpm.

Table A-2 Infiltration Model Parameters

Infiltration Parameter, (Chapter 3)	Reference in text, Chapter 3	Computer Program symbol	Definition	Units	limiting values, if any
α	Eq.(3-53)	AL	exponent parameter for decay curve	none	$0<\alpha<1$
B_p	Eq.(3-60)	B_p	ponding time parameter	dimensionless time	$0<B_p$
C_1	Eq.(3-64)	C	infiltration scaling parameter	time,(min)*	$0<C$
S_i	Eq.(3-64)	SI	initial volumetric relative water content	-	$0<S_i<<S_o$
S_o	Eq.(3-64)	SMAX	maximum volumetric water content under imbibition	-	$\sim.5<S_o<1.0$
v_r	Eq.(3-65)	ROC	volumetric relative rock content	-	$0<ROC<<1.0$

*minutes are used in subroutine only. Input option NTIME will govern data units used.

Table A-3 Example Infiltrometer Data
i = 0.1596 cm. per min.

Time (minutes)	Infiltration Rate (cm/min)
0	.1596
1	.1596
2	.1596
3	.150
4	.106
5	.099
7	.076
9	.073
12	.068
15	.062
20	.053
30	.047
50	.034
100	.028

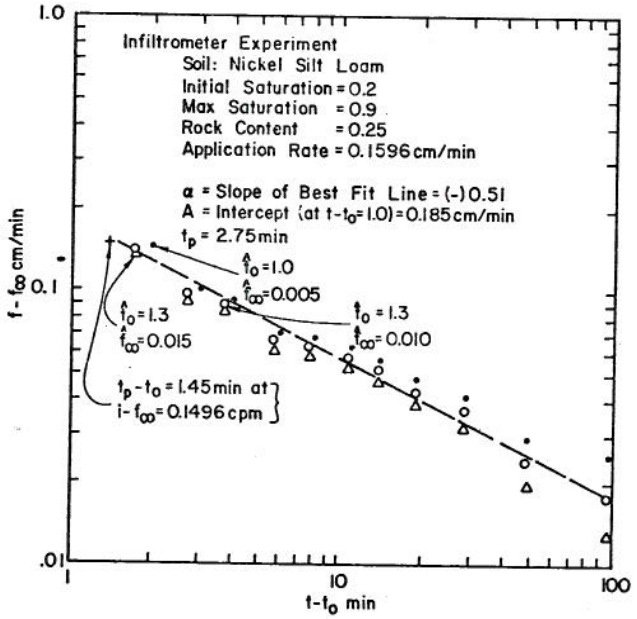

Fig. A-5 Graphical Fitting of Infiltrometer Data to Determine Infiltration Parameters α, A, t_o, and f_∞

Now Eq. (3-55) is used to determine T_o:

$$T_o = \frac{0.185}{(1-0.51)(.01)}^{1/.51} = 1236 \text{ min.}$$

T_o is used in Eq. (3-65) with v_r (which must be measured) and the measured variables S_i and S_{max} from the infiltrometer experiment data to obtain C_1:

$$C_1 = T_o/(S_o-S_i)/(1-v_r)$$

$$= 1236/(.9-.2)/(1-0.2)$$

$$= 2207 \text{ min.}$$

B_p is obtained by solving Eq. (3-60). F_{p*} is first obtained as

$$F_{p*} = i_* t_{p*} = \frac{i}{f_\infty}\frac{t_p}{T_o} = \frac{.1596}{.01}\frac{2.75}{1236} = .03551$$

Then from Eq. (3-60),

$$B_p = \frac{.03551}{\ln \frac{15.96}{14.96}} = .549$$

This completes the determination of necessary infiltration parameters. The data Card 10, for plane 3 will look thus:

Cols.	1	2 . . . . .
	b	$ THIRD J = 3, AL = 0.51, B = 0.55, C = 2207., SI = 0.6, SMAX = 0.9, RØC = 0.2 $

Note that FMIN on Card 9 is the IPH equilalent to 0.01 cpm of this example, and SI for the simulation problem is quite independent of the soil saturation SI from the infiltrometer experiment.

The remaining cards are prepared as described in the previous example.

Card 11.

Cols.	1	2. . . . .
	b	$ FIRST J = 4, NU = 7, NPRINT = 1 $

Card 12.

Cols.	1	2. . . . .
	b	$ SECOND J = 4, XL = 200., W = 100, S = 0.06, R1 = 0.05, R2 = 2000., FMIN = .2362 $

Card 13.

Cols.	1	2. . . . .
	b	$ THIRD J = 4, AL = 0.51, B = 0.55, C = 2207., SI = 0.6, SMAX = 0.9, RØC = 0.2 $

Card 14.

Cols.	1	2. . . . .
	b	$ FIRST J = 5, NU = 0, NR = 4, NL = 3, NC1 = 0, NC2 = 0, NCASE = 1, NPRINT = 1 $

Card 15.

Cols.	1	2. . . . .
	b	$ SECOND J = 5, XL = 100., W = 0., S = 0.04, ZL = 2., ZR = 2., A = 0.5, R1 = 0.020, FMIN = 0. $

Note that we have specified a channel with 1:2 side slopes and 0.5-ft. bottom width.

Card 16. The last element is to be a round conduit receiving input from channels 2 and 5. The card reads as follows:

Cols.	1	2. . . . .
	b	$ FIRST J = 6, NU = 0, NR = 0, NL = 0, NC1 = 2, NC2 = 5, NCASE = 2, NPRINT = 2 $

Card 17. We will use a 2.0 foot diameter conduit 150 feet long.

Cols.	1	2. . . . .
	b	$ SECOND J = 6, XL = 150., W = 0., S = 0.02, DIAM = 2.0, R1 = 0.012, FMIN = 0. $

Cards 18, 19. Plane no. 7 might conceptually be a parking lot contributing to a swale composed of planes 3 and 4 and channel 5. It is used here to illustrate both cascading of planes with disparate widths, and the flow from an impervious to a pervious plane, which the infiltration subroutine is designed to treat explicitly (statements 127 to 133). The plane will be assumed as follows:

Cols.	1	2. . . . .
	b	$ FIRST J = 7, NU = 0, NPRINT = 1 $
		$ SECOND J = 7, XL = 100, W = 200, S = 0.01, R1 = .012, R2 = 100., FMIN = 0. $

Card 20. We have finished describing the watershed and this card will contain rainfall data. We will use the same rainfall as in the previous example, but the time TI(ND) must again extend beyond TFIN. As specified by NUNITS, our dimensions are in inches per hour.

Cols.	1	2. . . . .
	b	$ RAIN QI(1) = 0.5, 1.0, 0.5, 0.0, 0.0, TI(1) = 0.0, 5.0, 10.0, 20.0, 95.0, ND = 5 $

PROGRAM OUTPUT

A portion of the computer output for the first example is shown in Fig. A-3. The identifying information and the rainfall data are shown first. HTRANS and QTRANS are the depth and discharge, respectively, at which the laminar flow equation and the Manning equation intersect. The next line shows MBT and NB. MBT is the index number in the temporary time-discharge storage vectors, QS(I), TS(I) where the hydrograph from the next element to be computed will be stored. NB(I) is the index number of the storage vector where the output from the element being computed is temporarily stored. This location information is only required for debugging if program changes are made. The message "plane No. 1 processes" means that all computations have been completed for this element. Any unprogrammed stop would then be caused by problems associated with the next element. The printout of the geometric parameters allows one to check the accuracy of input data.

The next several lines of output are optional and were printed by setting NPRINT = 2 in Card 6. A2(K), K = 1, NK is the cross-sectional area in square feet at each node point of channel 2 at the time (T(I)(in seconds)). QL(I) is the lateral inflow rate in cubic feet per second/ft. If this print-out is requested for a plane, the depth in feet is given for each node point. This information is normally not required but may be useful in special cases or if problems develop.

The final hydrograph, the volume of rainfall input and the volume of runoff are all printed automatically.

PROGRAM LISTING

A complete listing of KINGEN 75 follows. A card deck of this program in 026 code can be obtained before December 31, 1978 for the cost of cards, duplication, and postage by writing to:

Secretary, CSU Hydrology Papers
Engineering Research Center
Colorado State University Foothills Campus
Fort Collins, Colorado 80523

REFERENCE

Lane, Leonard J., D. A. Woolhiser, and V. M. Yevjevich. Influence of Simplifications in Watershed Geometry in Simulation of Surface Runoff. CSU Hydrology Paper No. 81, December 1975, 50 pp.

APPENDIX B

PROGRAM LISTING — KINGEN 75

```
      PROGRAM MAIN (INPUT,OUTPUT,TAPE5=INPUT,TAPE6=OUTPUT,DEBUG=OUTPUT)
      COMMON /IO/ IREAD,IWRITE
      COMMON /CNTRL/ NRES,NOPT,NTIME,NUNITS,NELE,CLEN,DELT,NLOG(20)
      COMMON /GEOM/ XL(20),W(20),S(20),R1(20),R2(20),FMIN(20),NL(20),NR(
     120),ND(20),NC1(20),NC2(20),NCASE(20),ZL(20),ZR(20),A(20),DIAM(20),
     2NP(20)
      COMMON /EVENT/ TFIN,ND,QI(100),TI(100),QOB(100),TOB(100),NO,SUMRCM
      COMMON /PLANE1/ H1(50),H2(50),QL(100),ALPHA(50),POWER(50),T(100),Q
     1(100),HUB(100),DX,DT,INDEX,THETA,ANU,GRAV,NB(20),QS(500),LENQ,LENQ
     2S,LENH1,L,QL1(50),QL2(50)
      COMMON /CIRC/ TH1(50),TH2(50),SIN1(50),SIN2(50),COS1(50),COS2(50),
     1SINIA,SIN2A,COS1A,COS2A,THUB(100),DFAC,UFAC,D
      COMMON /CHAN/ A1(50),A2(50),QUB(100),AUB(100),CO1,CO2,B,NI,NOQL
      COMMON /INFIL/ AL(20),BI(20),C(20),SI(20),SMAX(20),ROC(20)
      COMMON /LAWS/ ATURB,PTURB,ALAM,PLAM,HTRANS,WTRANS
      DIMENSION QD(100), QD2(100), QD3(100)
      DATA XL,W,S,R1,R2,FMIN,NL,NA,NU,NC1,NC2,NCASE,ZL,ZR,A,DIAM/20*-1.,
     120*-1.,20*0.,20*0.,20*0.,20*0.,20*0.,20*0.,20*0.,20*0.,20*0.,20*0.
     2,20*0.,20*-1.,20*0./
      DATA AL,B1,C,SI,SMAX,ROC/120*0./
      AREA=0.0
      CALL READER
      DO 105 I=1,NELE
         J=NLOG(I)
         AREA=AREA+W(J)*XL(J)
         IF (W(J).NE.0) CALL PLANE (J)
         IF (W(J).EQ.0) CALL CHANNL (J)
  105 CONTINUE
      CALL CONVERT (2)
      SUMRO=0.
      DO 110 L=1,NI
         QD(L)=Q(L)*AREA/43200.
         SUMRO=SUMRO+QD(L)*DELT
         QD2(L)=Q(L)*0.04233
  110 QD3(L)=QD(L)*0.028317
      AREM=AREA*.092951
      WRITE (IWRITE,135) AREA,AREM
      GO TO (115,120,125), NTIME
  115 WRITE (IWRITE,140) (T(L),QD(L),Q(L),QD2(L),QD3(L),L=1,NI)
      GO TO 130
  120 WRITE (IWRITE,145) (T(L),QD(L),Q(L),QD2(L),QD3(L),L=1,NI)
      GO TO 130
  125 WRITE (IWRITE,150) (T(L),QD(L),Q(L),QD2(L),QD3(L),L=1,NI)
  130 WRITE (IWRITE,155)
      SUMINCH=SUMRCM/2.54
      SMROIN=SUMRO/AREA*12.
      SMROCM=SMROIN*2.54
      SMROM=SUMRO*.028317
      WRITE (IWRITE,160) SUMINCH,SUMRCM
      WRITE (IWRITE,165) SMROIN,SMROCM,SUMRO,SMROM
      STOP
C
  135 FORMAT (20X,11HTOTAL AREA=,F20.5,12HSQ. FT.,  OR,F20.5,11H SQ. MET
     1ERS#/)
  140 FORMAT (35X,23H FINAL TOTAL HYDROGRAPH,/31X,10H TIME(SEC),20X,6HQ(
     1CFS),6X,6HQ(IPH),6X,6HQ(CPM),6X,7HQ(M3PS),/(31X,F7.2,21X,F8.5,4X,F
     28.6,4X,F8.6,4X,E10.4))
  145 FORMAT (35X,23H FINAL TOTAL HYDROGRAPH,/31X,10H TIME(MIN),20X,6HQ(
     1CFS),6X,6HQ(IPH),6X,6HQ(CPM),6X,7HQ(M3PS),/(31X,F7.2,21X,F8.5,4X,F
     28.6,4X,F8.6,4X,E10.4))
  150 FORMAT (35X,23H FINAL TOTAL HYDROGRAPH,/31X,10H TIME(HRS),20X,6HQ(
     1CFS),6X,6HQ(IPH),6X,6HQ(CPM),6X,7HQ(M3PS),/(31X,F7.2,21X,F8.5,4X,F
     28.6,4X,F8.6,4X,E10.4))
  155 FORMAT (1H ,//48X,31HEVENT TOTALS - INPUT AND OUTPUT)
  160 FORMAT (1H ,/9X,17HRAINFALL DEPTH = ,F7.3,12H INCHES, OR ,F7.3,4H
     1CM.,#//)
  165 FORMAT (1H ,28X,6HINCHES,5X,3HCM.,5X,15HCU.FT.     CU.M.,/9X,12HTOT
     1AL RUNOFF,4X,F10.4,1X,F9.4,1X,F8.2,2X,F8.3)
C
      END
      SUBROUTINE READER
      COMMON /IO/ IREAD,IWRITE
      COMMON /CNTRL/ NRES,NOPT,NTIME,NUNITS,NELE,CLEN,DELT,NLOG(20)
      COMMON /EVENT/ TFIN,ND,QI(100),TI(100),QOB(100),TOB(100),NO,SUMRCM
      COMMON /PLANE1/ H1(50),H2(50),QL(100),ALPHA(50),POWER(50),T(100),Q
     1(100),HUB(100),DX,DT,INDEX,THETA,ANU,GRAV,NB(20),QS(500),LENQ,LENQ
     2S,LENH1,L,QL1(50),QL2(50)
      DIMENSION KARD(8)
      NAMELIST  /BEGIN/ NELE,NRES,CLEN,TFIN,DELT,THETA,TEMP
      NAMELIST  /OPTION/ NOPT,NTIME,NUNITS
      NAMELIST  /ORDER/ NLOG
      NAMELIST  /FIRST/ J,NU,NR,NL,NC1,NC2,NCASE,NPRINT
      NAMELIST  /SECOND/ J,XL,W,S,ZR,ZL,A,DIAM,H1,R2,FMIN
      NAMELIST  /THIRD/ J,AL,B,C,SI,SMAX,ROC
      NAMELIST  /RAIN/ QI,TI,ND
      NAMELIST  /OBSERVV/ QOB,TOB,NO
      DATA IREAD,IWRITE/5,6/
      DATA NELE,NRES,CLEN,TFIN,DELT,TEMP,THETA/0,0,0.,0.,0.,0.,0.,0.7/
      DATA NLOG/20*0/
      DATA NOPT,NTIME,NUNITS/0,0,0/
      DATA NU,NR,NL,NC1,NC2,NCASE,NPRINT/0,0,0,0,0,0,1/
      DATA XL,W,S,ZR,ZL,A,DIAM,R1,R2,FMIN/-1.,-1.,0.,0.,0.,-1.,0.,0.,0.,
     10./
      DATA AL,B,C,SI,SMAX,ROC/6*0./
      DATA QI,TI,QOB,TOB,ND,NO/100<0.,100*0.,100*0.,100*0.,0.0/
C
C  ******************************************************************
C
C     READ IN DATA - DATA DECK SHOULD BE COMPOSED AS FOLLOWS
C     READ IN IDENTIFYING INFORMATION   80 COLUMNS OF ALPHANUMERIC INFO
C
      READ (IREAD,185) (KARD(I),I=1,8)
      IF (EOF(IREAD)) 105,110,105
  105 STOP
  110 WRITE (IWRITE,190) (KARD(I),I=1,8)
C
C         CARD1 - CONTAINS VARIBLES LISTED FOR NAMELIST/BEGIN
C         CARD2 - CONTAINS VARIBLES LISTED FOR NAMELIST/OPTION
C         CARD3 - CONTAINS VARIBLES LISTED FOR NAMELIST/ORDER
C         CARD4 - 1ST CARD OF INFO FOR ELEMENT J- CONTAINS INFO FOR OTHE
C                 CONTRIB ELEMENTS AND CHANNEL TYPE- SEE NAMELIST/FIRST
C         CARD5 - 2ND CARD OF INFO FOR ELEMENT J - CONTAINS ELEMENT
C                 GEOMETRY AND ROUGHNESS COEF - SEE NAMELIST/SECOND
C         CARD6 - OPTIONAL 3RD CARD OF INFO CONTAINING INFILTRATION
C                 CHARACTERISTICS OF PLANES - SHOULD NOT BE INPUT IF
C                 FMIN(J)=0.
C       CARDS 7-8,9-10...(N-3)-(N-2)  PAIRS OF CARDS FOR OTHER
C       ELEMENTS - SEE CARDS 4 AND 5
C       CARD(N-1) CONTAINS RAINFALL DATA OF STORM - SEE NAMELIST/RAIN
C       CARD(N) - CONTAINS OBSERVED RUNOFF FOR OPTIMIZATION IF DESIRED
C                 CARD IS OPTIONAL - SEE NAMELIST/OBSERV
C     THE FOLLOWING EXAMPLE CARDS ILLUSTRATE INPUT FOR CARDS 3,5,AND N-1
C
C     $OPTION  NLOG(1)=1,2,6,8,12,13,15,     $
C     $SECOND J=1,XL=200.,W=40.,S=0.05,R1=36.,R2=100., $
C     $RAIN QI(1)=1.,2.,0.,0.,TI(1)=0.,35.,200.,400.,ND=4  $
C
C     IN REGARDS TO DATA CARDS
C         1 - COLUMN 1 MUST BE BLANK FOR ALL DATA CARDS.
C          2 - EACH RECORD(EACH READ STATEMENT) MUST BEGIN WITH $ IN
C              COLUMN 2 AND END WITH $ AFTER ALL DATA HAS BEEN CODED.
C         3 - EACH RECORD MUST BE IDENTIFIED WITH A NAMELIST GROUP NAME
C             IMMEDIATELY FOLLOWING THE FIRST $.
C         4 - A MAX. OF 150 CHARACTERS ARE ALLOWED FOR EACH RECORD - THE
C             EXTRA CARD, IF NEEEDED, STARTS IN COL.2 (NOTHING IN COL.1)
C         5 - NO SUBSCRIPTS ON VARIABLES CAN BE USED ON NAMELIST/FIRST
C             AND NAMELIST/SECOND DATA CARDS (EVEN THOUGH THEY ARE SUB-
C             SCRIPTED LATER IN THE PROGRAM)
C         6 - THE SUBSCRIPT (1) IS REQUIRED FOR INPUT OF  ARRAYS NLOG,
C             QI,TI,QOB,AND TOB (SEE EXAMPLE DATA CARDS FOR ORDER AND
C             RAIN NAMELIST GROUP DATA INPUT CLAHIFICATION)
C         7 - ALL ASSIGNMENTS MUST BE FOLLOWED BY A COMMA,   EXCEPT  THE
C             LAST ONE.
C         8 - VARIABLES MAY BE LISTED IN ANY ORDER OR MAY BE OMITTED IF
C             NOT NEEDED FOR THE SITUATION - OMITTED VARIABLES WILL BE
C             SET TO ZERO - ERROR MESSAGES WILL BE ISSUED BY PROGRAM IF
C             ZERO IS NOT ALLOWED FOR A PARTICULAR VARIABLE.
C         9 - CARD PAIRS FOR EACH ELEMENT CAN BE ARRANGED IN ANY ORDER -
C             PROCESSING WILL STILL OCCUR AS SPECIFIED BY NLOG - HOWEVER
C             FIRST MUST PRECEED SECOND FOR EACH J ELEMENT.
C
C         10- A VALUE FOR J MUST BE SPECIFIED ON BOTH FIRST AND SECOND
C         11- A MAX OF 20 ELEMENTS MAY BE INPUT.
C         12 - DO NOT INPUT NAMELIST GROUP THIRD IF FMIN(J)=0 IN SECOND.
C
C     INPUT VARIABLES
C        NELE= NUMBER OF ELEMENTS, NRES=RESISTENCE LAW CODE(SEE COMMENTS
C        IN PLANE),CLEN=CHARACTERISTIC LENGTH,TFIN=TIME TO END PROCESS,
C        DELT=TIME INCREMENT FOR OUTPUT,TEMP=WATER TEMP.(IN DEGREES F-
C        DEFAULT IS 65F),THETA=WEIGHTING FACTOR IN IMPLICIT SOLUTION
C        FORMULAS (DEFAULT VALUE IS 1.)
C        NOPT-OPTIMIZATION CODE(SEE COMMENTS IN OPTIM),NTIME-TIME UNITS
C        CODE WHICH APPLIES TO INPUT( T FOR RAIN PATTERN, DELT, AND
C        INFILTRATION PARAMETH C), AND OUTPUT TIMES. CODE 1 = SEC., 2=
C        MIN., AND 3= HR.   NUNITS -ENGLISH OR METRIC UNITS CODE (1 =
C        ENGLISH -IPH, FT.  2 = METRIC -CPM, METERS
C        NLOG(20)-EACH ELEMENT OF ARRAY CONTAINS A J - WATERSHED
C        ELEMENTS ARE PROCESSED IN ORDER OF NLOG(I),I=1,NELE.
C        J-WATERSHED ELEMENT IDENTIFIER,NU(J)-J VALUE OF PLANE CONTRIB.
C        AT UPPER BOUND OF ELEMENT J,NR(J)-J VALUE OF PLANE CONTRIB. TO
C        RIGHT SIDE OF CHANNEL J,NL(J)-SAME EXCEPT TO LEFT SIDE,NC1(J)-J
C        VALUE OF CHAN. CONTRIB TO UPPER BOUND OF CHAN J,NC2(J)-SAME AS
C        NC1 (SECOND CONTRIB CHAN),NCASE(J)-CHANNEL TYPE CODE FOR CHAN J
C        (SEE COMMENTS IN CHANNL),NPRINT-PRINT CODE = 1 IF NO PRINTOUT
C         DESIRED, = 2 IF PRINTOUT DESIRED FOR THIS ELEMENT.
C        XL(J)-LENGTH OF ELEMENT J,W(J)-WIDTH OF ELEMENT J(FOR CHANNELS,
C        W(J)=0.),S(J)-SLOPE OF ELEMENT J,ZR(J)-SLOPE OF RIGHT SIDE OF
C        TRAPEZOIDAL CHANNEL J,ZL(J)-SAME AS ZR EXCEPT LEFT SIDE,A(J)-
C        WEIGHT OF EXCLUDED TRIANGLE FOR TRAPEZOID CHANNEL J,DIAM(J)-
C        DIAMETER OF CIRCULAR CHANNEL J,R1(J)-TURBULENT LAW ROUGHNESS
C        FACTOR(MANNING N OR CHEZY C) FOR ELEMENT J(REQUIRED),R2(J)-
C        LAMINAR ROUGHNESS FACTOR(REYNOLD-S K) FOR ELEMENT J (OPTIONAL),
C        FMIN(J)-MINIMUM INFILTRATION RATE FOR PLANE J,
C        AL(J),B(J),C(J) - INFILTRATION PARAMETERS DETERMINED BY SOIL
C        CHARACTERISTICS.  SEE R.E. SMITH-S PAPER IN JOURN.HYDROL.,V.17,
C        N.1/2,1972.,  SI(J) - INITIAL SOIL MOISTURE CONTENT OF PLANE J,
C        SMAX(J) - MAXIMUN MOISTURE STORAGE CAPAC. OF PLANE J, ROC(J) -
C        PERCENT ROCK CONTENT OF SOIL IN PLANE J
C        QI(100)-ARRAY CONTAINING RAINFALL RATE (IN/HR OR CM/HR)
C        TI(100)-TIMES CORRESPONDING TO QI ELEMENTS,NO-NUMBER OF RAIN-
C        FALL DATA PAIRS,QOB(100)-OBSERVED RUNOFF HYDROGRAPH FOR OPTIM-
C        IZATION (IN/HR OR CM/HR),TOB(100)-TIMES CORRESPONSING TO QOB
C        ELEMENTS,NO-NUMBER OF OBSERVED RUNOFF DATA PAIRS.
C
C     ...REMEMBER - DO NOT PUT SUBSCRIPTS ON  DATA GROUPS FIRST AND
C     SECOND .  HOWEVER, THE SUBSCRIPT (1) IS REQUIRED FOR ANY ARRAYS
C     IN DATA GROUPS ORDER,RAIN, OR OBSERV.....................
C
C  ******************************************************************
C
C     THE FOLLOWING ARE ARRAY DIMENSIONS USED AS CHECKS WITHIN THE PROGR
C     LENQS  -  SIZE OF QS
C     LENQ  -  SIZE OF Q
C     LENH1  -  SIZE OF H1
C
      LENQS=500
      LENQ=100
      LENH1=50
      GRAV=32.17
      ISUBR=6HREADER
      READ (IREAD,BEGIN)
C
C     ------------------------------
C
C     SUBROUTINE INSPEC CHECKS INPUT DATA FOR ANY OBVIOUS ERRORS OR
C     OMISSIONS.  SUBROUTINE RESET PLACES VALUES READ FROM FIRST,SECOND,
C     ,THIRD INTO THEIR APPROPRIATE ARRAY LOCATIONS IN COMMON/GEOM/INFIL
C
C     ------------------------------
C
      CALL INSPEC (1,0,0)
      READ (IREAD,OPTION)
      CALL INSPEC (2,0,0)
      READ (IREAD,ORDER)
      CALL INSPEC (3,0,0)
      JLST=NLOG(NELE)
```

```
      DO 115 I=1,NELE
         READ (IREAD,FIRST)
         JJ=J
         READ (IREAD,SECOND)
         IF (J.NE.JJ) CALL ERROR (ISUBR,5,JJ,J)
         IF (FMIN.GT.0.0001) READ (IREAD,THIRD)
         CALL RESET (J,XL,W,S,R1,R2,FMIN,NL,NR,NU,NC1,NC2,NCASE,ZR,ZL,A,
     1   DIAM,AL,B,C,SI,SMAX,ROC,NPRINT)
         CALL INSPEC (4,J,JLST)
         CALL INSPEC (6,J,0)
  115 CONTINUE
      READ (IREAD,RAIN)
      IF (TI(ND)-TFIN) 120,125,125
  120 ND=ND+1
      TI(ND)=TFIN
      QI(ND)=0.0
      WRITE (IWRITE,195)
  125 IF (NOPT.GT.0) READ (IREAD,OBSERV)
      CALL INSPEC (5,0,0)
      IF (NRES.NE.2.AND.NRES.NE.3) GO TO 130
C
C     COMPUTE KINEMATIC VISCOSITY IN SQ. FT./SEC.
C
      IF (TEMP.EQ.0.) TEMP=65.
      TEMP=(5./9.)*(TEMP-32.)
      XNU=(.00000017756/(1.+0.03368*TEMP+0.000221*TEMP*TEMP))
      XNU=XNU/(0.0254*0.0254*144.)
C
  130 DO 135 I=1,NELE
  135 NB(I)=0
      WRITE (IWRITE,200)
      GO TO (140,145,150), NTIME
  140 WRITE (IWRITE,205)
      FC=0.0166666667
      GO TO 155
  145 WRITE (IWRITE,210)
      FC=1.0
      GO TO 155
  150 WRITE (IWRITE,215)
      FC=60.
  155 SUMRCM=0.
      DO 180 I=1,ND
         GO TO (160,165), NUNITS
  160    QIE=QI(I)
         QIC=QIE*.042333
         GO TO 170
  165    QIE=QI(I)/.042333
         QIC=QI(I)
  170    WRITE (IWRITE,220) TI(I),QIE,QIC
         IF (ND-I) 180,180,175
  175    IP=I+1
         SUMRCM=SUMRCM+FC*(TI(IP)-TI(I))*QIC
  180 CONTINUE
C
C     --- CONVERT TIME INTO SECONDS AND DISCHARGE INTO CU.FT. PER SEC.
C
      CALL CONVERT (1)
      RETURN
C
  185 FORMAT (8A10)
  190 FORMAT (1H1,8A10)
  195 FORMAT (78H A POINT QI(ND+1),TI(ND+1) HAS BEEN ADDED TO RAIN DATA
     1SO THAT TI(ND+1) = TFIN)
  200 FORMAT (21H INPUT VALUES-   TIME,19X,8HRAINFALL)
  205 FORMAT (15X,5H(SEC),12X,5H(IPH),7X,8H(CM/MIN))
  210 FORMAT (15X,5H(MIN),12X,5H(IPH),7X,8H(CM/MIN))
  215 FORMAT (15X,5H(HRS),12X,5H(IPH),7X,8H(CM/MIN))
  220 FORMAT (13X,F10.2,5X,F10.3,5X,F10.5)
C
      END
      SUBROUTINE INSPEC (NREAD,J,JLST)
C
      COMMON /GEOM/ XL(20),W(20),S(20),R1(20),R2(20),FMIN(20),NL(20),NR(
     120),NU(20),NC1(20),NC2(20),NCASE(20),ZL(20),ZR(20),A(20),DIAM(20),
     2NP(20)
      COMMON /CNTRL/ NRES,NOPT,NTIME,NUNITS,NELE,CLEN,DELT,NLOG(20)
      COMMON /INFIL/ AL(20),B(20),C(20),SI(20),SMAX(20),ROC(20)
      COMMON /EVENT/ TFIN,ND,QI(100),TI(100),QOB(100),TOB(100),NO,SUMRCM
C
C     THIS SUBROUTINE INSPECTS THE INPUT DATA FOR ANY OBVIOUS ERRORS
C
      ISUBR=6HINSPEC
      GO TO (105,110,115,120,150,170), NREAD
  105 IF (NELE.EQ.0) CALL ERROR (ISUBR,3,4HNELE,0)
      IF (CLEN.EQ.0.) CALL ERROR (ISUBR,1,4HCLEN,0)
      IF (TFIN.EQ.0.) CALL ERROR (ISUBR,1,4HTFIN,0)
      IF (NRES.EQ.0) CALL ERROR (ISUBR,2,4HNRES,0)
      IF (DELT.EQ.0.) CALL ERROR (ISUBR,1,4HDELT,0)
      IF (NRES.GT.4) CALL ERROR (ISUBR,3,4HNRES,NRES)
      IF (NELE.GT.20) CALL ERROR (ISUBR,3,4HNELE,NELE)
      RETURN
  110 IF (NTIME.EQ.0) CALL ERROR (ISUBR,1,5HNTIME,0)
      IF (NUNITS.EQ.0) CALL ERROR (ISUBR,1,6HNUNITS,0)
      IF (NOPT.GT.1) CALL ERROR (ISUBR,3,4HNOPT,NOPT)
      IF (NTIME.GT.3) CALL ERROR (ISUBR,3,5HNTIME,NTIME)
      IF (NUNITS.GT.2) CALL ERROR (ISUBR,3,6HNUNITS,NUNITS)
      RETURN
  115 IF (NLOG(NELE).EQ.0) CALL ERROR (ISUBR,4,NLOG(NELE),NELE)
      RETURN
  120 IF (XL(J).LT.0.) CALL ERROR (ISUBR,2,2HXL,J)
      IF (W(J).LT.0.) CALL ERROR (ISUBR,2,1HW,J)
      IF (S(J).EQ.0.) CALL ERROR (ISUBR,2,1HS,J)
      IF (R1(J).EQ.0.) CALL ERROR (ISUBR,2,2HR1,J)
      IF (W(J).NE.0.) GO TO 140
      IF (XL(J).EQ.0..AND.J.NE.JLST) CALL ERROR (ISUBR,6,J,0)
      IF (NCASE(J).EQ.0) CALL ERROR (ISUBR,2,5HNCASE,J)
      IF (NCASE(J).GT.3) CALL ERROR (ISUBR,3,5HNCASE,J)
      GO TO (125,130,135), NCASE(J)
  125 IF (ZL(J).EQ.0.) CALL ERROR (ISUBR,2,2HZL,J)
      IF (ZR(J).EQ.0.) CALL ERROR (ISUBR,2,2HZR,J)
      IF (A(J).LT.0.) CALL ERROR (ISUBR,2,1HA,J)
      GO TO 145
  130 IF (DIAM(J).EQ.0.) CALL ERROR (ISUBR,2,4HDIAM,J)
      GO TO 145
  135 STOP 3333
  140 IF (XL(J).EQ.0.) CALL ERROR (ISUBR,3,2HXL,J)
      IF (NRES.EQ.2.AND.R2(J).EQ.0.) CALL ERROR (ISUBR,2,2HR2,J)
      IF (NRES.EQ.3.AND.R2(J).EQ.0.) CALL ERROR (ISUBR,2,2HR2,J)
  145 RETURN
  150 IF (ND.EQ.0) CALL ERROR (ISUBR,1,2HND,0)
      KK=0
      DO 155 I=1,ND
         IF (QI(I).NE.0.) KK=1
         IF (TI(I).EQ.0..AND.I.NE.1) CALL ERROR (ISUBR,8,2HTI,I)
  155 CONTINUE
      IF (KK.EQ.0) CALL ERROR (ISUBR,7,2HQI,4HRAIN)
      IF (NOPT.EQ.0) GO TO 165
      KK=0
      IF (NO.EQ.0) CALL ERROR (ISUBR,1,2HNO,0)
      DO 160 I=1,NO
         IF (QOB(I).NE.0.) KK=1
         IF (TOB(I).EQ.0..AND.I.NE.1) CALL ERROR (ISUBR,8,3HTOB,I)
  160 CONTINUE
      IF (KK.EQ.0) CALL ERROR (ISUBR,7,3HQOB,6HOBSERV)
  165 RETURN
  170 IF (FMIN(J).LE.0.0001) GO TO 175
      IF (AL(J).EQ.0.) CALL ERROR (ISUBR,2,2HAL,J)
      IF (B(J).EQ.0.) CALL ERROR (ISUBR,2,1HB,J)
      IF (C(J).EQ.0.) CALL ERROR (ISUBR,2,1HC,J)
      IF (SMAX(J).EQ.0.) CALL ERROR (ISUBR,2,4HSMAX,J)
  175 RETURN
C
      END
      SUBROUTINE RESET (I,XLT,WT,ST,R1T,R2T,FMINT,NLT,NRT,NUT,NC1T,NC2T,
     1NCASET,ZRT,ZLT,AT,DIAMT,ALT,BT,CT,SIT,SMAXT,ROCT,NPT)
      COMMON /INFIL/ AL(20),B(20),C(20),SI(20),SMAX(20),ROC(20)
      COMMON /GEOM/ XL(20),W(20),S(20),R1(20),R2(20),FMIN(20),NL(20),NR(
     120),NU(20),NC1(20),NC2(20),NCASE(20),ZL(20),ZR(20),A(20),DIAM(20),
     2NP(20)
      NU(I)=NUT
      NUT=0
      NR(I)=NPT
      NRT=0
      NL(I)=NLT
      NLT=0
      NC1(I)=NC1T
      NC1T=0
      NC2(I)=NC2T
      NC2T=0
      NCASE(I)=NCASET
      NCASET=0
      XL(I)=XLT
      XLT=-1.
      W(I)=WT
      WT=-1.
      S(I)=ST
      ST=0.
      ZR(I)=ZRT
      ZRT=0.
      ZL(I)=ZLT
      ZLT=0.
      A(I)=AT
      AT=-1.
      DIAM(I)=DIAMT
      DIAMT=0.
      R1(I)=R1T
      R1T=0.
      R2(I)=R2T
      R2T=0.
      FMIN(I)=FMINT
      FMINT=0.
      AL(I)=ALT
      ALT=0.
      B(I)=BT
      BT=0.
      C(I)=CT
      CT=0.
      SI(I)=SIT
      SIT=0.
      SMAX(I)=SMAXT
      SMAXT=0.
      ROC(I)=ROCT
      ROCT=0.
      NP(I)=NPT
      NPT=1
      RETURN
C
      END
      SUBROUTINE CONVERT (KEY)
      COMMON /CNTRL/ NRES,NOPT,NTIME,NUNITS,NELE,CLEN,DELT,NLOG(20)
      COMMON /GEOM/ XL(20),W(20),S(20),R1(20),R2(20),FMIN(20),NL(20),NR(
     120),NU(20),NC1(20),NC2(20),NCASE(20),ZL(20),ZR(20),A(20),DIAM(20),
     2NP(20)
      COMMON /EVENT/ TFIN,ND,QI(100),TI(100),QOB(100),TOB(100),NO,SUMRCM
      COMMON /PLANE1/ H1(50),H2(50),QL(100),ALPHA(50),POWER(50),T(100),Q
     1(100),HUB(100),DX,DT,INDEX,THETA,XNU,GRAV,NB(20),QS(500),LENQ,LENQ
     2S,LENH1,L,QL1(50),QL2(50)
      COMMON /CHAN/ A1(50),A2(50),QUB(100),AUB(100),C01,C02,B,NI,NOQL
      COMMON /INFIL/ AL(20),B1(20),C(20),SI(20),SMAX(20),ROC(20)
      GO TO (105,180), KEY
C
C     KEY=1...CONVERT INPUT UNITS TO THOSE OPERATED ON BY PROGRAM
C
C
C     THIS PORTION CONVERTS ALL TIMES TO SECONDS,METERS TO FEET,AND
C     CM/MIN OR IN/HR TO CU.FT./SEC.....
C
  105 GO TO (110,115,120), NTIME
  110 FAC=1.
      GO TO 125
  115 FAC=60.
      GO TO 125
  120 FAC=3600.
  125 TFIN=TFIN*FAC
      DELT=DELT*FAC
      DO 130 I=1,20
  130 C(I)=C(I)*FAC/60.
      DO 135 I=1,ND
         QI(I)=QI(I)/43200.
  135 TI(I)=TI(I)*FAC
      IF (NOPT.EQ.0) GO TO 145
      DO 140 I=1,NO
         QOB(I)=QOB(I)/43200.
  140 TOB(I)=TOB(I)*FAC
C
C     METRIC CONVERSION
C
  145 GO TO (175,150), NUNITS
  150 DO 155 I=1,ND
  155 QI(I)=QI(I)*23.622
      IF (NOPT.EQ.0) GO TO 165
```

```
      DO 160 I=1,NO
  160 QOB(I)=QOB(I)*23.622
  165 CLEN=CLEN*3.281
      DO 170 I=1,20
         XL(I)=XL(I)*3.281
         W(I)=W(I)*3.281
         A(I)=A(I)*3.281
         DIAM(I)=DIAM(I)*3.281
         FMIN(I)=FMIN(I)*23.622
  170 CONTINUE
  175 RETURN
C
C     KEY=2.. CONVERT UNITS BACK FOR CONVENIENT OUTPUT
C
C     CONVERT ALL CU.FT./SEC TO IN/HR,SECONDS TO DESIRED UNITS.....
C
  180 GO TO (185,190,195), NTIME
  185 DIV=1.
      GO TO 200
  190 DIV=60.
      GO TO 200
  195 DIV=3600.
  200 DO 205 I=1,NO
         TI(I)=TI(I)/DIV
  205 QI(I)=QI(I)*43200.
      IF (NOPT.EQ.0) GO TO 215
      DO 210 I=1,NO
         TOB(I)=TOB(I)/DIV
  210 QOB(I)=QOB(I)*43200.
  215 AREA=0.
      DO 220 I=1,NELE
         J=NLOG(I)
  220 AREA=AREA+(XL(J)*W(J))
      DO 225 I=1,NI
         T(I)=T(I)/DIV
  225 Q(I)=Q(I)*43200./AREA
      RETURN
C
      END
      SUBROUTINE PLANE (J)
      COMMON /IO/ IREAD,IWRITE
      COMMON /CNTRL/ NRES,NOPT,NTIME,NUNITS,NELE,CLEN,DELT,NLOG(20)
      COMMON /GEOM/ XL(20),W(20),S(20),R1(20),R2(20),FMIN(20),NL(20),NR(
     120),NU(20),NC1(20),NC2(20),NCASE(20),ZL(20),ZR(20),A(20),DIAM(20),
     2NP(20)
      COMMON /EVENT/ TFIN,NO,QI(100),TI(100),QOB(100),TOB(100),NO,SUMRCH
      COMMON /PLANE1/ H1(50),H2(50),QL(100),ALPHA(50),POWER(50),T(100),Q
     1(100),HUB(100),DX,DT,INDEX,THETA,ANU,GRAV,NB(20),QS(500),LENQ,LENQ
     2S,LENH1,L,QL1(50),QL2(50)
      COMMON /CHAN/ A1(50),A2(50),QUB(100),AUB(100),C01,C02,B,NI,NOQL
      COMMON /INFIL/ AL(20),BI(20),C(20),SI(20),SMAX(20),ROC(20)
      COMMON /LAWS/ ATURB,PTURB,ALAM,PLAM,HTRANS,QTRANS
      DIMENSION XIN(50), RF(100), QIPH(50), AVGINF(50)
      DATA BLANK/1H /
C
C     CALCULATE NUMBER OF DISTANCE INCREMENTS (NK) AND THE DISTANCE
C     INCREMENT SIZE (DX).
C
      SUM2=0.
      SUM1=SUM2
      NK=MAX1(15.*XL(J)/CLEN),3.0)
      IF (NK.LE.LENH1) GO TO 105
      WRITE (IWRITE,280)
      STOP
  105 DX=XL(J)/(FLOAT(NK)-1.)
C
C     INITIALIZE
C
      FMIN(J)=FMIN(J)/60.
      DO 110 K=1,NK
         QL1(K)=QI(1)
         QL2(K)=QI(1)
         H1(K)=0.0
  110 CONTINUE
      KB=2
      L=2
      T(1)=0.0
      Q(1)=0.0
      RF(1)=QI(1)
      T(L)=T(1)+DELT
      RF(L)=QI(1)
C
C
C     RESLAW CALCULATES VALUES TO BE  PLACED IN THE ARRAYS ALPHA(K) AND
C     POWER(K).  RESLAW RETURNS WITH VALUES FOR ATURB,PTURB,ALAM,AND
C     PLAM WHICH ARE THE ALPHA AND POWER VALUES FOR A   TURBULENT AND
C     THE LAMINAR OVERLAND FLOW MODELS  RESPECTIVELY.
C        NRES=1...MANNING
C        NRES=2...MANNING-LAMINAR
C        NRES=3...CHEZY-LAMINAR
C        NRES=4...CHEZY
C
C     CHGLAW PLACES THE APPROPRIATE VALES ALREADY CALCULATED IN RESLAW
C     INTO THE ARRAYS ALPHA(K) AND POWER(K), K=1,NK    DEPENDENT UPON
C     CHITERIA INVOLVING HTRANS AND QTRANS. IF IFLAG=0...ALPHA AND POWER
C     ARRAYS WILL BE BASSED ON A TUBULENT FLOW MODEL.  IF IFLAG =1 THESE
C     ARRAYS WILL BE BASED ON THE LAMINAR FLOW MODEL.
C
      CALL RESLAW (NRES,J)
      PRINT 285, HTRANS,QTRANS
C
C      CHECK FOR OTHER PLANES CONTRIBUTING.  NU(J)=0 - NO CONTRIBUTORS.
C
      IF (NU(J)-0) 115,125,115
C
C     OTHER PLANES ARE CONTRIBUTING -- CHECK TO SEE IF CORRECT LAW IS IN
C     EFFECT -- CALCULATE UPPER BOUND DEPTHS (HUB) FOR ALL TIME INCREMNT
C
  115 JJ=NU(J)
      MM=NB(JJ)-1
      IF (NB(JJ).EQ.0) CALL ERROR (5HPLANE,15,JJ,0)
      DO 120 M=1,NI
         IF (QS(M+MM)/W(J).GT.QTRANS) IFLAG=0
         IF (QS(M+MM)/W(J).LE.QTRANS) IFLAG=1
         CALL CHGLAW (IFLAG,1,NRES)
  120 HUB(M)=(QS(M+MM)/ALPHA(1)/W(J))**(1./POWER(1))
      HUB(MB)=HUB(NI)
      NB(JJ)=0
      GO TO 135
C
C     NO PLANES ARE CONTRIB. -- DEFINE MI (NO. OF TIME INCREMENTS)-- SET
C     ALL UPPER BOUND DEPTHS (HUB) TO ZERO.
C
  125 MB=IFIX(TFIN/DELT)+2
      NI=MB-1
         CALL CHGLAW (0,1,NRES)
      DO 130 M=1,MB
         HUB(M)=0.
  130 CONTINUE
C
C     CHECK TO SEE IF INTERNAL TIME INCREMENT LOOP IS FINISHED (LOOP IS
C     BETWEEN STMTS.500 AND 1100) -- ALSO MAKE SURE WE ALWAYS HAVE
C     COMPATABLE INPUT AND INTERNAL TIME (TI AND T RESPECTIVELY).
C
  135 RF(L)=QI(KB-1)
      RF(L-1)=RF(L)
      LFLAG=0
      IF (T(L).LE.TFIN) GO TO 140
      IF (T(L-1)+.0001.GE.TFIN) GO TO 230
      T(L)=TFIN
  140 IF (T(L).LT.TI(KB)-.0001) GO TO 145
      T(L)=TI(KB)
C
C     CALCULATE INITIAL ADVANCED TIME DEPTH (H2(1)) USING HUB AND A TIME
C     INTERPOLATION.
C
  145 MT=IFIX(T(L)/DELT)+1
      H2(1)=HUB(MT)+(HUB(MT+1)-HUB(MT))*((T(L)-(DELT*FLOAT(MT-1)))/DELT)
C
C     IMPLCT RETURNS WITH LOWER BOUND DEPTH (H2(NK)) -- CHECK TO MAKE
C     SURE CORRECT LAW IS IN EFFECT -- CALCULATE TOTAL DISCHARGE (CFS)
C     FROM PLANE J FOR TIME INCREMENT L.
C
      DT=T(L)-T(L-1)
C
C     TEST FOR IMPERVIOUS PLANE.  FMIN(J) .LE. 0.0001 - IMPERVIOUS PLANE
C
      TF=T(L)
      IF (FMIN(J).GT.0.0001) CALL XPLINP (H1,DT,T(L),RF(L),QL2,TF,NK,H2(
     11),NI,DELT,AL(J),BI(J),C(J),SI(J),SMAX(J),ROC(J),J)
      IF (NP(J).EQ.1) GO TO 155
      IF (FMIN(J).LT.0.0001) GO TO 155
      PPT=QI(KB-1)*43200.
      WRITE (IWRITE,290) T(L),PPT
      DO 150 I=1,NK
         QIPH(I)=QL2(I)*43200.
  150 CONTINUE
      WRITE (IWRITE,295) (QIPH(I),I=1,NK)
  155 IF (L.NE.2) GO TO 165
      DO 160 K=1,NK
         IF (QL2(K).EQ.0.) QL1(K)=0.
  160 CONTINUE
  165 IF (H2(1).NE.0.) GO TO 185
      DO 170 K=1,NK
         IF (QL2(K).LE.0..AND.H1(K).LE.0.) QL2(K)=0.
  170 CONTINUE
      DO 175 K=1,NK
         IF (QL1(K).NE.0.) GO TO 185
         IF (QL2(K).NE.0.) GO TO 185
         IF (H1(K).NE.0.) GO TO 185
  175 CONTINUE
      DO 180 K=2,NK
         GO TO (177,176,176,177) NRES
  176    POWER(K)=PLAM
         ALPHA(K)=ALAM
         GO TO 180
  177    POWER(K)=PTURB
         ALPHA(K)=ATURB
  180 H2(K)=0.
      IF (T(L).GE.TI(KB)-.0001) KB=KB+1
      GO TO 195
  185 IF (T(L).LT.TI(KB)-.0001) GO TO 190
      KB=KB+1
      IF (FMIN(J).LT..00001) LFLAG=1
  190 CALL IMPLCT (NK,J)
  195 CONTINUE
      Q(L)=ALPHA(NK)*(H2(NK)**POWER(NK))*W(J)
      IF (NU(J).NE.0) SUM1=SUM1+(ALPHA(1)*H2(1)**POWER(1)+ALPHA(1)*H1(1)
     1**POWER(1)),5*DT*W(J)
      SUM1=(RF(L))*XL(J)*DT*W(J)+SUM1
      SUM2=(Q(L)+Q(L-1))*DT/2.+SUM2
      DO 200 K=1,NK
  200 XIN(K)=(RF(L)-(QL1(K)+QL2(K))/2.)*DT
      XINS=(XIN(1)+XIN(NK))/2.
      STOR=(H2(1)+H2(NK))/2.
      NKM2=NK-2
      IF (NKM2.LT.1) GO TO 210
      DO 205 K=1,NKM2
         XINS=XINS+XIN(K+1)

  205 STOR=STOR+H2(K+1)
  210 STOR=STOR*DX*W(J)
      XINS=XINS*DX*W(J)
      SUM2=SUM2+XINS
      IF (NP(J).EQ.1) GO TO 215
      WRITE (IWRITE,300) (H2(K),K=1,NK)
C
C     CONTINUITY CHECK
C
      ER=(SUM1-SUM2-STOR)/SUM1*100.
      WRITE (IWRITE,305) SUM1,SUM2,STOR,ER
C
C     INCREMENT L AND INTERNAL TIME  -- REDEFINE LATERAL INFLOW (QL),AND
C     SET ADVANCE TIME DEPTHS (H2) EQUAL TO THE KNOWN DEPTHS (H1)
C
  215 L=L+1
      IF (L.LE.LENQ) GO TO 220
      WRITE (IWRITE,310)
      STOP
  220 T(L)=T(L-1)+DELT
      DO 225 K=1,NK
         QL1(K)=QL2(K)
         IF (LFLAG.LT.1) GO TO 225
         QL2(K)=QI(NP-1)
         QL1(K)=QL2(K)
  225 H1(K)=H2(K)
      GO TO 135
C
C     HAVE FINISHED PROCESSING THE PLANE THROUGH TIME TFIN, UNIF
C     CONVERTS Q OVER UNIFORM TIME INCREMENTS AND SAVES THIS STANDARD
C     HYDROGRAPH IN QS
C
  230 CONTINUE
```

```
      L=L-1
      LASTNB=NB(1)
      IF (NELE.EQ.1) GO TO 240
      DO 235 NE=2,NELE
         IF (NB(NE).GT.LASTNB) LASTNB=NB(NE)
  235 CONTINUE
  240 MBT=LASTNB+NI
      IF (LASTNB.EQ.0) MBT=1
      IF (MBT.LE.LENGS) GO TO 245
      WRITE (IWRITE,315)
      STOP
  245 CALL UNIF (Q,T,L,OS(MBT),NI,DELT)
      NB(J)=MBT
      WRITE (6,320) MBT,NB
      WRITE (IWRITE,325) J,XL(J),W(J),S(J)
      GO TO (250,255,260,265), NRES
  250 WRITE (IWRITE,330) R1(J)
      GO TO 270
  255 WRITE (IWRITE,335) R1(J),R2(J)
      GO TO 270
  260 WRITE (IWRITE,340) R1(J),R2(J)
      GO TO 270
  265 WRITE (IWRITE,345) R1(J)
  270 IF (FMIN(J).LE..00001) GO TO 275
      WRITE (IWRITE,350) FMIN(J),AL(J),BI(J),C(J),SI(J),SMAX(J),ROC(J)
      RETURN
  275 WRITE (IWRITE,355)
      RETURN
C
  280 FORMAT (56H H1,H2   ,ALPHA, AND POWER NEED TO BE DIMENSIONED LARGE
     1R)
  285 FORMAT (5X,8H RTRANS=,1PE12.5,8H QTRANS=,1PE12.5)
  290 FORMAT (5X,7HTIME IS,F11.5,20H SEC.,  RAIN RATE IS ,F15.5,4H IPH)
  295 FORMAT (1X,3HQL(IPH)=,12(2X,F8.5))
  300 FORMAT (1X,11HH2(I=1,NK)=,12(2X,F8.5))
  305 FORMAT (10H   INFLOW=,E10.3,11H   OUTFLOW=,E10.3,11H   STORAGE=,E1
     10.3,7H ERROR=,E10.3,8H PERCENT)
  310 FORMAT (38H T AND Q NEED TO BE DIMENSIONED LARGER)
  315 FORMAT (34H OS NEEDS TO BE DIMENSIONED LARGER)
  320 FORMAT (5H MBT=,I4,10X,3HNB=,2I4)
  325 FORMAT (10X,9HPLANE NO ,I4,19H PROCESSED.//5X,28HGEOMETRIC PARAMET
     1ERS      L=,F7.1,4H  W=,F7.1,4H  S=,F7.4)

  330 FORMAT (15X,11HMANNINGS N=,F5.3)
  335 FORMAT (15X,11HMANNINGS N=,F5.3,12H  LAMINAR K=,F8.1)
  340 FORMAT (15X,8HCHEZY C=,F6.1,12H  LAMINAR K=,F8.1)
  345 FORMAT (15X,8H CHEZY C=,F6.1)
  350 FORMAT (15X,30HINFILTRATION PARAMETERS  FMIN=,F8.5,3H A=,F8.2,4H
     1B=,F8.2,4H  C=,F9.2,5H  SI=,F8.2,2H  SMAX=,F8.2,6H  ROC=,F8.2)
  355 FORMAT (15X,16HIMPERVIOUS PLANE)
C
      END
      SUBROUTINE XPLINF (H1,DT,T,RF,QL2,TF,NK,HUP,NI,DELT,ALF,BIN,CIN,SI
     1N,SO,ROCK,J)
C
C     THIS SUBROUTINE WAS DEVELOPED BY R. E. SMITH, ARS, AND MODIFIED
C     FOR  WSF WITH KINGEN75
C     REFERENCE..SMITH,R. E., THE INFILTRATION ENVELOPE-RESULTS FROM A T
C     INFILTROMETER, JOURNAL OF HYDROLOGY, V.17,N.1/2,1972.
C     SUBROUTINE COMPUTES INFILTRATION AND RETURNS EXCESS RAINFALL FOR A
C     TIME INCREMENT
C
C      OPERATING DIMENSIONS ARE INCHES AND MINUTES
C
      COMMON /IO/ IREAD,IWRITE
      COMMON /GEOM/ XL(20),W(20),S(20),R1(20),R2(20),FMIN(20),NL(20),NR(
     120),NW(20),NC1(20),NC2(20),NCASE(20),ZL(20),ZR(20),A(20),DIAM(20),
     2NP(20)
      DIMENSION QL2(50), TOS(50), DTS(50), SI(50), H1(50), DELTS(50), QO
     1S(50), SINT(50), QSD(50), NRN(50), NRO(50), NMODE(50), QSTAR(50)
      DECF(S,C)=EXP(ALF*(.04/(ALOG(S*TON)-CL)/(C+.55)/(C+.55))**.8)
      DELT=DELT/60.
      DT=DT/60.
      T=T/60.
      TF=TF/60.
      RF=RF*720.
      DO 105 I=1,NK
  105 QL2(I)=QL2(I)*720.
      RST=RF/FMIN(J)
      J1=1
      IRO=0
      IF (T.GT.DT) GO TO 115
      GAM=ALF/(1.-ALF)
      M=1
      JRP=0
      DO 110 K=1,NK
         SINT(K)=SIN
         QSTAR(K)=0
         NRO(K)=0
         NMODE(K)=0
  110 NRN(K)=0
  115 CONTINUE
C
C **  BIN IS DIMENSIONLESS PARAMETER WHICH CONTROLS TIME OF PONDING.
C     IT IS THEORETICALLY EQUAL TO NONDIMENSIONALIZED SORPTIVITY SQUARED
C     DIVIDED BY (2.*FMIN)  (SEE PHILIP+DSS+1957). THIS IS NOT THE SAME
C     B USED BY SMITH, 1972
C     --SOLVE FOR TIME WHEN PONDING(RUNOFF BEGINS) WILL OCCUR
C
      IF (NRO(2).NE.0) GO TO 145
      TON=CIN*(SO-SINT(2))*(1.-ROCK)
      QON=FMIN(J)*TON
      T=T-DT
C
      IF (RST.LT.1E-6) GO TO 130
      DT=((BIN*ALOG(RST/(RST-1.))-QSTAR(2))*QON/RF)+0.0001
      IF (DT) 120,120,125
  120 IRO=2
      GO TO 130
  125 IF (T+DT-TF) 135,130,130
  130 DT=TF-T
      T=TF
      GO TO 140
  135 T=T+DT
  140 CONTINUE
      IF (NP(J).EQ.1) GO TO 150
      WRITE (6,355) DT,T
C
  145 CONTINUE
  150 DO 345 I=J1,NK
C
C     --CONVERT FEET TO INCHES
C
      S1(I)=12.*H1(I)
      IF (IRO) 155,155,195
  155 IF (NMODE(I)) 160,160,265
  160 IF (NRO(I)) 180,165,220
  165 IF (JRP) 170,170,190
  170 IF (I-J1) 175,175,190
  175 IF (HUP-.000001) 190,190,265
  180 IF (RST-1.) 240,240,185
C
C     ------  UNPONDED, RAINING, PLANE CASE
C
  185 H1(I)=0.
      IF (I.GE.NK) WRITE (6,360) (SINT(K),K=1,NK)
      JRP=1
  190 CONTINUE
      TON=CIN*(SO-SINT(I))*(1.-ROCK)
      QON=FMIN(J)*TON
      NRO(I)=0
      IF (RST-1.) 200,200,195
  195 QPS=BIN*ALOG(RST/(RST-1.))
      QST=QSTAR(I)+RF*DT/QON
      IF (QST-QPS) 200,205,205
  200 QSTAR(I)=QSTAR(I)+(RF*DT+S1(I))/QON
      QL2(I)=0.
      IF (NP(J).EQ.1) GO TO 345
      WRITE (IWRITE,370) QST,QPS
      GO TO 345
C
C     SO TOS IS VERTICAL ASYMPTOTE OF INFIL. DECAY CURE.
C     QOS IS HYPOTHETICAL INFIL. DEPTH PARAMETER WHICH IS SET SO THAT
C     THE INFIL CURVE PASSES THRU RF(TPS) AT T=TPS.
C     NOTE QSTAR AND QOS ARE USED IN DEFINING INFIL DECAY TO CORRECTLY A
C      COUNT FOR PERIODS WITHIN THE RAIN PATTERN WHEN RF .LT. INFIL.CAP.
C      (OTHERWISE, FOR SIMPLE PATTERNS WITH RF.GT.F+F IS DEFINED BY T
C      AND TOS ALONE).
C
C     ----- CALCULATE TOST AND QO(I) FOR INFILTRATION DECAY CURVE
C
  205 NRO(I)=2
      TS=T/TON
      DST=((1.-ALF)/(RST-1.))**(1./ALF)
      QOS(I)=QPS-DST**(1.-ALF)-DST
      IF (QPS-QSTAR(I)) 215,215,210
  210 TPS=TS
      TOS(I)=TPS-DST
      QSTAR(I)=QSTAR(I)+RF*DT/QON
      QL2(I)=0.
      GO TO 345
  215 TPS=(T-DT)/TON
      QPS=QSTAR(I)
      TOS(I)=TPS-DST
      QOS(I)=QPS-DST**(1.-ALF)-DST
      FCL=RST
      GO TO 230
  220 TON=CIN*(SO-SINT(I))*(1.-ROCK)
      QON=FMIN(J)*TON
      TS=T/TON
     TLS=(T-DT)/TON
      RFST=PST+S1(I)/DT/FMIN(J)
      IF (RFST-1.) 240,225,225
  225 FCL=(1.-ALF)/(QSTAR(I)-TLS+TOS(I)-QOS(I))**GAM+1.
C
C     --LET INFIL.CONTINUE AT MAX RATE
C
      IF (RFST-FCL+1.E-04) 235,230,230
  230 QSTAR(I)=QOS(I)+(TS-TOS(I))**(1.-ALF)+TS-TOS(I)
      FCN=(1.-ALF)/(QSTAR(I)-TS+TOS(I)-QOS(I))**GAM+1.
      QL2(I)=RF-FMIN(J)*0.5*(FCN+FCL)
      GO TO 345
  235 QSTAR(I)=QSTAR(I)+(RF*DT+S1(I))/QON
      QL2(I)=-1.*(S1(I)/DT+RF)
      GO TO 345
  240 IF (S1(I)-0.5*FMIN(J)*DT) 245,235,235
  245 IF (NRO(I)) 255,255,250
  250 NRO(I)=-1
C
C     -- RESET INTIAL SOIL WATER TO NEAR SATURATION AT ZERO PRESSURE
C
      SINT(I)=SO-0.01
      QSDEM=QSTAR(I)*QON
      QSTAR(I)=0.
      IF (NP(J).LE.1) GO TO 260
      WRITE (6,365) QSDEM,I
      GO TO 260
C
C     --EMPIRICAL DRAINAGE FUNCTION
C
  255 SINT(I)=SINT(I)*(1.-.02*(1.-RST))**DT
  260 QL2(I)=-S1(I)/DT-.0001
      GO TO 345
C
C     --THIS SECTION IS GENERALLY NOT USED.. IT IS USED IF IMPERV. PLANE
C     --ONTO PERV. PLANE
C     ------ SUDDEN PONDING SITUTATION
C
  265 NMODE(I)=2
      IF (NRN(I)) 270,270,300
  270 NRN(I)=2
      IF (RF-FMIN(J)) 275,275,280
  275 TOS(I)=(T-DT)/TON
      DELTS(I)=0.
      QOS(I)=QSTAR(I)
      GO TO 290
  280 QPS=BIN*ALOG(RF/(RF-FMIN(J)))
      QSS=QSTAR(I)+RF*DT/TON
      RATIO=QSS/QPS
      IF (RATIO-1.) 285,205,205
  285 DTS(I)=((1.-ALF)/(RF/FMIN(J)-1.))**(1./ALF)
C
C     ----- EMPIRICAL RELATION FOR DELTS/
C
      DELTS(I)=DTS(I)*RATIO**(1./ALF)
      TOS(I)=(T-DT)/TON-DELTS(I)
      QOS(I)=QSTAR(I)-DELTS(I)**(1.-ALF)-DELTS(I)
      DELTS(I)=DELTS(I)*TON
      CL=ALOG(DELTS(I))
      TN=T/TON-TOS(I)
      DCF=DECF(TN,DELTS(I))
      FCN=1.+(1.-ALF)/TN**ALF*DCF
      IF ((FCN-1.)/DCF+1.*(S1(I)/DT+RF)/FMIN(J)) 295,295,290
  290 QSTAR(I)=QSTAR(I)+(RF*DT+S1(I))/QON
```

```
      QL2(I)=0.
      GO TO 345
  295 DTT=DT/TON
      QSTAR(I)=QSTAR(I)+DTT*TN**(1.-ALF)-(TN-DTT)**(1.-ALF)
      QL2(I)=RF-FCN*FMIN(J)
      GO TO 345
C
C****** CHECK THIS ON RECESSION FROM PONDING
C
  300 TL=(T-DT)/TON-TOS(I)
      IF (DELTS(I)-0.00001) 310,310,305
  305 CONTINUE
      CL=ALOG(DELTS(I))
      DCF=DECF(TL,DELTS(I))
      GO TO 315
  310 DCF=1.0
  315 CONTINUE
      DENO=QSTAR(I)-TL-QOS(I)
      IF (DENO) 275,275,320
  320 FCL=1.+(1.-ALF)/DENO**GAM*DCF
      IF (FCL-(RF+S1(I)/DT)/FMIN(J)) 325,325,290
  325 TS=T/TON-TOS(I)
      IF (DELTS(I)-0.00001) 330,330,335
  330 DCF=1.
      GO TO 340
  335 DCF=DECF(TS,DELTS(I))
  340 CONTINUE
      QSTAR(I)=QSTAR(I)+DT/TON*(TS**(1.-ALF)-TL**(1.-ALF))
      FCN=1.+(1.-ALF)/(QSTAR(I)-TS-QOS(I))**GAM*DCF
      QL2(I)=RF-FMIN(J)*0.5*(FCN+FCL)
  345 CONTINUE
      RF=RF/720.
      DELT=DELT*60.
      DT=DT*60.
      T=T*60.
      TF=TF*60.
      DO 350 I=1,NK
         QL2(I)=QL2(I)/720.
  350 QSD(I)=QSTAR(I)*QON
      RETURN
C
  355 FORMAT (1H ,16HDT(FROM XPLINF)=,F10.3,5X,3HT= ,F10.3)
  360 FORMAT (1X,10F10.5)
  365 FORMAT (1H ,9X,23HTOTAL ACCUM INFIL(IN.)=,F8.4,8HAT NODE ,I3)
  370 FORMAT (6H  QST=,F10.5,5H QPS=,F10.5)
C
      END
      SUBROUTINE CHANNL (J)
      COMMON /IO/ IREAD,IWRITE
      COMMON /CNTRL/ NRES,NOPT,NTIME,NUNITS,NELE,CLEN,DELT,NLOG(20)
      COMMON /GEOM/ XL(20),W(20),S(20),R1(20),R2(20),FMIN(20),NL(20),NR(
     120),NU(20),NC1(20),NC2(20),NCASE(20),ZL(20),ZR(20),A(20),DIAM(20),
     2NP(20)
      COMMON /EVENT/ TFIN,ND,QI(100),TI(100),QOB(100),TOB(100),NO,SUMRCM
      COMMON /PLANE1/ H1(50),H2(50),QL(100),ALPHA(50),POWER(50),T(100),Q
     1(100),HUB(100),DX,DT,INDEX,THETA,ANU,GRAV,NB(20),QS(500),LENQ,LENQ
     25,LENH1,L,QL1(50),QL2(50)
      COMMON /CHAN/ A1(50),A2(50),QUB(100),AUB(100),CO1,CO2,B,NI,NOQL
      COMMON /CIRC/ TH1(50),TH2(50),SIN1(50),SIN2(50),COS1(50),COS2(50),
     1SIN1A,SIN2A,COS1A,COS2A,THUB(100),DFAC,QFAC,D
      COMMON /LAWS/ ATURB,PTURB,ALAM,PLAM,HTRANS,QTRANS
      DATA BLANK/1H /
C
C     CALCULATE NK AND DX  AND NI
C
      NK=MAX1((15.*XL(J)/CLEN),3.)
      IF (NK.LE.LENH1) GO TO 105
      WRITE (IWRITE,280)
  105 DX=XL(J)/(FLOAT(NK)-1.)
      NI=IFIX(TFIN/DELT)+1
C
C     CHOOSE TURBULENT OVERLAND FLOW RESISTANCE LAW
C           NRES=1 OR NRES=2.....MANNING FORMULA
C           NRES=3 OR NRES=4....CHEZY FORMULA
C
      IF (NRES.EQ.1.OR.NRES.EQ.2) NREST=1
      IF (NRES.EQ.3.OR.NRES.EQ.4) NREST=4
      CALL RESLAW (NREST,J)
      DO 365 K=1,NK
  365 CALL CHGLAW (0,K,NREST)
C
C     CHECK TO SEE WHAT TYPE OF CHANNEL
C        NCASE=1...TRAPEZOIDAL SHAPED CHANNEL CROSS-SECTION
C        NCASE=2...CIRCULAR SHAPED CROSS-SECTION
C        NCASE=3,...IRREGULAR SHAPED CROSS-SECTION
C
      GO TO (110,115,275), NCASE(J)
  110 CO1=1./ZR(J)+1./ZL(J)
      CO2=(1.+1./(ZR(J)*ZR(J)))**0.5+(1.+1./(ZL(J)*ZL(J)))**0.5
      B=W(J)
      GO TO 120
  115 D=DIAM(J)
C
C     SUBROUTINE ADD RETURNS WITH UPPER BOUND AREAS (AUB) AND COMBINED
C     LATERAL INFLOW INTO CHANNEL J.   IF CHANNEL IS A CIRCULAR CONDUIT,
C     ADD RETURNS WITH AND UPPER BOUND THETA ANGLE (THUB) INSTEAD OF AHE
C
  120 CALL ADD (J)
      IF (XL(J)) 265,265,125

C
C     ROUTE TO CORRECT CHANNEL GEOMETRY
C
  125 GO TO (130,155,275), NCASE(J)
C
C     TRAPAZOIDAL SHAPED CROSS-SECTION
C     CALCULATE AREAS AT EACH DX POINT FOR ALL TIME INCREMENTS
C
  130 Q(1)=0.0
      T(1)=0.0
      DO 139 K=1,NK
  135 A1(K)=0.0
      DO 150 L=2,NI
         T(L)=T(L-1)+DELT
         A2(1)=AUB(L)
         BT=DELT
         CALL IMPLCT (NK,J)
         DUM=(B*B+2.*A2(NK)/CO1)**0.5
         WPERIM=(DUM-B)*CO2+B*CO1
         Q(L)=ALPHA(NK)*A2(NK)**POWER(NK)/WPERIM**(POWER(NK)-1.)
         IF (NP(J).EQ.1) GO TO 140
         WRITE (IWRITE,285) (A2(K),K=1,NK)
         WRITE (IWRITE,290) L,T(L),L,Q(L),L,QL(L)
  140    DO 145 K=1,NK
            A1(K)=A2(K)
  145    CONTINUE
  150 CONTINUE
      GO TO 205
C
C     CIRCULAR CONDUIT CHANNEL
C
  155 T(1)=0.
      Q(1)=0.
      DT=DELT
      DO 160 K=1,NK
         TH1(K)=0.0
         SIN1(K)=0.0
         COS1(K)=1.0
  160 CONTINUE
      INIT=1
      DO 170 L=2,NI
         LL=L-1
         Q(L)=0.0
         T(L)=T(LL)+DELT
         TH1(1)=THUB(LL)
         IF (TH1(1).LE.0.0.AND.THUB(L).LE.0.) GO TO 165
         SIN1(1)=SIN(TH1(1)/2.)
         COS1(1)=SQRT(1.-SIN1(1)*SIN1(1))
         INIT=L
  165    IF (NP(J).LE.1) GO TO 170
         WRITE (IWRITE,295) (TH1(K),K=1,NK)
         WRITE (IWRITE,290) L,T(L),L,Q(L),L,QL(L)
         IF (INIT.EQ.L) GO TO 175
  170 CONTINUE
  175 DO 200 L=INIT,NI
         TH2(1)=THUB(L)
         SIN1A=SIN((TH1(1)+TH2(1))/2.)
         COS1A=SQRT(1.-SIN1A*SIN1A)
         NOQL=0
         CALL IMPLCT (NK,J)
         SINX=SIN(TH2(NK))
         IF (TH2(NK).NE.0.) GO TO 180
         Q(L)=0.
         GO TO 185
  180    Q(L)=(D*D*(TH2(NK)-SINX)/8.)**POWER(NK)/(D*TH2(NK)/2.)**(POWER(
     1   NK)-1.)*ALPHA(NK)
         IF (NP(J).EQ.1) GO TO 190
  185    WRITE (IWRITE,300) (TH2(K),K=1,NK)
         WRITE (IWRITE,290) L,T(L),L,Q(L),L,QL(L)
  190    DO 195 K=1,NK
            TH1(K)=TH2(K)
            SIN1(K)=SIN2(K)
            COS1(K)=COS2(K)
  195    CONTINUE
  200 CONTINUE

C
C     HAS FINISHED PROCESSING THROUGH TIME TFIN. STORE HYDROGRAPH IN QS
C
  205 WRITE (IWRITE,305) J,XL(J),S(J)
      GO TO (210,215), NCASE(J)
  210 WRITE (IWRITE,310) ZL(J),ZR(J),A(J)
      GO TO 220
  215 WRITE (IWRITE,315) DIAM(J)
  220 GO TO (225,230,235,240), NRES
  225 WRITE (IWRITE,320) R1(J)
      GO TO 245
  230 WRITE (IWRITE,325) R1(J),R2(J)
      GO TO 245
  235 WRITE (IWRITE,330) R1(J),R2(J)
      GO TO 245
  240 WRITE (IWRITE,335) R1(J)
  245 WRITE (IWRITE,340) NC1(J),NC2(J),NL(J),NR(J)
      LASTNB=NB(1)
      DO 250 NE=2,NELE
         IF (NB(NE).GT.LASTNB) LASTNB=NB(NE)
  250 CONTINUE
      MBT=LASTNB+NI
      IF (LASTNB.EQ.0) MBT=1
      IF (MBT.LE.LENQS) GO TO 255
      WRITE (IWRITE,345)
  255 DO 260 L=1,NI
         MM=L-1
         QS(MM+MBT)=Q(L)
  260 CONTINUE
      NB(J)=MBT
      WRITE (IWRITE,350) MBT,NB
      GO TO 270
C
C     IF XL=0 WE MERELY OUTPUT THE ADDED UPPER BOUND DISCHARGE (QUB
C     WHICH WAS CALCULATED IN ADD.
C
  265 T(1)=0.0
      Q(1)=QUB(1)
      DO 360 L=2,NI
         T(L)=T(L-1)+DELT
         Q(L)=QUB(L)
  360 CONTINUE
      WRITE (IWRITE,355) J
      NSIG=1
  270 RETURN
  275 STOP 6666
C
  280 FORMAT (53H  A1,A2,ALPHA,AND POWER NEED TO BE DIMENSIONED LARGER)
  285 FORMAT (1H ,11HA2(K=1,NK)=,15(1X,F7.4))
  290 FORMAT (5H   T(,I3,2H)=,1PE12.5,3X,4H  Q(,I3,2H)=,1PE12.5,3X,4H QL
     1(,I3,2H)=,1PE12.5)
  295 FORMAT (1H ,11HTH1(K=1,NK),15(1X,F7.4))
  300 FORMAT (1X,11HTH2(K=1,NK),15(1X,F7.4))
  305 FORMAT (10X,10HCHANNEL NO,I4,10H PROCESSED.//5X,24HGEOMETRIC PARAM
     1ETERS  L=,F8.1,4H  S=,F7.4/10X,13HCROSS SECTION)
  310 FORMAT (5X,30HTRAPEZOIDAL SHAPE  LEFT SLOPE=,F7.5,13H RIGHT SLOPE=
     1,F7.5,3H A=,F8.2)
  315 FORMAT (5X,26HCIRCULAR SHAPE   DIAMETER=,F8.5)
  320 FORMAT (15X,11HMANNINGS N=,F5.3)
  325 FORMAT (15X,11HMANNINGS N=,F5.3,12H  LAMINAR K=,F8.1)
  330 FORMAT (15X,8HCHEZY C=,F6.1,12H  LAMINAR K=,F8.1)
  335 FORMAT (15X,9H CHEZY C=,F6.1)
  340 FORMAT (10X,29HCHANNEL IDENTIFICATION   NC1=,I4,5H NC2=,I4/10X,25H
     1PLANE IDENTIFICATION  NL=,I4,4H NR=,I4)
  345 FORMAT (34H QS NEEDS TO BE DIMENSIONED LARGER)
  350 FORMAT (5H MBT=,I4,10X,3HNB=,20I4)
  355 FORMAT (20H OUTPUT FOR ELEMENT ,I2,24H IS THE FINAL HYDROGRAPH)
C
```

```
      END
      SUBROUTINE RESLAW (NRES,J)
      COMMON /GEOM/ XL(20),A(20),S(20),R1(20),R2(20),FMIN(20),NL(20),NR(
     120),NW(20),NC1(20),NC2(20),NCASE(20),ZL(20),ZH(20),A(20),DIAM(20),
     2NP(20)
      COMMON /PLANE1/ H1(50),H2(50),QL(100),ALPHA(50),POWER(50),T(100),Q
     1(100),HUB(100),DX,DT,INDEX,THETA,XNU,GRAV,NB(20),QS(500),LENQ,LENQ

     2S,LENM1,L,QL1(50),QL2(50)
      COMMON /LAWS/ ATURB,PTURB,ALAM,PLAM,HTRANS,QTRANS
C
C     THIS SUBROUTINE CALCULATES THE VALUES TO BE USED FOR ALPHA(K) AND
C     POWER(K) IN DEPTH AND DISCHARGE CALCULATIONS. ATURB AND PTURB ARE
C     THE VALUES BASED ON A TURBULENT OVERLAND FLOW MODEL WHILE ALAM AND
C     PLAM ARE THOSE BASED ON A LAMINAR FLOW MODEL.
C        FOR NRES=1...CALCS. ONLY MANNING TURBULENT FLOW VALUES.
C            NRES=2...CALCS. BOTH MANNING TURBULENT FLOW AND DARCY-
C                     WIESBACH LAMINAR FLOW VALUES.
C            NRES=3...CALCS. BOTH CHEZY TURBULENT  FLOW AND DARCY-
C                     WIESBACH LAMINAR  FLOW VALUES.
C            NRES=4...CALCS. ONLY CHEZY TURBULENT FLOW VALUES.
C     ALSO CALCULATED  IN THIS ROUTINE ARE THE TRANSITION POINTS FOR
C     DEPTH (HTRANS) AND FOR DISCHARGE(QTRANS) WHICH ARE THE VALUES
C     WHERE WE CHANGE FROM TURBULENT TO LAMINAR FLOW. FOR NRES=1 AND
C     NRES=4, HTRANS AND QTHANS ARE MADE NEGATIVE SO THAT THE PROGRAM
C     WILL ALWAYS OPERATE WITH TURBULENT FLOW PARAMETERS.
C
      GO TO (105,105,110,110), NRES
C
C     MANNING TURBULENT FLOW
C
  105 ATURB=(1.49/R1(J))*(S(J)**0.5)
      PTURB=5./3.
      GO TO 115
C
C     CHEZY TURBULENT FLOW
C
  110 ATURB=R1(J)*S(J)**0.5
      PTURB=3./2.
  115 GO TO (135,120,120,135), NRES
C
C     DARCY-WEISBACH LAMINAR FLOW
C
  120 ALAM=S(J)*8.*GRAV/(XNU*R2(J))
      PLAM=3.
      GO TO (125,130), NRES-1
C
C     TRANSITONS POINTS FOR MANNING-LAMINAR
C
  125 HTRANS=(1.49*XNU*R2(J)/(8.*GRAV*R1(J)*S(J)**0.5))**0.75
      QTRANS=(1.49*S(J)**0.5*HTRANS**(5./3.))/R1(J)
      GO TO 140
C
C     TRANSITION POINTS FOR CHEZY-LAMINAR
C
  130 HTRANS=(R1(J)*XNU*R2(J)/(8.*GRAV*R1(J)*S(J)**0.5))**(2./3.)
      QTRANS=R1(J)*S(J)**0.5*HTRANS**1.5
      GO TO 140
C
C     FIX SO THAT ONLY TURBULENT MODEL WILL BE EXPRESSED FOR NON-LAMINAR
C     MODELS. ONLYFOR NRES=1 OR NRES=4.
C
  135 HTRANS=-1.
      QTRANS=-1.
  140 RETURN
C
      END
      SUBROUTINE CHGLAW (IFLAG,K,NRES)
      COMMON /PLANE1/ H1(50),H2(50),QL(100),ALPHA(50),POWER(50),T(100),Q
     1(100),HUB(100),DX,DT,INDEX,THETA,XNU,GRAV,NB(20),QS(500),LENQ,LENQ
     2S,LENM1,L,QL1(50),QL2(50)
      COMMON /LAWS/ ATURB,PTURB,ALAM,PLAM,HTRANS,QTRANS
C
C     THIS SUBROUTINE CHANGES HYDRAULIC RESISTENCE LAWS (TURBULENT TO
C     LAMINAR OR VICE VERSA) AS DICTATED BY THE TRANSTION POINTS FOR
C     DEPTH AND DISCHARGE (HTRANS AND QTRANS).
C
      IF (IFLAG) 110,105,110
  105 X=ATURB
      Y=PTURB
      GO TO 115
  110 X=ALAM
      Y=PLAM
  115 CONTINUE
      ALPHA(K)=X
      POWER(K)=Y
      RETURN
C
      END
      SUBROUTINE UNIF (Q,T,NIN,QO,NI,DELT)
      DIMENSION Q(NIN), T(NIN), QO(NI)
C
C     THIS SUBROUTINE TAKES THE VALUES OF Q AT THEIR CORRESPONDING TIME
C     CONVERTS THEM INTO VALUES WITH EQUAL TIME INTERVALS (DELT).  THESE
C     VALUES ARE STORED IN QO.
C     Q  =  INPUT DATA ARRAY
C     T  =  INPUT TIME ARRAY
C     NIN  =  LENGTH OF Q AND T ARRAYS
C     QO  =  OUTPUT DATA ARRAY
C     NI  =  LENGTH OF QO
C     DELT  =  TIME INCREMENT
C
      I=2
      K=1
      QO(1)=Q(1)
      TO=0.
  105 TO=TO+DELT
  110 IF (T(K).GE.TO) GO TO 115
      K=K+1
      GO TO 110
  115 IF (ABS(T(K)-TO).LE.1.E-5) GO TO 125
      QO(I)=Q(K-1)+(TO-T(K-1))/(T(K)-T(K-1))*(Q(K)-Q(K-1))
  120 I=I+1
      IF (I.GE.NI) GO TO 130
      GO TO 105
  125 QO(I)=Q(K)
      GO TO 120
  130 QO(NI)=Q(NIN)
      RETURN
C
      END
      SUBROUTINE IMTHUB (X,FX,DERF)
      COMMON /CHAN/ A1(50),A2(50),QUB(100),AUB(100),C01,C02,B,NI,NOQL
      COMMON /PLANE1/ H1(50),H2(50),QL(100),ALPHA(50),POWER(50),T(100),Q
     1(100),HUB(100),DX,DT,INDEX,THETA,XNU,GRAV,NB(20),QS(500),LENQ,LENQ
     2S,LENM1,L,QL1(50),QL2(50)
      COMMON /CIRC/ TH1(50),TH2(50),SIN1(50),SIN2(50),COS1(50),COS2(50),
     1SIN1A,SIN2A,COS1A,COS2A,THUB(100),DFAC,QFAC,D
      J=INDEX
      SINX=SIN(X)
      X1=X+.000001
      SINX1=SIN(X1)
      PM1=POWER(1)-1.
      FAC1=(D/4.)*(1.-SINX1/X1)
      F1=ALPHA(1)*(FAC1**PM1)*D*D*(X1-SINX1)/8.-QUB(J)
      FAC=(D/4.)*(1.-SINX/X)
      FX=ALPHA(1)*(FAC**PM1)*D*D*(X-SINX)/8.-QUB(J)
      DERF=(F1-FX)/.000001
      RETURN
C
      END
      SUBROUTINE IMPOCF (X,FX,DERFX)
      COMMON /PLANE1/ H1(50),H2(50),QL(100),ALPHA(50),POWER(50),T(100),Q
     1(100),HUB(100),DX,DT,INDEX,THETA,XNU,GRAV,NB(20),QS(500),LENQ,LENQ
     2S,LENM1,L,QL1(50),QL2(50)
      J=INDEX
      JP1=J+1
      P=POWER(J)
      PP=POWER(J+1)
      PM1=P-1.
      PPM1=PP-1.
      TH=THETA
      T1=1.-THETA
      PA=H2(J)+X-H1(J)-H1(JP1)
      PB=12.*DT/DX)*(TH*(ALPHA(JP1)*X**PP-ALPHA(J)*H2(J)**P)+T1*(ALPHA(J
     1P1)*H1(JP1)**PP-ALPHA(J)*H1(J)**P))
      PC=BT*(QL2(J)+QL2(JP1))
      FX=PA+PB-PC

      DERFX=1.+(2.*DT*(ALPHA(JP1)*PP*THETA*(X**PPM1)/DX))
      RETURN
C
      END
      SUBROUTINE IMPCHA (X,FX,DERF)
      COMMON /CHAN/ A1(50),A2(50),QUB(100),AUB(100),C01,C02,B,NI,NOQL
      COMMON /PLANE1/ H1(50),H2(50),QL(100),ALPHA(50),POWER(50),T(100),Q
     1(100),HUB(100),DX,DT,INDEX,THETA,XNU,GRAV,NB(20),QS(500),LENQ,LENQ
     2S,LENM1,L,QL1(50),QL2(50)
      DIMENSION DQDA(2)
      DQDAFCT(AL,A,D1,D2,P,PM1,C)=AL*(A/D2)**PM1*(P-(PM1*A*C/(D1*D2)))
      ZFUNC(B,AREA,C01)=(B*B+2.*AREA/C01)**0.5
C
C     CONSTANTS
C
      IF (B.EQ.0.) B=.000001
      J=INDEX
      C=C02/C01
      XK=B*GO1
      P=POWER(1)
      PM1=P-1.
      PM2=P-2.
      THETA1=1.-THETA
C
C     CALCULATE DERIVATIVES OF THE DISCHARGE EQN. (DQ/DA)
C
      AREA1=(A1(J)+A1(J+1))/2.
      DUM11=ZFUNC(B,AREA1,C01)
      DUM21=(DUM11-B)*C02*XK
      DQDA(1)=DQDAFCT(ALPHA(1),AREA1,DUM11,DUM21,P,PM1,C)
      AREA2=(X+A2(J))/2.
      DUM12=ZFUNC(B,AREA2,C01)
      DUM22=(DUM12-B)*C02*XK
      DQDA(2)=DQDAFCT(ALPHA(1),AREA2,DUM12,DUM22,P,PM1,C)
C
C     CALCULATE SECOND DERIVATIVE OF DISCHARGE EQN WITH RESPECT TO X
C     (D2Q/DADX)
C
      IF (AREA2.EQ.0.) GO TO 105
      FAC=(AREA2/DUM22)
      TERM1=FAC**PM2*PM1*(1.-X*C/(DUM12*DUM22))/(2.*DUM22)
      TERM2=FAC**PM1*C*PM1*(1.-AREA2*(C*DUM22/(C01*DUM12)))/(DUM12*DUM22)
     1)/(2.*DUM12*DUM22)
      D2QDAX=ALPHA(J)*(TERM1-TERM2)
      GO TO 110
  105 D2QDAX=0.
  110 CONTINUE
C
C     FINITE DIFFERENCE EQN. AND ITS DERIVATIVE
C
      FX=(AREA2-AREA1)/(DT*2.)+(THETA/DX)*DQDA(2)*(X-A2(J))+(THETA1/DX)*
     1DQDA(1)*(A1(J+1)-A1(J))-0.5*(QL(L+1)+QL(L))
C
      DERF=1./(2.*DT)+(THETA/DX)*(DQDA(2)+D2QDAX*(X-A2(J)))
      RETURN
C
      END
      SUBROUTINE IMPCIR (X,FX,DERF)
      COMMON /PLANE1/ H1(50),H2(50),QL(100),ALPHA(50),POWER(50),T(100),Q
     1(100),HUB(100),DX,DT,INDEX,THETA,XNU,GRAV,NB(20),QS(500),LENQ,LENQ
     2S,LENM1,L,QL1(50),QL2(50)
      COMMON /CIRC/ TH1(50),TH2(50),SIN1(50),SIN2(50),COS1(50),COS2(50),
     1SIN1A,SIN2A,COS1A,COS2A,THUB(100),DFAC,QFAC,D
      COMMON /IO/ IREAD,IWRITE
      DIMENSION DADTH(2), DQDTH(2)
      NC=0
      J=INDEX
      JP1=J+1
      OMEGA=THETA
      P=POWER(J)
      PM1=P-1.
      PM2=P-2.
      IF (X.EQ.0.) X=0.0001
      ANGL2A=(X+TH1(JP1))/2.
      ANGL1Q=(TH1(J)+TH1(JP1))/2.

      ANGL2Q=(X+TH2(J))/2.
      SIN2A=SIN(ANGL2A)
      SIN1Q=SIN1(J)
      SIN2Q=SIN(ANGL2Q)
      COS2A=COS(ANGL2A)
      COS1Q=COS1(J)
      COS2Q=COS(ANGL2Q)
      AREA1Q=D*D*(ANGL1Q-SIN1Q)/8.
```

```
      AREA2Q=D*D*(ANGL2Q-SIN2Q)/8.
      DADTH(1)=D*D*(1.-COS1A)/8.
      DADTH(2)=D*D*(1.-COS2A)/8.
      IF (ANGL1Q.NE.0.) GO TO 105
      FAC1=0.
      GO TO 110
  105 FAC1=(2.*AREA1Q/(ANGL1Q*D))**PM1
  110 FAC2=(2.*AREA2Q/(ANGL2Q*D))**PM1
      TERM11=P*D*D*(1.-COS1Q)/8.
      IF (ANGL1Q.NE.0.) GO TO 115
      TERM12=0.
      GO TO 120
  115 TERM12=AREA1Q*PM1/ANGL1Q
  120 TERM21=P*D*D*(1.-COS2Q)/8.
      TERM22=AREA2Q*PM1/ANGL2Q
      DQDTH(1)=ALPHA(J)*FAC1*(TERM11-TERM12)
      DQDTH(2)=ALPHA(JP1)*FAC2*(TERM21-TERM22)
      FAC3=FAC2*D*ANGL2Q/(2.*AREA2Q)
      DADX=P*D*(1.-COS2Q)/16.
      DERIV=2.*DADX/(D*ANGL2Q)-AREA2Q/(ANGL2Q*ANGL2Q*D)
      TERM1=FAC2*(P*D*D*SIN2Q/16.-PM1*DADX/ANGL2Q*AREA2Q*PM1/(2.*ANGL2Q*
     1ANGL2Q))
      TERM2=FAC3*PM1*DERIV*(TERM21-TERM22)
      D2QDTX=ALPHA(1)*(TERM1+TERM2)
      D2ADTX=D*D*SIN2A/16.
      FX=(1./(2.*DT))*(DADTH(1)*(TH2(J)-TH1(J))+DADTH(2)*(X-TH1(JP1)))+(
     1OMEGA/DX)*DQDTH(2)*(X-TH2(J))+((1.-OMEGA)/DX)*DQDTH(1)*(TH1(JP1)-T
     2H1(J))
      DERF=(1./(2.*DT))*(D2ADTX*(X-TH1(JP1))+DADTH(2))+(OMEGA/DX)*(D2QDT
     1X*(X-TH2(J))+DQDTH(2))
      SIN2(J)=SIN2Q
      COS2(J)=COS2Q
      RETURN
C
      END
      SUBROUTINE IMPAUB (X,FX,DERF)
      COMMON /CHAN/ A1(50),A2(50),QUB(100),AUB(100),CO1,CO2,B,NI,NOQL
      COMMON /PLANE1/ H1(50),H2(50),QL(100),ALPHA(50),POWER(50),T(100),Q
     1(100),HUB(100),DX,DT,INDEX,THETA,XNU,GRAV,NB(20),QS(500),LENQ,LENQ
     2S,LENM1,L,QL1(50),QL2(50)
      DQDAFCT(AL,A,D1,D2,P,PM1,C)=AL*(A/D2)**PM1*(P-(PM1*A*C/(D1*D2)))
      N=0
  105 KFLAG=0
      J=INDEX
      IF (X.EQ.0..AND.QUB(J).EQ.0.) QUB(J)=0.0000001
      P=POWER(1)
      PM1=P-1.
      C=CO2/CO1
      DUM1=(B*B+2.*X/CO1)**0.5
      DUM2=(DUM1-B)*CO2+B*CO1
      FX=ALPHA(1)*X**P/DUM2**PM1-QUB(J)
C
C     CALCULATE DERIVATIVE OF ERROR FUNCTION (DERF)
C
      DERF=DQDAFCT(ALPHA(1),X,DUM1,DUM2,P,PM1,C)
C
C     DUE TO MISBEHAVIOR OF THE ERROR FUNCTION IN SOME CASES, THE FOL -
C     LOWING CORRECTION OF X MAY BE NECESSARY FOR CONVERGENCE
C
      IF (QUB(J-1).EQ.0.) GO TO 110
      IF (QUB(J)/5..GT.QUB(J-1)) KFLAG=1
      IF (KFLAG.EQ.0) GO TO 110
      IF (DERF.LT.0..AND.FX.LT.0.) GO TO 115
  110 RETURN
  115 X=X*10.
      N=N+1
      IF (N.GT.2) CALL ERROR (6HIMPAUB,10,0)
      GO TO 105
C
      END
      SUBROUTINE ADD (J)
      COMMON /IO/ IREAD,IWRITE
      COMMON /CHAN/ A1(50),A2(50),QUB(100),AUB(100),CO1,CO2,B,NI,NOQL
      COMMON /CIRC/ TH1(50),TH2(50),SIN1(50),SIN2(50),COS1(50),COS2(50),
     1SIN1A,SIN2A,COS1A,COS2A,THUB(100),DFAC,QFAC,D
      COMMON /PLANE1/ H1(50),H2(50),QL(100),ALPHA(50),POWER(50),T(100),Q
     1(100),HUB(100),DX,DT,INDEX,THETA,XNU,GRAV,NB(20),QS(500),LENQ,LENQ
     2S,LENM1,L,QL1(50),QL2(50)
      COMMON /GEOM/ XL(20),W(20),S(20),R1(20),R2(20),FMIN(20),NL(20),NR(
     120),NU(20),NC1(20),NC2(20),NCASE(20),ZL(20),ZR(20),A(20),DIAM(20),
     2NP(20)
C
C
C     THIS ROUTINE DOES TWO THINGS  1) IT CALCULATES THE UPPER BOUNDARY
C     AREA FOR INPUT INTO THE CHANNEL ROUTINE FOR CASES WHERE THERE IS A
C     EITHER A CONVERGING PLANE OR CHANNELS CONTRIBUTING TO THE UPPER
C     BOUNDARY OF CHANNEL J...2)IT ADDS TOGETHER ALL LATERAL INFLOW FROM
C     ANY CONTRIBUTING LATERAL PLANES.
C     NOTE THAT THE INDEX (N) IN THIS ROUTINE IS ON TIME.
C
C
      EXTERNAL IMPAUB,IMTHUB
      NOQL=1
      NCHN=0
      NPA=NCHN
      NUT=NU(J)
      NC1T=NC1(J)
      NC2T=NC2(J)
      DO 105 N=1,NI
  105 AUB(N)=0.0
C
C     CHECK FOR CONTRIB. ELEMENTS AT UPPER END AND SEND TO APPROP. LOOP
C
  110 IF (NUT.NE.0) GO TO 115
      IF (NC1T.NE.0) NCHN=NCHN+1
      IF (NC2T.NE.0) NCHN=NCHN+1
      IF (NCHN.EQ.0) GO TO 215
      GO TO (125,135), NCHN
C
C     CONVERGING PLANE AT UPPER END OF CHANNEL
C
  115 IF (NC1T.NE.0.OR.NC2T.NE.0) CALL ERROR (3HADD,14,J,0.)
      IF (NB(NUT).EQ.0) CALL ERROR (3HADD,15,NUT,0.)
      MU=NB(NUT)
      DO 120 N=1,NI
         MM=N-1
         QUB(N)=QS(MM+MU)
  120 CONTINUE
      NB(NUT)=0
      NUT=0
      GO TO 145
C
C     ONE CHANNEL AT UPPER END
C
  125 M=NB(NC1T+NC2T)
      IF (NB(NC1T+NC2T).EQ.0) CALL ERROR (3HADD,15,NC1T+NC2T,0.)
      DO 130 N=1,NI
         MM=N-1
         QUB(N)=QS(MM+M)
  130 CONTINUE
      NB(NC1T+NC2T)=0
      NC2T=0
      NC1T=NC2T
      NCHN=0
      GO TO 145
C
C     TWO CHANNELS AT UPPER END
C
  135 M1=NB(NC1T)
      M2=NB(NC2T)
      IF (NB(NC1T).EQ.0) CALL ERROR (3HADD,15,NC1T,0.)
      IF (NB(NC2T).EQ.0) CALL ERROR (3HADD,15,NC2T,0.)
      DO 140 N=1,NI
         MM=N-1
         QUB(N)=QS(M1+MM)+QS(M2+MM)
  140 CONTINUE
      NB(NC1T)=0
      NB(NC2T)=0
      NC2T=0
      NC1T=NC2T
      NCHN=0
      GO TO 145
C
C     CALCULATE NECESSARY UPPER BOUND PARAMETERS--EITHER AREAS OR ANGLES
C     VALUES ARE SOLVED FOR BY NEWTONS ITERATION METHOD.
C
  145 GO TO (150,170,210), NCASE(J)
C
C     TRAPEZOIDAL CASE -- UPPER BOUND AREA (AUB)
C
  150 IF (XL(J).EQ.0) RETURN
      AUB(1)=0.
      IEND=15
      XST=(QUB(2)*B*CO1/ALPHA(1))**(1./POWER(1))
      DO 165 N=2,NI
         INDEX=N
         IF (QUB(N).EQ.0.) GO TO 160
         IF (B.GT..000001) GO TO 155
         AUB(N)=((QUB(N)/ALPHA(1))*(2.*CO2*CO2/CO1)**(.5*(POWER(1)-1.)))
     1   **(1./(.5*(POWER(1)+1.)))
         GO TO 165
  155    IF (XST.EQ.0.) XST=0.001
         CALL ITER (AUB(N),FA,DERFA,IMPAUB,XST,0.0001,IEND,IER)
         IER=IER+1
         IF (IER.EQ.3) AUB(N)=0.
         IF (IER.EQ.3) IER=1
         IF (IER.EQ.4) AUB(N)=0.
         IF (IER.EQ.4) IER=1
         IF (AUB(N).LT.0.0001) AUB(N)=0.
         XST=AUB(N)
         GO TO (165,185,190,195,200), IER
  160    AUB(N)=0.
  165 CONTINUE
      GO TO 110
C
C     CIRCULAR CONDUIT CASE - UPPER BOUND ANGLE (THUB)
C
  170 PI=ACOS(-1.)
      D=DIAM(J)
      DFAC=(D/2.)**(1.-1./POWER(1))
      QMAX=ALPHA(1)*PI*D*(D/4.)**POWER(1)
      IEND=10
      XSP=PI/5.
      THUB(1)=0.
      DO 180 N=2,NI
         INDEX=N
         IF (QUB(N).EQ.0.) GO TO 175
         IF (QUB(N)/10..GT.QUB(N-1)) XSP=5.*THUB(N-1)
         IF (XSP.EQ.0.) XSP=PI/5.
         IF (QUB(N).GT.QMAX) GO TO 205
         QFAC=(QUB(N)/ALPHA(1))**(1./POWER(1))
         CALL ITER (THUB(N),FT,DERFT,IMTHUB,XSP,0.005,IEND,IER)
         IER=IER+1
         IF (IER.EQ.3) THUB(N)=0.
         IF (IER.EQ.3) IER=1
         IF (IER.EQ.4) THUB(N)=0.
         IF (IER.EQ.4) IER=1
         IF (THUB(N).LT.0.005) THUB(N)=0.
         XSP=THUB(N)
         GO TO (180,185,190,195,200), IER
  175    THUB(N)=0.
  180 CONTINUE
      GO TO 240
  185 CALL ERROR (3HADD,10,IEND,0.)
  190 CALL ERROR (3HADD,11,N,0.)
  195 CALL ERROR (3HADD,13,N,0.)
  200 CALL ERROR (3HADD,17,J,1)
  205 WRITE (IWRITE,255) J,D,QMAX,N,QUB(N)
  210 STOP 555
C
C
C     CHECK FOR NUMBER OF CONTRIB. PLANES ON SIDES AND SEND TO CORRECT
C     LOOP.  AFTER THIS IS DONE, RETURN.
C
  215 NRT=NR(J)
      NLT=NL(J)
      IF (NRT.NE.0) NPA=NPA+1
      IF (NLT.NE.0) NPA=NPA+1
      IF (NPA.EQ.0) GO TO 240
      GO TO (220,230), NPA
C
C     ONE SIDE LATERAL INFLOW ONLY
C
  220 M=NB(NLT+NRT)
      IF (NB(NRT+NLT).EQ.0) CALL ERROR (3HADD,15,NRT+NLT,0.)
      DO 225 N=1,NI
         MM=N-1
         QL(N)=(QS(MM+M))/XL(J)
  225 CONTINUE
      NPA=0
      NB(NLT+NRT)=0
      NLT=0
```

```
      NRT=NLT
      GO TO 250
C
C     BOTH LEFT AND RIGHT LATERAL INFLOW
C
  230 MR=NB(NRT)
      ML=NB(NLT)
      IF (NB(NRT).EQ.0) CALL ERROR (3HADD,15,NRT,0.)
      IF (NB(NLT).EQ.0) CALL ERROR (3HADD,15,NLT,0.)
      DO 235 N=1,NI
         MM=N-1
         QL(N)=(QS(MM+MR)+QS(MM+ML))/XL(J)
  235 CONTINUE
      NPA=0
      NB(NLT)=0
      NB(NRT)=NB(NLT)
      NLT=0
      NRT=NLT
      GO TO 250
C
C     NO LATERAL INFLOW
C
  240 DO 245 N=1,NI
         QL(N)=0.0
  245 CONTINUE
      NOQL=2
  250 RETURN
C
  255 FORMAT (//,1X,120(1H*),/,5X,9HPIPE NO. ,I2,15H WITH DIAMETER=,F7.3
     1,40H WAS EXCEEDED ITS FLOW CAPACITY OF QMAX=,1PE12.5,/,5X,32HOVERF
     2LOW  OCCURRED AT TIME STEP ,I3,10H WITH QUB=,1PE12.5,/1X,120(1H*),
     31X)
C
      END
      SUBROUTINE IMPLCT (NK,I)
      COMMON /IO/ IREAD,IWRITE
      COMMON /CNTRL/ NRES,NOPT,NTIME,NUNITS,NELE,CLEN,DELT,NLOG(20)
      COMMON /GEOM/ XL(20),W(20),S(20),R1(20),H2(20),FMIN(20),NL(20),NR(
     120),NU(20),NC1(20),NC2(20),NCASE(20),ZL(20),ZR(20),A(20),DIAM(20),
     2NP(20)
      COMMON /EVENT/ TFIN,ND,QI(100),TI(100),QUB(100),TUB(100),NO,SUMRCM
      COMMON /PLANE1/ H1(50),H2(50),QL(100),ALPHA(50),POWER(50),T(100),Q
     1(100),HUR(100),DX,DT,INDEX,THETA,ANU,GRAV,NB(20),QS(500),LENQ,LENQ
     2S,LENM1,L,QL1(50),QL2(50)
      COMMON /CHAN/ A1(50),A2(50),QUB(100),AUB(100),C01,C02,B,NI,NOQL
      COMMON /CIRC/ TH1(50),TH2(50),SIN1(50),SIN2(50),COS1(50),COS2(50),
     1SIN1A,SIN2A,COS1A,COS2A,THUB(100),DFAC,QFAC,D
      COMMON /LAWS/ ATURB,PTURB,ALAM,PLAM,HTRANS,QTHANS
      EXTERNAL IMPOCF,IMPCHA,IMPCIR
      DATA EPS,IEND/0.0001,50/
      NKM1=NK-1
C
C     CHECK TO SEE IF PLANE OR CHANNEL
C
      IF (W(I).EQ.0) GO TO 160
C
C*****************************************************************
C
C     PLANE CASE -- ADVANCE TIME DEPTH (H2) IS SOLVED IMPLICITLY BY
C     NEWTON-S ITERATIVE METHOD IN ITER.  ROUTINE IMPOCF  IS THE ROUTINE
C     WHICH CALCULATES  THE FINITE DIFFERENCE EQN. USED BY ITER.  NOTE
C     THAT THE CORRECT RESISTENCE LAW IS CHOSEN BEFORE EACH CALL TO ITER
C
      DO 155 J=1,NKM1
         INDEX=J
         JP1=J+1
         XST=H2(J)
         IF (XST.EQ.0.) XST=H1(JP1)
         IF (H1(JP1).GT.HTRANS.OR.H2(J).GT.HTRANS) IFLAG=0
         IF (H1(JP1).LE.HTRANS.OR.H2(J).LE.HTRANS) IFLAG=1
         CALL CHGLAW (IFLAG,JP1,NRES)
C
C     CHECK FOR NEGATIVE LATERAL INFLOW.  IF SO,     CHECK TO SEE IF IT
C     IS SUFFICIENT TO DRY UP H2(J+1). IF SO, SET TO 0 AND CONTINUE.
C
         QTEST=0.5*(QL2(J)+QL2(JP1))*DT
         IF (QTEST.GT.0.) GO TO 105
         QTEST=-QTEST
         IF (QTEST.LT.H1(JP1)) GO TO 105
         H2(JP1)=0.
         GO TO 155
  105    IF (J-1) 110,110,120
  110    IF (H2(1)+H1(2)) 115,115,120
  115    H2(2)=DT*QL2(2)
         IER=1
         GO TO 125
  120    CALL ITER (H2(JP1),FH2,DERFH2,IMPOCF,XST,.00001,IEND,IER,10.0)
         IER=IER+1
  125    H2(J+1)=AMAX1(0.,H2(J+1))
C
C     INTERPRET ERROR FLAG FOR TOO MANY NEG. TRIAL VALUES AS CONVERGENCE
C     AT ZERO.  ONLY POSSIBLE DURING RECESSION PERIOD OF HYDROGRAPH AND
C     WITH KINEMATIC SHOCK CONDITION.
C
         IF (IER.NE.4) GO TO 140
         IF (QL2(J)+QL2(JP1).GT.0.) GO TO 140
         IF (JP1.EQ.NK) GO TO 135
         DO 130 JK=JP1,NK
            IF (H2(JK).GT.0.) GO TO 135
  130    CONTINUE
         GO TO 140
  135    H2(JP1)=0.
         GO TO 155
  140    GO TO (155,275,150,285,300), IER
  145    H2(JP1)=H1(JP1)+QTEST
         WRITE (IWRITE,310) J
         GO TO 155
  150    WRITE (IWRITE,315) JP1,T(L),I
  155 CONTINUE
      RETURN
C
C*****************************************************************
C
C     CHECK FOR TYPE OF CHANNEL
C
  160 GO TO (165,220), NCASE(I)
C
C     TRAPEZOIDAL CHANNEL -- SOLUTION FOR ADVANCE TIME AREA(A2).
C     SINCE ROUTINE WILL NOT CONVERGE AT ZERO AND SINCE THE ERROR FLAG
C     FOR TOO MANY CORRECTED NEGATIVE TRIAL VALUES IS SET WHENEVER CON-
C     VERGENCE AT ZERO IS ATTEMPTED. THIS ERROR FLAG IS RECOGNIZED AS
C     CONVERGENCE AT ZERO.  FOR NO LATERAL INFLOW CASES (NOQL=2) ZERO
C     CONVERGENCE IS POSSIBLE EITHER BEFORE RUNOFF REACHES THE CHANNEL
C     FROM ABOVE OR DURING THE RECESSION PERIOD OF THE HYDROGRAPH.  IF
C     LATERAL INFLOW OCCURS (NOQL=1) THEN ZERO IS ONLY POSSIBLE FOR
C     RECESSION.
C
  165 DO 215 J=1,NKM1
         INDEX=J
         JP1=J+1
         XST=A2(J)
         GO TO (175,170), NOQL
  170    IF (A1(JP1).EQ.0.) XST=0.
  175    CALL ITER (A2(JP1),FA2,DERFA2,IMPCHA,XST,EPS,IEND,IER,1000.)
         IER=IER+1
         IF (IER.EQ.4) GO TO 180
         IF (A2(JP1).EQ.0.) GO TO 180
         IF (A2(JP1).LT.EPS) A2(JP1)=0.
         GO TO 205
C
C     CHECK TO SEE IF ZERO VALUE IS DUE TO PRE- RUNOFF PERIOD OR TO
C     RECESSION
C
  180    JP1=J+1
         DO 185 JK=JP1,NK
            IF (A1(JK).GT.0.) GO TO 200
  185    CONTINUE
         GO TO (205,190), NOQL
C
C     RUNOFF HAS NOT REACHED  J+1
C
  190    DO 195 JJ=JP1,NK
            A2(JJ)=0.
  195    CONTINUE
         RETURN
C
C     RECESSION ZERO VALUE
C
  200    A2(JP1)=0.
         GO TO 215
  205    GO TO (215,275,280,285,300), IER
  210    A2(J+1)=(QL(L)+QL(L-1))*.5*DT
         WRITE (IWRITE,320) J
  215 CONTINUE
      RETURN
C
C     CIRCULAR CONDUIT CASE -- SOLUTION FOR ADVANCE TIME THETA ANGLE
C     (TH2).  NOTE THAT THERE IS NO LATERAL INFLOW, SO THE SAME CONDITIO
C     APPLY TO CONVERGENCE AT ZERO  AS DISCUSSED ABOVE UNDER THE TRAPEZO
C     NO LATERAL INFLOW CASE.
C
  220 DO 270 J=1,NKM1
         INDEX=J
         JP1=J+1
         IF (TH2(J)+TH1(J)+TH1(JP1).NE.0.) GO TO 230
  225    TH2(JP1)=0.
         SIN1A=0.
         SIN2(J)=SIN1A
         COS1A=1.
         COS2(J)=COS1A
         GO TO 270
  230    CONTINUE
         XSP=TH2(J)
         IF (XSP.EQ.0.) XSP=0.01
         CALL ITER (TH2(JP1),FTH2,DERFTH2,IMPCIR,XSP,0.00001,IEND,IER,6.
     1   26)
         SIN1A=SIN2A
         COS1A=COS2A
         IER=IER+1
         IF (TH2(JP1).EQ.0.) GO TO 240
C
         IF (IER-4) 260,235,260
C
C     CHECK TO SEE IF ZERO VALUE IS DUE TO PRE-RUNOFF PERIOD OR TO RECES
C     SION.
C
  235    TH2(JP1)=0.
         SIN2(J)=SIN(TH2(J)/2.)
         COS2(J)=SQRT(1.-SIN2(J)*SIN2(J))
         SIN1A=SIN(TH1(JP1)/2.)
         COS1A=SQRT(1.-SIN1A*SIN1A)
         GO TO 270
  240    JP1=J+1
         DO 245 JK=JP1,NK
            IF (TH1(JK).GT.0.) GO TO 255
  245    CONTINUE
C
C     PRE-RUNOFF ZERO VALUE
C
         SIN2(J)=0.
         COS2(J)=1.
         DO 250 JJ=JP1,NK
            TH2(JJ)=0.
            SIN2(JJ)=0.
            COS2(JJ)=1.
  250    CONTINUE
         RETURN
C
C     RECESSION ZERO VALUE
C
  255    TH2(JP1)=0.
         SIN1A=SIN(TH1(JP1)/2.)
         COS1A=SQRT(1.-SIN1A*SIN1A)
         SIN2(J)=0.
         COS2(J)=1.
         GO TO 270
  260    GO TO (265,275,280,290,305), IER
  265    IF (TH2(JP1).LT.0.005) GO TO 225
  270 CONTINUE
      RETURN
C
C     ERROR RETURNS
C
  275 CALL ERROR (6HIMPLCT,10,IEND,0.)
  280 IP1=INDEX+1
      CALL ERROR (6HIMPLCT,11,IP1,0.)
  285 IP1=INDEX+1
      IF ((H1(J).EQ.H1(J+1)).AND.(H2(J).GT.(H1(J)+QTEST))) GO TO 145
      GO TO 295
  290 IP1=INDEX+1
      IF ((A1(J).EQ.A1(J+1)).AND.(A2(J).GT.((QL(L-1)+QL(L))*.5*DT))) GO
     1TO 210
  295 CALL ERROR (6HIMPLCT,13,IP1,0.)
```

```
      RETURN
  300 IP1=INDEX+1
      CALL ERROR (6HIMPLCT,17,I,IP1)
  305 IP1=INDEX+1
      CALL ERROR (6HIMPLCT,16,I,IP1)
      RETURN
C
  310 FORMAT (2X,25H  NO POSITIVE ROOT AT J= ,I3,/,10X,24HH2(J+1)=H1(J+1
     1)+(QL)(DT))
  315 FORMAT (2X,34H NEGATIVE DEPTH CALLED ZERO AT J= ,I2,3HAT ,F10.2,15
     1H MIN. ON PLANE ,I2)
  320 FORMAT (2X,23H NO POSITIVE ROOT AT J=,I3,/,10X,29HA2(J+1)=(QL(1)+Q
     1L(2))(.5)(DT))
C
      END
      SUBROUTINE ITER (X,F,DERF,FCT,XST,EPS,IEND,IER,XMAX)
C     ******************************************************************
C
C     SUBROUTINE  ITER
C
C     THIS ROUTINE SOLVES GENERAL NONLINEAR EQUATIONS OF THE FORM F(X)=0
C     BY MEANS OF THE NEWTON ITERATION  METHOD.
C
C     DESCRIPTION OF PARAMETERS
C        X  - RESULTANT ROOT OF EQUATION F(X)=0
C        F  - RESULTANT FUNCTION VALUE AT ROOT X.
C        DERF-RESULTANT  VALUE OF DERIVATIVE AT ROOT X.
C        FCT - NAME OF THE EXTERNAL SUBROUTINE USED. IT COMPUTES  TO
C              GIVEN ARGUMENT X FUNCTION VALUE F AND DERIVATIVE DERF. IT
C              PARAMETER LIST MUST BE X,F,DERF
C        XST - INPUT VALUE WHICH SPECIFIES THE INITIAL GUESS OF THE
C              ROOT X.
C        EPS - INPUT VALUE WHICH SPECIFIES THE UPPER BOUND OF THE ERROR
C              OF RESULT X.
C        IEND- MAXIMUM NUMBER OF ITERATION STEPS SPECIFIED.
C        IER - RESULTANT ERROR PARAMETER CODED AS FOLLOWS
C                IER=0 - NO ERROR
C                IER=1 - NO CONVERGENCE AFTER IEND ITERATION STEPS
C                IER=2 - AT ANY ITERATION STEP DERIVATIVE DERF WAS
C                        EQUAL TO ZERO.
C                IER=3 - X HAS  TAKEN ON A NEGATIVE VALUE 5 CONSECUTIVE
C                        TIMES  FOLLOWING CORRECTION TO A POSTIVE VALUE.
C
C     ******************************************************************
C
C     PREPARE ITERATION
C
      COMMON /IO/ IREAD,IWRITE
      IER=0
      NC=0
      X=XST
      TOL=X
      CALL FCT (TOL,F,DERF)
      DX=F/DERF
      X=X-DX
      NSIGN=0
      IF (DERF.LT.0.) NSIGN=1
      TOLF=100.*EPS
C
C
C     START ITERATION LOOP
C
      DO 145 I=1,IEND
         IF (F) 105,155,105
C
C     EQUATION IS NOT SATISFIED BY X
C
  105    IF (DERF) 110,160,110
C
C     ITERATION IS POSSIBLE
C
C     IF X TAKES A NEGATIVE VALUE, CORRECT X TO BE HALF ITS OLD VALUE.
C     IF NOT, MAKE SURE NC=0 AND CONTINUE.
C
  110    IF (X) 115,120,120
  115    NC=NC+1
         X=(X+DX)/(1.+FLOAT(NC))
         IF (NC-5) 135,170,170
  120    NC=0
         IF (X-XMAX) 130,130,125
  125    LC=LC+1
         X=0.9*XMAX
         IF (LC-5) 135,135,175
  130    LC=0
  135    TOL=X
         CALL FCT (TOL,F,DERF)
         NCK=0
         IF (DERF.LT.0.) NCK=1
         IF (NSIGN-NCK.NE.0) GO TO 165
         DX=F/DERF
         X=X-DX
C
C     TEST ON SATISFACTORY ACCURACY
C
         TOL=EPS
         IF (ABS(DX)-TOL) 140,140,145
  140    IF (ABS(F)-TOLF) 155,155,145
  145 CONTINUE
C
C     END OF ITERATION LOOP
C
      GO TO 150
C
C     NO CONVERGENCE AFTER IEND ITERATION STEPS, ERROR RETURN
C
  150 IER=1
  155 RETURN
C
C     ERROR RETURN IN CASE OF ZERO DIVISION
C
  160 IER=2
      RETURN
  165 WRITE (IWRITE,180)
C
C     FLAGGED RETURN IN CASE OF 5 CORRECTED NEGATIVE X VALUES
C
  170 IER=3
      RETURN
C
C ***  FLAGGED RETURN AFTER CONVERGENCE TO GT. MAX VALUE OF X
C
  175 IER=4
      RETURN
C
  180 FORMAT (17X,36HERROR STOP ON CHANGE OF SIGN IN DERF)
C
      END
      SUBROUTINE ERROR (ISUBR,I,IVAR,KVAR)
      COMMON /IO/ IREAD,IWRITE
      DATA IUP/15/
      WRITE (IWRITE,200) I,ISUBR
      IF ((I.GE.1).AND.(I.LE.IUP)) GO TO 105
      WRITE (IWRITE,205)
      GO TO 195
  105 GO TO (110,115,120,125,130,135,140,145,150,155,160,165,170,175,180
     1,185,190), I
  110 WRITE (IWRITE,215)
      WRITE (IWRITE,210) IVAR
      WRITE (IWRITE,225)
      GO TO 195
  115 WRITE (IWRITE,215)
      WRITE (IWRITE,225)
      WRITE (IWRITE,220) IVAR,KVAR
      GO TO 195
  120 WRITE (IWRITE,215)
      WRITE (IWRITE,230) IVAR,KVAR
      GO TO 195
  125 WRITE (IWRITE,235) KVAR,KVAR
      GO TO 195
  130 WRITE (IWRITE,240) IVAR,KVAR
      GO TO 195
  135 WRITE (IWRITE,245) IVAR
      GO TO 195
  140 WRITE (IWRITE,250) IVAR,KVAR
      GO TO 195
  145 WRITE (IWRITE,255) IVAR,KVAR
      GO TO 195
  150 WRITE (IWRITE,260) IVAR
      GO TO 195
  155 WRITE (IWRITE,265) IVAR
      GO TO 195
  160 WRITE (IWRITE,270) IVAR
      GO TO 195
  165 WRITE (IWRITE,275)
      GO TO 195
  170 WRITE (IWRITE,280) IVAR
      RETURN
  175 WRITE (IWRITE,285) IVAR
      GO TO 195
  180 WRITE (IWRITE,290) IVAR
      GO TO 195
  185 WRITE (IWRITE,295) IVAR,KVAR
      GO TO 195
  190 WRITE (IWRITE,300) IVAR,KVAR
  195 WRITE (IWRITE,305)
      STOP
C
  200 FORMAT (1H0,132(1H*)//11H ERROR NO. ,I3,13H CALLED FROM ,A6)
  205 FORMAT (47H0ERROR NUMBER OUT OF RANGE.  CALLED FROM ERROR.)
  210 FORMAT (58H IT APPEARS THAT NO VALUE HAS BEEN INPUT FOR THE VARIAB
     1LE ,A8,2H .)
  215 FORMAT (16H0DATA CARD ERROR,/)
  220 FORMAT (58H IT APPEARS THAT NO VALUE HAS BEEN INPUT FOR THE VARIAB
     1LE ,A8,30H FOR WATERSHED ELEMENT WITH J=,I3)
  225 FORMAT (79H AT LEAST UNDER THE CONDITIONS SPECIFIED, INPUT FOR THI
     1S  VARIABLE IS REQUIRED.)
  230 FORMAT (34H THE VALUE INPUT FOR THE VARIABLE ,A8,79H IS ILLEGAL. T
     1HIS VALUE OR ARRAY ELEMENT SUBSCRIPT (IFVARIABLE IS AN ARRAY) IS ,
     2I4)
  235 FORMAT (96H APPARENTLY ALL WATERSHED ELEMENTS HAVE NOT BEEN ASSIGN
     1ED TO THE ORDER OF PROCESSING ARRAY NLOG,/,11H THERE ARE ,I3,19H
     2ELEMENTS,BUT NLOG(,I3,4H)=0.)
  240 FORMAT (82H DATA CARDS FOR GROUPS 1ST AND 2ND ARE FOR TWO DIFFEREN
     1T NOS. ELEMENTS. ON 1ST, J=,I3,14H AND ON 2ND J=,I3)
  245 FORMAT (11H ELEMENT J=,I3,93H HAS BEEN SPECIFIED AS AN ADDER CHANN
     1EL  (XL=0.) BUT IS NOT THE LAST ELEMENT TO BE PROCESSED.)
  250 FORMAT (11H THE ARRAY ,A5,33H IS REQUIRED INPUT ON GROUP CARD ,A8,
     147H , APPARENTLY IT IS MISSING FROM THE DATA INPUT)
  255 FORMAT (11H FOR ARRAY ,A5,16H EITHER ELEMENT ,I3,55H IS ILLEGAL(=0
     1.) OR THE ENTIRE ARRAY HAS NOT BEEN INPUT)
  260 FORMAT (47H THE NUMBER OF GEOMETRIC ELEMENTS EXCEEDS 20.  ,1H=,I10
     1,1H=)
  265 FORMAT (22H NO CONVERGENCE AFTER ,I4,17H ITERATION STEPS.)
  270 FORMAT (18H DERIVATIVE OF  X(,I4,6H) = 0.)
  275 FORMAT (17H BLANK CARD READ.)
  280 FORMAT (92H 5 CONSECUTIVE NEGATIVE VALUES WERE OBTAINED FOR NEW VA
     1LUES IN THE ITERATIVE SOLUTION OF  X(,I3,1H))
  285 FORMAT (9H ELEMENT ,I2,40H HAS A PLANE AND CHANNEL(S) AT UPPER END
     1)
  290 FORMAT (9H ELEMENT ,I3,27H HAS NOT BEEN PROCESSED YET)
  295 FORMAT (86H  CENTRAL INTERCEPT ANGLE CALCULATED TO BE GT. 2PI, IMP
     1LYING FULL PIPE FLOW IN CONDUIT,I3,6H AT X(,I2,1H))
  300 FORMAT (27H  AREA OR DEPTH ON ELEMENT ,I2,6H AT X(,I2,42H) IS CALC
     1ULATED TO EXCEED MAXIMUM ALLOWED )
  305 FORMAT (1H0,132(1H*))
C
      END
```

Key Words: Computer, Hydrograph, Infiltration, Kinematic, Overland Flow, Rural, Storm Sewers, Urban

Abstract: A parametric infiltration model is incorporated with a surface routing model, based upon a kinematic cascade of planes and channels to constitute a watershed model. Relationships are developed to compute flows by the kinematic approximation in channels of circular cross-section for routing through storm drains. The infiltration model is tested on some infiltrometer experiments; model parameters are estimated from measured data and by comparison to characteristics of soils used in a previous study. Two types of flow resistance relationships are considered: the Chezy formula and a friction relationship that is initially laminar and then becomes turbulent (Chezy) above a transition Reynolds number. The watershed model is used to compute discharge from: a) a 0.6 acre impervious experimental rainfall-runoff facility, b) a 27 acre experimental agricultural watershed, and c) a 165 acre urban watershed.

Key Words: Computer, Hydrograph, Infiltration, Kinematic, Overland Flow, Rural, Storm Sewers, Urban

Abstract: A parametric infiltration model is incorporated with a surface routing model, based upon a kinematic cascade of planes and channels to constitute a watershed model. Relationships are developed to compute flows by the kinematic approximation in channels of circular cross-section for routing through storm drains. The infiltration model is tested on some infiltrometer experiments; model parameters are estimated from measured data and by comparison to characteristics of soils used in a previous study. Two types of flow resistance relationships are considered: the Chezy formula and a friction relationship that is initially laminar and then becomes turbulent (Chezy) above a transition Reynolds number. The watershed model is used to compute discharge from: a) a 0.6 acre impervious experimental rainfall-runoff facility, b) a 27 acre experimental agricultural watershed, and c) a 165 acre urban watershed.

Key Words: Computer, Hydrograph, Infiltration, Kinematic, Overland Flow, Rural, Storm Sewers, Urban

Abstract: A parametric infiltration model is incorporated with a surface routing model, based upon a kinematic cascade of planes and channels to constitute a watershed model. Relationships are developed to compute flows by the kinematic approximation in channels of circular cross-section for routing through storm drains. The infiltration model is tested on some infiltrometer experiments; model parameters are estimated from measured data and by comparison to characteristics of soils used in a previous study. Two types of flow resistance relationships are considered: the Chezy formula and a friction relationship that is initially laminar and then becomes turbulent (Chezy) above a transition Reynolds number. The watershed model is used to compute discharge from: a) a 0.6 acre impervious experimental rainfall-runoff facility, b) a 27 acre experimental agricultural watershed, and c) a 165 acre urban watershed.

A computer program of a general kinematic watershed model is described and documented. This program, called KINGEN 75 may be used to predict hydrographs of individual storms for small rural and urban watersheds, based on basin topography and field measurements of infiltration parameters.

Reference: Rovey, Edward W., David A. Woolhiser and Roger E. Smith; Colorado State University, Hydrology Paper No. (July 1977), A Distributed Kinematic Model of Upland Watersheds.

A computer program of a general kinematic watershed model is described and documented. This program, called KINGEN 75 may be used to predict hydrographs of individual storms for small rural and urban watersheds, based on basin topography and field measurements of infiltration parameters.

Reference: Rovey, Edward W., David A. Woolhiser and Roger E. Smith; Colorado State University, Hydrology Paper No. (July 1977), A Distributed Kinematic Model of Upland Watersheds.

A computer program of a general kinematic watershed model is described and documented. This program, called KINGEN 75 may be used to predict hydrographs of individual storms for small rural and urban watersheds, based on basin topography and field measurements of infiltration parameters.

Reference: Rovey, Edward W., David A. Woolhiser and Roger E. Smith; Colorado State University, Hydrology Paper No. (July 1977), A Distributed Kinematic Model of Upland Watersheds.

A computer program of a general kinematic watershed model is described and documented. This program, called KINGEN 75 may be used to predict hydrographs of individual storms for small rural and urban watersheds, based on basin topography and field measurements of infiltration parameters.

Reference: Rovey, Edward W., David A. Woolhiser and Roger E. Smith; Colorado State University, Hydrology Paper No. (July 1977), A Distributed Kinematic Model of Upland Watersheds.

LIST OF PREVIOUS 25 PAPERS

No. 68 Stochastic Analysis of Groundwater Level Time Series in Western United States, by Albert G. Law, May 1974.

No. 69 Efficient Sequential Optimization in Water Resources, by Thomas E. Croley II, September 1974.

No. 70 Regional Water Exchange for Drought Alleviation, by Kuniyoshi Takeuchi, November 1974.

No. 71 Determination of Urban Watershed Response Time, by E. F. Schulz, December 1974.

No. 72 generation of Hydrologic Samples, Case Study of the Great Lakes, by V. Yevjevich, May 1975.

No. 73 Extraction of Information on Inorganic Water Quality, by William L. Lane, August 1975.

No. 74 Numerical Model of Flow in Stream-Aquifer System, by Catherine E. Kraeger Rovey, August 1975.

No. 75 Dispersion of Mass in Open-Channel Flow, by William W. Sayre, August 1975.

No. 76 Analysis and Synthesis of Flood Control Measures, by Kon Chin Tai, September 1975.

No. 77 Methodology for the Selection and Timing of Water Resources Projects to Promote National Economic Development, by Wendim-Agegnehu Lemma, August 1975.

No. 78 Two-Dimensional Mass Dispersion in Rivers, by Forrest M. Holly, Jr., September 1975.

No. 79 Range and Deficit Analysis Using Markov Chains, by Francisco Gomide, October 1975.

No. 80 Analysis of Drought Characteristics by the Theory of Run, by Pedro Guerrero-Salazar and Vujica Yevjevich, October 1975.

No. 81 Influence of Simplifications in Watershed Geometry in Simulation of Surface Runoff, by L. J. Lane, D. A. Woolhiser and V. Yevjevich, January 1976.

No. 82 Distributions of Hydrologic Independent Stochastic Components, by Pen-chih Tao, V. Yevjevich and N. Kottegoda, January 1976.

No. 83 Optimal Operation of Physically Coupled Surface and Underground Storage Capacities, by Dragoslav Isailovic, January 1976.

No. 84 A Salinity Management Strategy for Stream-Aquifer Systems, by Otto J. Helweg, and J. Labadie, February 1976.

No. 85 Urban Drainage and Flood Control Projects Economic, Legal and Financial Aspects, by Neil S. Grigg, Leslie H. Botham, Leonard Rice, W. J. Shoemaker, and L. Scott Tucker, February 1976.

No. 86 Reservoir Capacity for Periodic-Stochastic Input and Periodic Output, by Kedar Nath Mutreja, September 1976.

No. 87 Area-Deficit-Intensity Characteristics of Droughts, by Norio Tase, October 1976.

No. 88 Effect of Misestimating Harmonics in Periodic Hydrologic Parameters, by K. L. Bullard, V. Yevjevich, and N. Kottegoda, November 1976.

No. 89 Stochastic Modeling of Hydrologic, Intermittent Daily Processes, by Jerson Kelman, February 1977.

No. 90 Experimental Study of Drainage Basin Evolution and Its Hydrologic Implications, by Randolph S. Parker, June 1977.

No. 91 A Model of Stochastic Structure of Daily Precipitation Series Over an Area, by C. W. Richardson, July 1977.

No. 92 Effects of Forest and Agricultural Land Use on Flood Unit Hydrographs, by Wiroj Sangvaree and Vujica Yevjevich, July 1977.